THE UNIVERSITY OF CHICAGO

THE CONTRIBUTION OF SOX2+ CELLS TO PROSTATE EPITHELIUM DEVELOPMENT, REGENERATION, AND HYPERPLASIA

A DISSERTATION SUBMITTED TO

THE FACULTY OF THE DIVISION OF THE BIOLOGICAL SCIENCES

AND THE PRITZKER SCHOOL OF MEDICINE

IN CANDIDACY FOR THE DEGREE OF

DOCTOR OF PHILOSOPHY

DEPARTMENT OF PATHOLOGY

BY

ERIN MARIE MCAULEY

CHICAGO, ILLINOIS

JUNE 2018

For my family

TABLE OF CONTENTS

LIST OF FIGURES

LIST OF TABLES

ACKNOWLEDGEMENTS

I would like to express my appreciation and gratitude for my dissertation advisor, Dr. Donald Vander Griend, especially for his tireless cheerleading. I am also grateful for the feedback and advice of my co-PI, Russell Szmulewitz.

To George and Linda Plopper, thank you for your mentorship and friendship as I've navigated academia.

I'd also like to acknowledge past lab mates that I have had the good fortune of working with, including Le Shen, Chris Weber, Mary Buschmann, Karen Edelblum, Sheng-Ru Shiou, Yitang Wang, and Jack Kach. To Isabel Romero-Calvo, my lifelong buddy, I am grateful for your friendship and strength over the years.

I would like to thank current members of the Vander Griend and Szmulewitz labs that I have also had the privilege of working with. Thank you to Hannah Brechka for your sunny disposition. To Marc Gillard, my French homie and nook-mate, your optimism and energy were truly appreciated. Thank you to Tiha Long for your advice and friendship. To Ryan Brown, I thank you for your enthusiasm for science. To Lari de Wet, thank you for making the lab a joy to work in. Thank you to Phillip Selman, for all that you do to ensure the lab operates smoothly. To Anthony Williams, thank you for teaching me how to become a better communicator. An enormous thank you to and Raj Bhanvadia, Calvin VanOpstall, and Dan Moline for your scientific expertise and comradery, you are long-haul friends. An extra thanks to Dan and Sophia Lamperis, for continuing to develop this project and shape it into your own.

I am grateful for the support given to me by the members of my thesis committee: Dr. Deb Lang, Dr. Victoria Prince, Dr. Xiaoyang Wu, and Dr. Mark Lingen. I am particularly

indebted to Deb and Vicky, who put a lot of thought and energy into thinking about what was best for me.

I am thankful for the expertise and support given by several core facilities, including the Human Tissue Resource Center, Integrated Light Microscopy Core Facility, Animal Resource Center, Integrated Animal Imaging Core, and the Institutional Animal Care and Use Committee. I thank the Biomedical Sciences Cluster Office as well as the Office of Graduate and Postdoctoral Affairs for administrative support. Additionally, I am grateful for the UChicagoGRAD and myCHOICE programs and their staff. I would also like to thank my program support, including Steve Meredith and Ben Glick.

I am so thankful for all of the book clubs, wine and cheese clubs, potlucks and game nights I've experienced with my graduate school friends and their partners. Thank you for your commiseration and friendship: Hannah and Patrick Brechka, Anna Dembo and Daniel Medina, Ryan Ohr and Leidy Gutierrez, Scott Biering and Brittany Nelson, Andrew and Hallie Kirkley, and Andrew Belcher.

An eternal thanks to my parents, John and Donna, for encouraging my love of reading and learning, and always providing me the means to pursue extra educational opportunities. And to my brothers, Frank and John, for their love and support.

Finally, I wish to express my gratitude to my best friend and wonderful husband, Ryan, whose friendship and love have made all the difference.

ABBREVIATIONS

AP (Anterior Prostate); AR (Androgen Receptor); BMI1 (B cell-specific Moloney murine leukemia virus integration site 1); BPH (Benign Prostatic Hyperplasia); BOO (Bladder Outlet Obstruction); CARBs (Castration-Resistant Bmi1-expressing cells); CARNs (Castration-Resistant Nkx3.1-expressing cells); CCO (Cytochrome C Oxidase); CD (Cluster of Differentiation); ChIP (Chromatin Immunoprecipitation); CK (Cytokeratin); c-MYC (v-myc avian myelocytomatosis viral oncogene homolog); CZ (Central Zone); DBD (DNA-binding domains); DLP (Dorsolateral Prostate); DWI (Diffusion-weighted Imaging); DCE (Dynamic Contrast-enhanced); DT (Diphtheria Toxin); DTR (Diphtheria Toxin Receptor); ERα (Estrogen Receptor alpha); ESC (Embryonic Stem Cell); EYFP (Enhanced Yellow Fluorescent Protein); FFPE (Formalin-Fixed, Paraffin Embedded); FOV (Field-of-view); GAPDH (glyceraldehyde-3-phosphate dehydrogenase); GFP (Green Fluorescent Protein); GR (Glucocorticoid Receptor); IFN-γ (Interferon Gamma); IL (Interleukin); iPSCs (induced Pluripotent Stem Cells); Klf4 (Kruppel-like factor 4); IACUC (Institutional Animal Care and Use Committee); ICM (Inner Cell Mass); IRB (Institutional Review Board); LUTS (Lower Urinary Tract Symptoms); MDM2 (Mouse double minute 2 homolog); MRI (Magnetic Resonance Imaging); NE (Neuroendocrine); NPC (Neural Progenitor Cells); OCT (Optimal Cutting Temperature); PrEC (Prostate Epithelial Cell); Pax2 (Paired box protein-2); PCR (Polymerase Chain Reaction); (Prostate Epithelial Cell); PZ (Peripheral Zone); Q-RT-PCR (Quantitative Reverse Transcription PCR); RNA-seq (Ribonucleic Acid Sequencing); SCC (Squamous Cell Carcinoma); Sox2 [SRY (sex determining region Y)-box 2]; SV (Seminal Vesicle); T (Testosterone); TE (Trophectoderm); T+E (Testosterone + Estrogen); TGF-α (Transforming Growth Factor-alpha); TGF-β (Transforming Growth Factor-beta); TOF (Time-of-flight); TSCs (Trophoblast Stem Cells); TSS

(Transcriptional Start Site); TUNEL (Terminal deoxynucleotidyl transferase (TdT) dUTP Nick-End Labeling); TZ (Transition Zone); UGS (Urogenital Sinus); UGSE (Urogenital Sinus Epithelium); UGSM (Urogenital Sinus Mesenchyme); VP (Ventral Prostate)

CHAPTER I

INTRODUCTION

BACKGROUND AND SIGNIFICANCE

Adult stem cells: characteristics and function

Epithelia are tightly linked cells that line inner (e.g., digestive and respiratory tracts) and outer (e.g., epidermis) surfaces of the body in continuous sheets. Epithelial cells perform the crucial protective function of separating internal tissue from external environments and in doing so are subjected to chronic insults and injury. Subsequently, most epithelial tissues need to constantly replace damaged or dead cells throughout the life of the animal. This process of continual cell replacement is called tissue homeostasis and is critical for the maintenance of adult tissues (Slack, 2000; Moore and Lemischka, 2006; Blanpain et al., 2007; Li and Clevers, 2010; Varga and Greten, 2017). In some tissues, homeostasis is orchestrated via stochastic replication of existing cells. In other tissues, particularly those with a greater demand for regenerative capacity (e.g., skin, intestine, and blood), adult stem cells represent the major source of new tissue-specific cells.

In many tissues, epithelial homeostasis is achieved via tissue-specific adult stem cells, capable of self-renewal and potency, in which they can give rise to multiple cell lineages to repopulate the tissue (Hall and Watt, 1989; Potten and Loeffler, 1990). Traditionally, epithelial stem cells are thought to exist at the top of a defined hierarchy. As a cell progresses through this hierarchy, it becomes more differentiated and less plastic, and is assumed to have lost properties

of stem identity. Typically stem cells undergo asymmetric cell division, in which each division gives rise to an undifferentiated copy of the stem cell and a more differentiated daughter cell. This transit-amplifying cell can undergo several more divisions, yielding the function-performing and terminally differentiated cells of the tissue. The transit-amplifying cell ultimately undergoes differentiation.

It should be noted that the first ground-breaking experiments done to begin to understand general stem cell biology utilized the hematopoietic system. These experiments produced a model in which a multipotent, self-renewing hematopoietic stem cell sat atop a well-defined hierarchy and could generate terminally differentiated cells of the blood by sequential differentiation. This progressive differentiation process was thought to be hierarchical, unidirectional and importantly, prototypical of other adult tissues.

Recently, however, accumulating evidence has highlighted other methods by which adult, tissue-specific stem cells can support developmental and homeostatic processes in specialized tissues (Varga and Greten, 2017). Indeed, multiple cell populations or types in many epithelial organs have been identified as multipotent progenitors, especially in models of tissue injury. In addition to the idea of dormant or facultative stem cells, recent studies have highlighted dedifferentiation in cells previously thought to be quiescent and terminally differentiated. These cells can transiently acquire stem-like properties, including multipotency (Rompolas et al., 2013; Tata et al., 2013; Rios et al., 2014; Tetteh et al., 2015; Kopp et al., 2016; Tetteh et al., 2016). Therefore, it is crucial to keep challenging previously established paradigms of adult stem cell biology and cellular phenotype.

Indeed, emerging evidence indicates that a hierarchical framework is not always representative of adult stem cells and that varying mechanisms of cell plasticity can exist in different tissues (Varga and Greten, 2017). Multiple models of plasticity have been reported, including cellular dedifferentiation (reversing its hierarchical progression) and transdifferentiation, a direct conversion of one cell type to another, without entering a more plastic intermediate (summarized in **Figure 1.1**) (Cieślar-Pobuda et al., 2017; Firas and Polo, 2017). These processes can be achieved by expression of so-called master regulators, expression of which are often sufficient to push committed cells of one lineage to adopt a completely different lineage (Chan and Kyba, 2013). Examples include transcription factors MyoD and SCL, expression of which can drive non-mesoderm cells to acquire a myogenic phenotype, and non-hematopoietic cells to behave as hematopoietic precursors, respectively (Chan and Kyba, 2013).

In light of these data, it is critical to understand that the processes of tissue homeostasis and repair may not be supported by the same population of stem cells. Indeed, several of the previously-mentioned mechanisms may be used to regenerate the tissue, depending on several parameters. Particularly in the case of tissue repair, the nature of the injury can also serve as a determinant for which recovery mechanism is initiated in the tissue. Seminal research in the liver and pancreas has highlighted the ability of a subset of differentiated cells to adopt "stem-like" capabilities in response to tissue injury, termed facultative stem cells (Zipori, 2004). Essentially, these quiescent cells can achieve the function of stem cells and potentially recapitulate their characteristics, in response to a defined stimulus. Interestingly, this paradigm was first suspected and subsequently established in amphibians (Brockes, 1997).

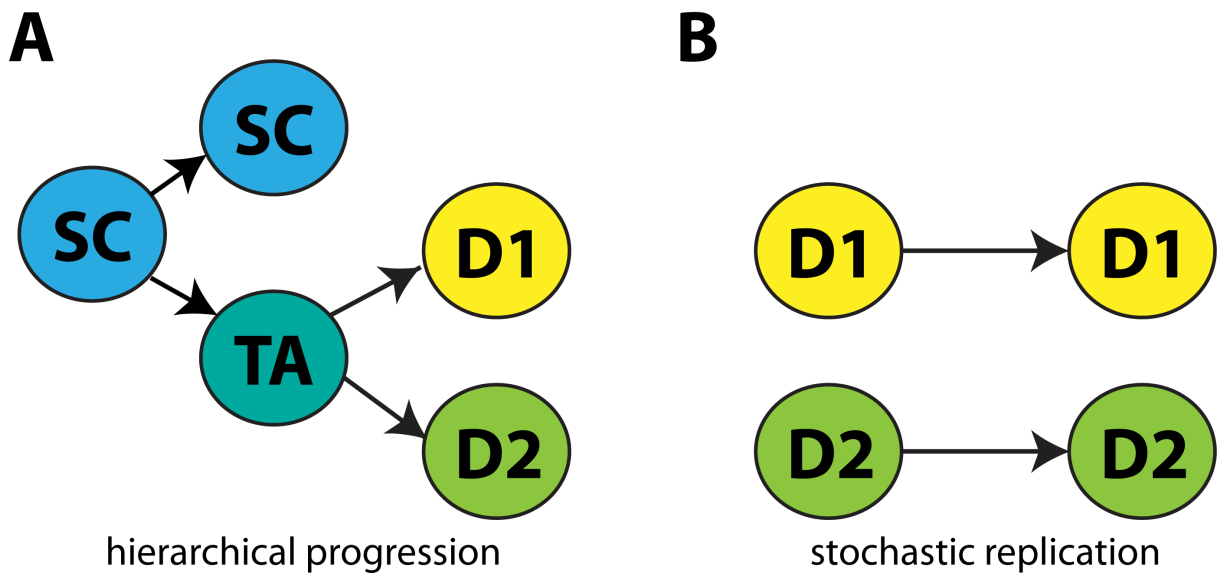

Figure 1.1: Mechanisms used for maintaining homeostasis and in various adult mammalian tissues. A: A prototypical mechanism for tissue regeneration involves a hierarchical progression from a pool of undifferentiated stem cells (SC, shown in blue) toward tissue-specific and differentiated lineages (D1 and D2, shown in yellow and green respectively). Often this process goes through an intermediate compartment, the transit-amplifying pool (TA, shown in teal). Representative examples of tissues supported by resident stem cells include the intestine, skin, and blood. **B**: Another model of tissue homeostasis depends on stochastic replication of differentiated cells. Representative examples of tissues supported by this method of homeostasis include bone, kidney, and cartilage.

Epithelial adult stem cells are largely considered to be developmentally committed, in that their division yields more of the differentiated cells of their resident tissue type, but not cells of any other type (Slack, 2000). This restricted capability is usually referred to as uni- (one lineage), bi- (two lineages) or multi-, sometimes oligo-, potency (several tissue-specific lineages). This is in contrast to pluripotent embryonic stem cells, which can yield each of the three embryonic germ layers: endoderm, mesoderm, and ectoderm. Often, adult stem cells are thought to lack putative markers of differentiation, and traditionally were thought of as quiescent or slow-cycling. Interestingly, it has been shown in several tissues that both quiescent (non-dividing) and active stem cell subpopulations exist, and they can reside in spatially separate, sometimes adjoining, locations (Li and Clevers, 2010).

Epithelial stem cell maintenance, activation, and differentiation are commonly controlled by both intrinsic and extrinsic mechanisms (Blanpain et al., 2007). A primary extrinsic mechanism is the interaction with the surrounding microenvironment, termed the stem cell niche. It is thought that the niche cells actively protect neighboring stem cells from harmful stimuli that can cause differentiation (resulting in a loss of self-renewal and potency properties), apoptosis, or otherwise depletion of stem cell reserves (Moore and Lemischka, 2006). Additionally, niche signaling represents one mechanism by which asymmetric cell division can be regulated: mitotic spindle orientation of the stem cell can predispose the daughter cell closer to the niche to remain undifferentiated, whereas the other daughter cell, located outside the niche, undergoes a terminally differentiation event (Knoblich, 2008; Yamashita et al., 2010). Well-characterized stem cell niches include the bone marrow for hematopoietic progenitors, the hair follicle for epidermal progenitors, and the intestinal crypt.

Intrinsic mechanisms of adult epithelial stem cell biology often include cell type-specific transcription factors and their interplay with specific chromatin regulators. In the following section I discuss the transcription factor Sox2 (SRY [sex determining region Y]-box 2) as one such intrinsic regulator.

Sox2 as a regulator of adult stem cell plasticity

Recently, Sox2 has been reported as a marker and driver of stemness in adult tissues. Sox2 has been shown to mark potentially long-lived populations in the testes, forestomach, glandular stomach, anus, cervix, esophagus, lens, as well as the trachea and cervix (Arnold et al., 2011). Additionally, genetic lineage tracing experiments have demonstrated that Sox2+ cells derive all lineages of the murine dental incisor as well as taste buds (Juuri et al., 2012; Martin et al., 2016; Ohmoto et al., 2017). Interestingly, the expression pattern of Sox2 overlaps with Lgr5,

a putative stem cell marker in other epithelia (Barker et al., 2007; oz et al., 2012; Wang et al., 2015), in these tissues. Sox2 deletion also results in a decrease in Lgr5 expression (Ohmoto et al., 2017; Sanz-Navarro et al., 2017).

Surprisingly, Sox2-expressing stem cells do not appear to be required for tissue homeostasis in all organs investigated. Indeed, Sox2 expression appears to be dispensable for gastric stem cell and epithelial self-renewal (Sarkar et al., 2016). Additionally, Sox2-expressing stem cells in the pituitary gland also appear to be dispensable for tissue homeostasis or remodeling (Roose et al., 2017). These data suggest that Sox2+ stem cells in these organs may constitute a specialized stem cell reserve, or may have other as-of-yet unknown critical roles. These two studies did not formally investigate potential compensatory mechanisms by other proteins, or alternative stem cell populations. In a particularly plastic tissue such as the dental incisor, deletion of Sox2 specifically in putative Sox2+ stem cells resulted in *de novo* upregulation of Sox2 in another cell population (Sanz-Navarro et al., 2017). This compensatory upregulation of Sox2 in stellate reticulum cells restored morphogenetic defects in the labial cervical loop caused as a result of Sox2 deletion. These findings highlight potential heterogeneity and plasticity in a Sox2-expressing cell population: expression of Sox2 may be transient and occur in multiple cell types that are not statically maintained.

In addition to promoting tissue homeostasis, Sox2 and Sox2+ cell populations can be involved in tissue repair. In general, tissue injury or aging has been shown to induce *in vivo* reprogramming by Sox2, in conjunction with other pluripotency factors, indicating that this expansion of plasticity is a required step for tissue repair (Mosteiro et al., 2016). For example, in a mouse model of neuronal injury, upregulation of Sox2 was coincident with enhanced progenitor cell capacity, which was blocked upon Sox2 deletion (Lin et al., 2017). However, the

Sox2+ population has also specifically been shown to contribute to downstream processes involved in tissue repair. In a chemically-induced model of tracheal epithelium damage, Sox2-deficient tracheal cells failed to undergo efficient tissue repair and recover wildtype levels of basal, ciliated and Clara cell populations in a comparable time course to wildtype animals (Que et al., 2009).

Remarkably, forced expression of Sox2, in combination with Oct4, Klf4, and c-Myc, can confer pluripotency onto somatic fibroblast cells, yielding induced pluripotent stem cells (iPSCs) (Takahashi and Yamanaka, 2006). Importantly, forced overexpression of Sox2 alone, in combination with specific culture conditions, can drive the reprogramming of both mouse and human fibroblasts to robust cultures of inducible neural progenitor cells. These cultures are reported to be expandable, multipotent and capable of engraftment, in that they do not form tumors (Ring et al., 2012). These findings underscore the wide-reaching consequences that Sox factor signaling has on differentiated cells, namely endowment of plasticity.

Multiple studies have linked Sox2 expression and the Sox2-expressing lineage to tumor initiation processes in multiple tissues. Importantly, Sox2 is often expressed heterogeneously throughout the cells of many tumor types. In a mouse model of skin squamous-cell carcinoma (SCC), lineage ablation of SOX2-expressing cells resulted in significant tumor regression. Sox2 deletion in pre-existing skin papilloma and SCC resulted in tumor regression as well as a marked decrease in ability of cancer cells to be propagated upon transplantation into immunodeficient mice (Boumahdi et al., 2014; Siegle et al., 2014). Taken together, these data highlight a critical role of SOX2 as a driver of cancer malignancy and stemness, as well as a contribution of SOX2-expressing cells to tumor maintenance. Indeed, in a mouse model of medulloblastoma, rare and quiescent Sox2+ cells were shown to be responsible for tumor initiation and propagation.

Following chemotherapy, Sox2+ cells were observed to be enriched via genetic lineage trace, suggesting that these Sox2-expressing cells are resistant to therapy and contribute to cancer relapse (Vanner et al., 2014). Notably, a detailed correlation of Sox2 expression to human patient prognosis and tumor phenotype in more than twenty cancers has recently been published (Wuebben and Rizzino, 2017).

Given the relationship between Sox2 and adult stem cells in other tissues, Sox2 has begun to be studied in the malignant prostate epithelium. Our group has previously shown that forced overexpression of Sox2 can promote castration-resistant tumor growth (Kregel et al., 2013). Additionally, we and others have also shown that silencing of Sox2 results in significant growth suppression of prostate cancer cells (Kregel et al., 2013; Kar et al., 2017). Taken together these data highlight a potential role of Sox2 to drive pro-survival and proliferative signaling in prostate cancer. More recently, using a novel mouse model of aggressive prostate cancer, it was hypothesized that tumor cells acquire lineage plasticity via upregulation of Sox2 as a driving mechanism to escape luminal cell-specific frontline drug therapies that target the androgen receptor (Ku et al., 2017; Mu et al., 2017). Functional consequences of Sox2 expression throughout the natural history of prostate cancer, as well as a result of different treatments, remain incompletely understood.

Sox2 as a regulator of embryonic stem cell pluripotency

Stem cells, characterized by a specialized capacity to self-renew and potential to differentiate into multiple cellular lineages, are of great interest in regenerative biology. While embryonic and adult stem cells are capable of both of these criteria, there is a significant restriction in plasticity between the two. Embryonic stem cells (ESCs) are pluripotent, giving rise to all embryonic lineages (endoderm, mesoderm, and ectoderm). ESCs are derived from the inner

cell mass (ICM) of the developing blastocyst, an early-stage pre-implantation embryo. In contrast, somatic or adult stem cells are found in developed organs and give rise to one or more committed lineages. Notably, adult stem cell lineages are restricted to the specialized cells of the tissues they reside in. The cell fate decision between self-renewal or differentiation is a complicated dance, orchestrated by transcription factors that control expression of downstream actors, as well as chromatin remodelers that can allow or prohibit access of some parts of the genome. While some of these actors and remodelers have been identified, the underpinning mechanisms by which they act remain incompletely understood.

The very first lineage specification decision in the mammalian embryo occurs upon the formation of the trophectoderm (TE) and inner cell mass (ICM) within the blastocyst (Marikawa and Alarcón, 2009; Rossant and Tam, 2009; 2017). Lineage tracing in the mouse has demonstrated that cells of the ICM can yield all embryonic tissues as well as components of the extraembryonic yolk sac, whereas the TE derives placental lineages (Marikawa and Alarcón, 2009). Several essential transcription factors coordinate the correct generation of the TE and ICM in mouse blastocyst development. Lineage specification and cell fate restriction occur upon expression of unique and early markers, including Cdx2 in the TE and Sox2 in the ICM (Avilion et al., 2003; Wicklow et al., 2014; Rossant and Tam, 2017). Sox2 is initially expressed in both the TE and ICM (Avilion et al., 2003) and is required for the segregation of both lineages (Keramari et al., 2010). Sox2 expression then becomes restricted to ICM progenitors during blastocyst formation by activation of Hippo signaling (Wicklow et al., 2014). This process appears to occur independently of Cdx2, which represses expression of two other canonical pluripotency factors, Oct4 and Nanog, in the TE (Wicklow et al., 2014).

In ESCs, Sox2 appears to be required for maintenance of pluripotency by regulating the expression of Oct4 and Nanog as well as other downstream genes (Boyer et al., 2005). In both human and mouse ESCs, chromatin-immunoprecipitation experiments demonstrated that Oct4 and Sox2 regulate target genes synergistically through joint Oct-Sox enhancers (Boyer et al., 2005). These target genes include transcription factors that can regulate their own downstream genes, some of which are involved in cell cycle progression, differentiation, and chromatin remodeling. Importantly, Oct4, Sox2, and Nanog can cooperate in auto-regulatory and feedforward signaling loops to tune their own expression (Boyer et al., 2005). Feedforward loop networks are especially useful and specialized in the case of ESCs, as this setup enables consistent activity that is largely insensitive to transient changes in input. Indeed, overexpression of Oct4 appears to partially compensate for the loss of Sox2 (Masui et al., 2007). Additionally, Sox2 expression leads to functional repression of TE-related genes through its upregulation of Oct4 (Nichols et al., 1998; Niwa et al., 2005; Le Bin et al., 2014; Wicklow et al., 2014; Frum and Ralston, 2015). Interestingly, while Sox2 is required for regulation of target genes responsible for Oct4 expression, it is dispensable for Oct-Sox enhancer activation in mouse ES cells (Masui et al., 2007). Taken together these data suggest that the critical function of Sox2 is to stabilize ESCs in a pluripotent state by maintaining levels of Oct4 expression.

Notably, Sox2-deficient embryos fail to derive ESCs from the ICM as well as trophoblast stem cells (TSCs) from the TE (Avilion et al., 2003). Furthermore, deletion of *Sox2* in already established ESCs results in their inappropriate differentiation into TE-like cells (Masui et al., 2007). Taken together these data indicate that Sox2 is critical for the maintenance of ESCs. However, perhaps paradoxically, overexpression of Sox2 in ESCs results in downregulation of the gene, in addition to other well-known target genes of Oct-Sox enhancers, including Nanog

(Boer et al., 2007). Furthermore, small increases in Sox2 expression in ESCs triggers differentiation into a wide range of cell types, including neuroectoderm, mesoderm, and trophectoderm. Interestingly, endoderm tissue is not produced (Kopp et al., 2008). These data strongly highlight that it is the levels of Sox2 expression that are critical for ESC pluripotency – expression of Sox2 needs to be tightly maintained within a narrow range in order to influence cell fate decisions (Kopp et al., 2008).

Upon the conclusion of gastrulation and subsequent exit from pluripotency, Sox2 signaling persists in tissues from all three germ layers during fetal development (Sarkar and Hochedlinger, 2013). Notably, Sox2 appears to be critical for formation and function of the nervous system (Zappone et al., 2000; Avilion et al., 2003; Graham et al., 2003; Ellis et al., 2004). Sox2 expression is noted in the embryonic nervous system from the earliest stage of its development, and is chiefly found to be enriched in actively proliferating, undifferentiated neural precursor cells (NPCs). Strikingly, these results are conserved between multiple model organisms, including chicken, mouse, and human embryos. Related proteins are also observed in *Drosophila Melanogaster* to achieve similar functions (Pevny and Nicolis, 2010).

Briefly, division of NPCs generates daughter cells that undergo further differentiation into specialized cell types, including glial cells (e.g., astrocytes, oligodendrocytes) and a wide range of phenotypically distinct, post-mitotic neurons. During neurogenesis, progenitor cells exit the cell cycle, migrate toward the marginal zone and begin to express neuronal-specific markers (Bylund et al., 2003). In seminal chick embryo studies, Sox2, in concert with Sox1 and Sox3, was shown to suppress neuronal differentiation and maintain NPCs in an undifferentiated state. Conversely, overexpression of any of these factors induces progenitor cell proliferation (Bylund et al., 2003; Graham et al., 2003). These studies were corroborated in additional

experiments using neonatal and adult mouse brains (Ferri, 2004; Cavallaro et al., 2008). Additionally, fate-mapping experiments in the murine brain revealed that Sox2+ cells in the subgranular zone are multipotent, giving rise to neurons and astrocytes, and can respond to mitotic signals with increased proliferation, indicating an active role in both neonatal and adult neurogenesis (Suh et al., 2007). Part of the mechanism by which Sox2 controls neuronal differentiation of NPCs may be through competition with repressive epigenetic modulators (Amador-Arjona et al., 2015).

Given that true *Sox2* deficiency is embryonic lethal early in post-implantation (Avilion et al., 2003), studies of its function in fetal development have largely focused on partial loss-of-function (e.g., hypomorphic or conditional) mutants. Neural-specific compound hypomorphic mutants (which retained only 25-30% activity of Sox2 as compared to wildtypes) showed significant defects in brain morphology with a host of motor and neurological deficiencies (Ferri, 2004; Cavallaro et al., 2008). NPCs from these mice produced remarkably fewer numbers of mature neurons with altered morphology, but generated normal glial cells (Cavallaro et al., 2008). A deficiency in the number of GABAergic neurons, often involved in epilepsy, was also observed. In humans, heterozygous Sox2 deficiency is associated with eye abnormalities (micro- or anophthalmia), malformation of the hippocampus, and epilepsy (Fantes et al., 2003).

Strikingly, these data highlight major defects in neuronal differentiation with relatively unaltered self-renewal capabilities as a result of altered Sox2 expression. Interestingly, Sox2 overexpression in murine neural cells at early, but not late, stages of differentiation, rescued the neuronal maturation defect (Cavallaro et al., 2008). Taken together, these data suggest that Sox2 is not only crucial for self-renewal of NPCs but also for differentiation of subsets of neurons (Cavallaro et al., 2008). Furthermore, the function of Sox2 is not always limited to the

maintenance of stem or progenitor cells.

Sox2 signaling has been found to be crucial for the embryonic formation and postnatal development of the anterior foregut endoderm and its derivatives, including the trachea, lung, tongue, esophagus, stomach, as well as the anus and cervix (Que et al., 2007; Okubo et al., 2009b). Furthermore, Sox2 has also been shown to be critical for development and persist into adult cell populations of the inner ear (Gálvez et al., 2017; Steevens et al., 2017), the retina (Taranova et al., 2006), and the skin (Lesko et al., 2013).

It is important to understand underpinning mechanisms by which Sox2, and related Sox family proteins, achieve a multifunctional role as critical regulator of multiple and distinct lineages and stem cell states. As transcription factors, the chief responsibility of Sox family proteins involves binding to sequence-specific DNA to orchestrate selective gene expression. DNA binding specificity is bestowed on Sox family proteins through the High Mobility Group (HMG) domain, which recognize 6-7 base pair DNA sequences. This domain was first identified in Sry (sex determining region Y), a crucial factor involved in mammalian male sex determination, and is a defining characteristic of the Sox family: proteins containing this domain with higher than 50% amino acid similarity to the HMG domain of Sry are referred to as Sox proteins (Sry-related HMG box) (Gubbay et al., 1990). In contrast to most DNA-binding domains, HMG domains are unique in that they can interact with the minor groove of the DNA helix, and induce a marked bend in the DNA (Ferrari et al., 1992; Grosschedl et al., 1994; Wegner, 2010). The HMG box, typically contained between the N- and C- terminal domains, also contains nuclear localization signals that allow Sox family proteins to shuttle to the cell nucleus (Zhao and Koopman, 2012).

Despite scant conservation of components outside the HMG box, most Sox family proteins also harbor a transactivation or transrepression domain, enabling them to act as typical transcription factors. Based on HMG box sequence similarity (greater than 80%), Sox family proteins are catalogued into subgroups, whose members are expected to share biochemical properties and thus, overlapping function (Wegner, 2010). Despite global similarities in composition and protein structure, it may be these smaller, specific differences that allow for a wide range of Sox family function. Indeed, in the case of Sox2, a member of the SoxB1 subgroup, Sox1 and Sox3 have been shown to either achieve a similar function alongside Sox2 (Bylund et al., 2003; Adikusuma et al., 2017) or at least partially compensate for loss of function of Sox2 in a given context (Corsinotti et al., 2017).

SoxB1 proteins were first identified in two independent reports. First, in ESCs, Sox2 was identified as the binding partner of Oct4 at the FGF4 gene, which is essential for limb patterning and development (Yuan et al., 1995). Strikingly, neither Sox2 or Oct4 in isolation could initiate transcriptional activation –synergistic action of both proteins was required. The second report identified Sox2 as a regulator of crystalline genes, differentiation factors specific to the lens epithelium (Kamachi et al., 1995). In a follow-up study it was revealed that activation of these crystalline-gene enhancers required the presence of Pax6 at a flanking sequence (Kamachi et al., 2001). These results highlight a common theme: specification of gene expression is achieved through a particular Sox factor in conjunction with a partner factor (Kondoh and Kamachi, 2010). Partner factor binding is largely determined by flanking DNA sequences, adjacent to the Sox binding site, and the availability of the partner factor in the cell (Kamachi et al., 2000; Kamachi and Kondoh, 2013).

It should be noted that some reports have highlighted the ability of Sox2 to act as a pioneer factor: to access closed chromatin, independent of presence of other binding factors (Soufi et al., 2012; Soufi and Zaret, 2013; Soufi et al., 2015). These data do not necessarily undermine and are not mutually exclusive with the Sox-partner code, especially as this debate continues in the field (Iwafuchi-Doi et al., 2016; Zaret et al., 2016). Specifically, Sox2 has been shown to bind its canonical motifs, either partial or degenerate, in nucleosome-free and nucleosome-bound loci (Soufi et al., 2012). While some pioneer factors derive their chromatin-opening capability from their structural similarity to linker histones, this does not appear to be the whole case with Sox2 (Hou et al., 2016). Sox2 binding to nucleosomes is a combination of sequence-specific and non-specific interactions, which can be efficiently competed by non-specific DNA (Soufi et al., 2015). Although it seems to be sufficient to access closed chromatin (and thus fulfilling pioneer factor criteria), Sox2 appears to probe chromatin in a nonspecific manner for other transcription factors. Indeed, single molecule tracking studies in live ESCs suggest that Sox2 binds first to cognate Oct-Sox enhancers, and subsequently recruits Oct4 (Chen et al., 2014). It is also possible that Sox family proteins can direct transcriptional regulation and reorganize chromatin in parallel. Whether the pioneering ability of Sox2 is sufficient to allow its binding to all closed genomic loci in the absence of other co-factors, and the potential mechanisms of how such binding might occur, remain incompletely understood. More recent reports would suggest that the pioneer activity of Sox2 may be conditional on multiple determinants – key residues in the Sox2 DNA-binding domain, rotational position of the Sox motif in nucleosome, and presence of accessory proteins – and not equivalent at all genomic loci (Liu and Kraus, 2017).

In addition to requisite partner factors, target gene selectivity can also be achieved via posttranslational modifications or dimerization of Sox factors (homo- or hetero-), and recruitment of other co-factors (Wegner, 2010; Sarkar and Hochedlinger, 2013). As mentioned, post-translational modifications of Sox proteins can also regulate DNA-binding activity and capability for transactivation, in addition to protein stability and nuclear localization (Lefebvre et al., 2007; Bernard and Harley, 2010; Malki et al., 2010; Kamachi and Kondoh, 2013). For example, acetylation appears to increase the rate of nuclear export of Sox2 in ESCs. Importantly, increased acetylation leads to increased ubiquitination of Sox2 and subsequent proteasomal degradation (Baltus et al., 2009). Phosphorylation of Sox2 in a serine-rich region of the C-terminus seems to be a prerequisite step for sumoylation of a nearby lysine, which impairs Sox2-DNA binding, thus negatively regulating transcriptional activity (Tsuruzoe et al., 2006; Van Hoof et al., 2009). Interestingly, phosphorylation of the N-terminal part of human Sry has been shown to have the opposite effect, positively regulating transcriptional activity (Desclozeaux et al., 1998). Methylation of Sox2 at Arg113 via CARM1, an arginine methyltransferase, has been shown to promote more Sox2 self-association and facilitate Sox2-mediated transactivation (Zhao et al., 2011). O-linked glycosylation in the C-terminal part of Sox2 is considered a putative hallmark of pluripotency and is lost upon cell differentiation (Jang et al., 2012). All of these examples serve to highlight a common theme: Sox2-mediated signaling can be regulated via post-translational modifications of Sox2 to change its protein stability, degradation rate, subcellular localization, and DNA-binding capability. Notably, these regulatory capabilities may or may not change between differentiated, adult, or embryonic progenitor cells.

Overview of prostatic embryogenesis and development

Given the relationship between Sox2 and embryonic stemness, it is important to

understand the mechanisms of embryonic prostatic morphogenesis, and whether it is involved in this process.

In both humans and mice, the prostate develops from the embryonic urogenital sinus, the endodermal anlagen tissue present at an ambisexual embryonic stage (Marker et al., 2003). Androgen receptor-mediated paracrine signaling from the surrounding urogenital sinus mesenchyme (UGSM) orchestrates the first wave of tissue outgrowth of the urogenital sinus epithelium (UGSE). The UGSE buds out into the UGSM, yielding a system of ducts comprised of solid epithelial cords. These solid cords undergo further canalization to form the ductal lumen, which becomes fully functional upon a proximal-distal wave of cytodifferentiation, to give rise to fully differentiated cell types. Circulating androgens then maintain the process of branching morphogenesis and ductal outgrowth through birth and pre-pubertal stages, until the prostate undergoes a final maturation upon the onset of puberty.

Signaling pathways that drive the processes of prostate epithelial formation, budding, differentiation and branching are similar in rodents and humans (Toivanen and Shen, 2017). Multiple gene families have been documented to participate in prostate development, including common and organ-specific nuclear transcription factors (e.g., homeobox (Hox) and Forkhead box (Fox) genes) as well as several secreted signaling ligands encoded by conserved multigene families including Notch, Hedgehogs, Wnts, FGFs, Bmps and TGF-β (Bhatia-Gaur et al., 1999; Huang et al., 2007; Prins and Putz, 2008; Pritchard and Nelson, 2008; Thomson, 2008; Timms, 2008; Javed and Langley, 2013; Nishan et al., 2015; Okazawa et al., 2015). Interestingly, Sox9 has also been implicated as an essential and early transcription factor in prostate epithelial specification, as knockout results in either absence or defective prostate formation and differentiation (Thomsen et al., 2008; Huang et al., 2012).

Although signaling pathways for prostate patterning are largely conserved, there are species-specific differences in developmental kinetics of these morphogenetic processes. While human prostate epithelial budding occurs relatively early during embryogenesis, rodent budding initiates at late fetal stages. This translates into a difference of interrupted phases of morphogenesis (postnatal, quiescence, pubertal) in humans, as compared to continuous morphogenesis in rodents (postnatal through pre-pubertal) (Cunha et al., 1987).

Following prostatic bud formation, the epithelium undergoes extensive proximal-distal outgrowth and branching morphogenesis. In the rodent, this outgrowth results in an organ comprised of histologically and functionally distinct lobes: the ventral (VP), anterior (AP), and dorsolateral lobes (DLP) (Sugimura et al., 1986). These lobes are located circumferentially around the urethra, the distal ends of which float freely in the pelvic cavity. Additionally, the stromal compartment of the murine prostate is sparse, instead of the more contained anterior fibromuscular region found in the human prostate (Oliveira et al., 2015).

The multi-lobular arrangement of the rodent prostate is in contrast to the human prostate, which is uni-lobular and divided into three distinct glandular regions: the peripheral zone (PZ), a central zone (CZ), a transition zone (TZ), and the aforementioned non-glandular anterior fibromuscular stroma region (McNeal, 1981) (compared in **Figure 1.2**). The PZ surrounds the proximal prostatic urethra, the CZ surrounds the vas deferens and the TZ encircles the distal prostate urethra (Oliveira et al., 2015). Some reports have used gene expression analysis and comparison to posit that the mouse DLP is homologous to the human PZ (Berquin et al., 2005). However, the current consensus in the field is that there is no clear correspondence between mouse prostate lobes and human prostate zones (Shappell et al., 2004; Ittmann et al., 2013; Toivanen and Shen, 2017).

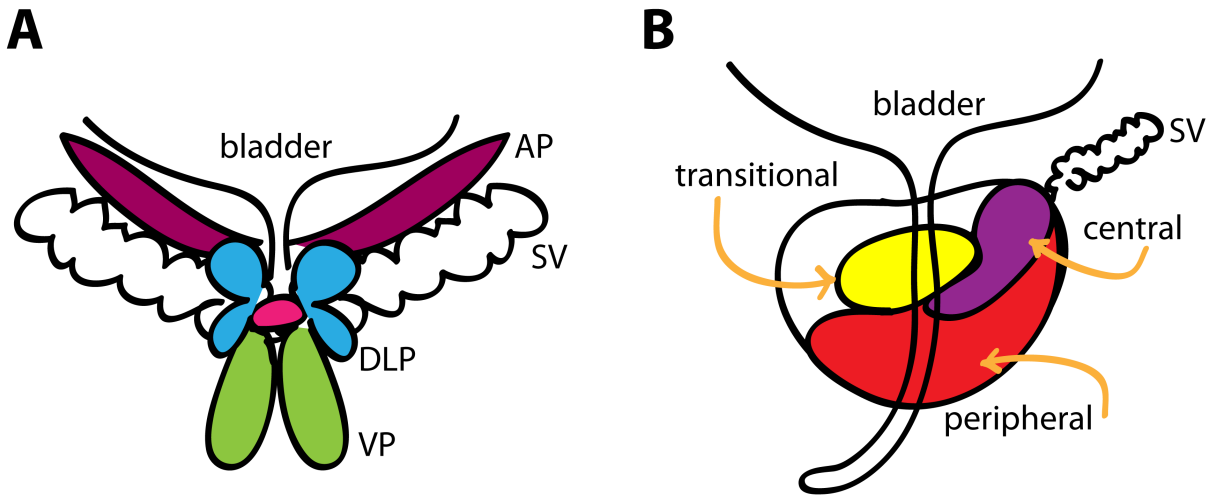

Figure 1.2: Comparison of mouse and human prostate. A: The mouse prostate sits below the bladder and is divided into pairs of lobes arranged circumferentially around the urethra (shown in pink). The anterior prostate (AP, purple), sometimes called the coagulating glands, sit cranially on and are bilaterally attached to the seminal vesicles (SV, uncolored). Despite differences in histology, the dorsal and lateral prostate lobes, usually referred to as one unit (DLP, shown in blue), are located bilaterally at the base of the seminal vesicles. The ventral prostate (VP, green) sits anterior to the urethra and caudal with respect to the bladder. Each of the distal ends of each of the lobes are not anchored to the pelvic floor and thus float freely in the murine pelvic cavity. Each of the proximal ends of the lobes drain into the urethra. It is thought that the proximal prostate, located adjacent to the urethra, houses the prostatic epithelial stem cells in a niche-like configuration. **B:** In contrast, the human prostate is instead organized into zones as determined by distinct histology. The peripheral zone (PZ, shown in red) surrounds the proximal prostatic urethra. The transitional zone (TZ, shown in yellow), surrounds the distal prostate urethra, and is often the site of clinical benign prostatic hyperplasia. Finally, the central zone (CZ, shown in purple) surrounds the vas deferens (not pictured). The human prostate also contains a non-glandular anterior fibro-muscular stromal region (uncolored), in contrast to the sparse arrangement in the murine prostate. Both are represented here in a coronal view. Figure adapted from Peng et al., 2015.

Broadly, the psuedostratified epithelium of both the human and mouse prostate is comprised of three cell types (summarized in Figure 1.3). Terminally differentiated, androgen-dependent luminal cells produce prostatic secretory proteins. Luminal cells are tall and columnar, expressing cytokeratins (CK) 8 and 18, as well as Nkx3.1 and androgen receptor (AR). Non-secretory basal cells express p63, CK5 and CK14 and line the basement membrane (Signoretti et al., 2000; Wang et al., 2001; Xin et al., 2003). The function of basal cells remains incompletely understood (Kurita, 2004). In the developing and adult prostate, rare, intermediate cells expressing both luminal (CK8 and/or CK18) and basal (CK5 and/or CK14) markers are present, although their significance remains unclear (Xue et al., 1998; Hudson et al., 2001; Shen and Abate-Shen, 2010). The third cell type is the rare neuroendocrine (NE) cell, which is thought to produce paracrine factors to regulate the secretory epithelium (Abrahamsson, 1999). The majority of NE cells are thought to derive from the migratory neural crest during embryogenesis and therefore are not suspected to share a common progenitor with the prostate epithelium (Szczyrba et al., 2017).

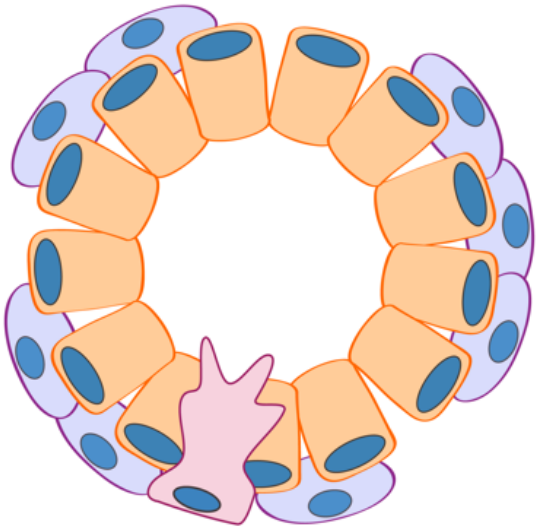

Figure 1.3: Representative arrangement of glandular unit in murine prostate. In the murine and human prostates, the terminally differentiated luminal cells (shown here in orange) line the lumen of the glandular unit. Secretory proteins are secreted into the lumen and drained into the urethra. The luminal cells sit atop a layer of basal cells (shown here in purple). The basal cells contact the basement membrane and receive stromal signals. In the mouse, the basal cell layer is discontinuous, whereas it is continuous in the human. Rare neuroendocrine cells (shown here in pink) are observed throughout the prostate epithelium.

Mouse-based techniques for studying specific cell populations

Genetic lineage tracing is a classic technique with which to answer questions about self-renewal and longevity of a given cell population, two major criteria of stem cells. By bestowing an indelible and permanent markers on a cell population or type of interest, one can monitor cellular dynamics throughout homeostatic tissue turnover as well as cell lineage plasticity in homeostasis, injury or regeneration, and tumorigenesis (Fink et al., 2015; Papaioannou, 2016). One of the most important tools in performing lineage tracing studies in mice is the CreERT2/loxP site-specific recombination system. A tamoxifen-responsive Cre recombinase (CreERT2) is knocked in at an endogenous promoter of interest. A lox-STOP-lox-EYFP group is homozygous expressed at the ROSA26 locus. Upon tamoxifen administration, Cre will act on the loxP sites to recombine out the STOP codon, allowing permanent and inheritable expression of enhanced yellow fluorescent protein (EYFP) in cells that express the gene of interest. In Chapter 2 I describe the use of a tamoxifen-inducible Cre allele that has been knocked into the endogenous Sox2 locus to fate-map Sox2+ cells and resultant progeny during embryonic development as well as adult homeostasis and development.

Upon cellular division, each daughter cell will inherit EYFP. If the cell promoter of interest does indeed mark a stem cell, cellular division will yield an undifferentiated stem cell, theoretically maintaining expression of the gene of interest and EYFP, and a more differentiated daughter cell, which is expected to turn off expression of the gene of interest but retain EYFP expression. Frequency of EYFP+ cells at each time point, especially over longer periods of chase, can indicate longevity and self-renewal of the cell population of interest (depicted in Figure 1.4). Composition of EYFP-labeled cells at each time point can be dissected using immunofluorescence microscopy to examine co-labeling of putative lineage markers with EYFP,

demonstrating potency of the cell type of interest. Ideally, tamoxifen-mediated induction frequency is low enough so that subsequent tracing events have a high chance of originating from a single labeled cell (Fink et al., 2015; Wuidart et al., 2016). Importantly, homeostatic lineage tracing that does not involve any model of injury or repair is contingent upon the rate of epithelial turnover in that tissue.

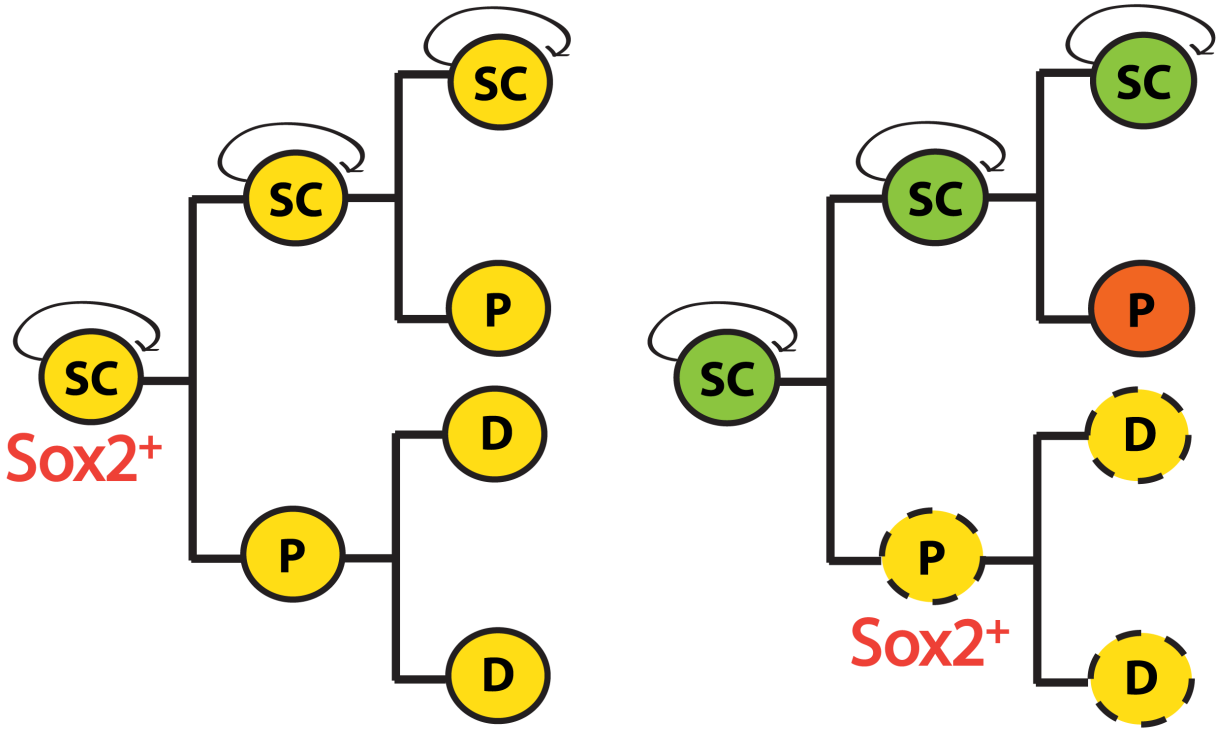

Figure 1.4: Possible outcomes of Sox2 lineage tracing cohorts. If Sox2 labels a stem cell compartment in the prostate (SC, shown in yellow), these progenitors should express EYFP upon tamoxifen administration, thereby giving rise to permanently-labeled YFP+ cells. Cellular division of these YFP+/Sox2+ stem cells may yield a YFP+ transit-amplifying compartment (P, yellow) as well as a YFP+ labeled differentiated cell lineage (D, yellow). In contrast, if Sox2 did not label true stem cells in the prostate, derivative lineages (such as the transit-amplifying or differentiated luminal cells, labeled as P and D respectively) would only be transiently labeled with YFP (indicated by dashed lines). Over longer periods of chase this YFP+ signal would be lost or outcompeted by unlabeled cells. Figure adapted from Arnold et al., 2011.

Notably, gene expression is not necessarily a constant variable -- although a specific gene may mark a given cell population at one time point, it may be subject to change throughout development and homeostasis (Papaioannou, 2016). Indeed, expression of one gene, however transiently, may have little connection with the eventual fate of the resultant progeny. Lineage tracing may interrogate some criteria of progenitor cells, but does not fully examine whether a gene of interest plays a consequential role in the dynamics of cellular differentiation and/or survival.

While the YFP+ cells in the genetic lineage tracing mice at one point derived from a Sox2+ cell, YFP+ expression does not always correlate with endogenous or *de novo* upregulation of Sox2 after tamoxifen labeling. Reporter mice, in which a target gene has been genetically marked for the purpose of monitoring its promoter activity, can help supplement genetic fate-mapping studies. Reporter mice offer the additional functionality where expression of a fluorescent reporter can be tightly coupled to endogenous expression of a target gene, allowing for discrete isolation of cells expressing the target gene. In Chapter 2, I describe the use of Sox2 reporter mice. In these mice, the coding sequences of enhanced green fluorescence protein (eGFP) has replaced the coding sequence of one copy of Sox2. These reporter mice are critical to any flow cytometry studies, as live cells can be isolated based on eGFP expression (whereas cells would need to be fixed and stained to study intracellular Sox2 expression, limiting their use in downstream applications). Both mouse models are summarized in **Figure 1.5**.

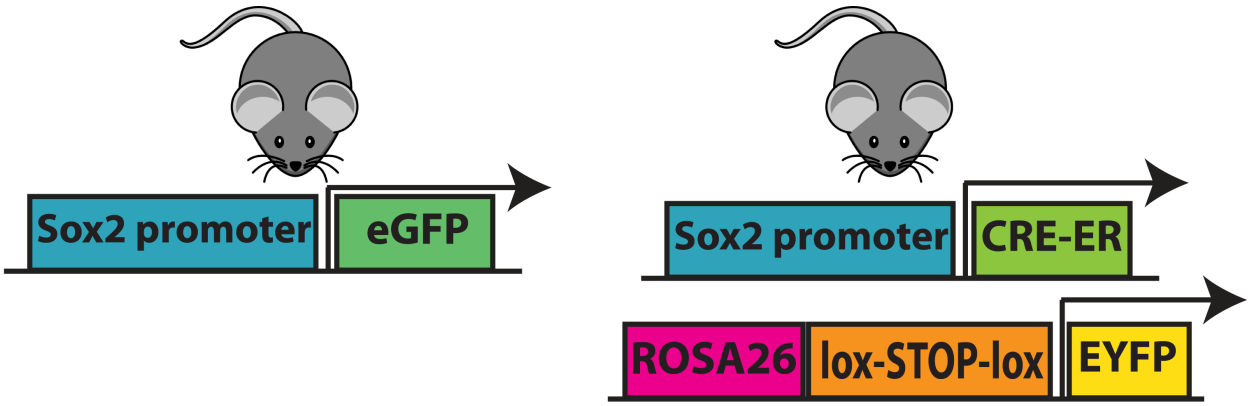

Figure 1.5: Overview of mouse models used to dissect the role of Sox2 in prostate epithelial homeostasis. Importantly, Sox2-eGFP mice can be used to understand *de novo* expression pattern of Sox2 in different prostatic epithelial lineages. In these mice, eGFP expression is a high-fidelity marker of Sox2 activity, as eGFP is knocked into the endogenous promoter of Sox2. In contrast, Sox2CreER;ROSA26-loxSTOPlox-EYFP mice (referred to elsewhere as Sox2-YFP or Sox2-LT mice) are used to fate-map Sox2-expressing cells throughout tissue homeostasis and regeneration. Therefore, YFP expression in these mice does not always correlate to Sox2 expression (but often does at pulse time points).

Progenitor cells in the adult prostate

Although questions still remain about underpinning mechanisms of prostate epithelial cell specification, relationships between the epithelial lineages have recently become clearer. In general, there appears to be plasticity restriction in progenitors, from multipotency during postnatal development to unipotency throughout post-pubescent homeostasis (Wuidart et al., 2016).

Data generated via *in vivo* genetic lineage tracing are often inconsistent with results found in *ex vivo* cell culture and tissue grafting assays of both mouse and human prostate tissue. Historically, *ex vivo* assays have demonstrated that adult basal cells can serve as luminal progenitors, particularly during inflammation and wound repair (Lawson et al., 2007; Goldstein et al., 2008; Wang et al., 2013; Kwon et al., 2014; Höfner et al., 2015; Toivanen et al., 2016). More recently, luminal cells have also been shown to harbor stem properties in these *ex vivo* assays (Karthaus et al., 2014; Chua et al., 2014a; Kwon et al., 2015). It is likely that these assays drive cells to be much more plastic, which is not reflective of post-pubescent prostate tissue. Therefore, lineage tracing methodologies are considered a gold standard approach for monitoring physiologically relevant progenitor populations (Snippert and Clevers, 2011).

In the human prostate, lineage tracing can be achieved by studying distribution and clonality of sporadic mitochondrial DNA mutations such as cytochrome *c* oxidase (CCO) deficiency. Such a method has recently demonstrated that the maintenance of adult human prostate epithelium relies upon multipotent basal stem cells, located in the proximal prostate near the urethra (Moad et al., 2017). These basal stem cells constantly self-renew to yield bipotent basal progenitors, which then migrate out along the proximal-distal axis of ducts. As they migrate along the ductal network, basal progenitors can give rise to luminal cells to support

tissue homeostasis. Although lineage-restricted luminal stem cells were observed, they were largely confined to the proximal prostate, and provided only a minor contribution to prostate epithelial homeostasis. These data argue in favor of an overlapping progenitor pool for both basal and luminal cells in the adult human prostate (Moad et al., 2017). These findings are in stark contrast to lineage tracing data in the adult murine prostate, which favors lineage-restricted progenitors.

During murine prostate development, basal cells appear to serve as multipotent progenitors, as they are able to generate both luminal and neuroendocrine cells (Ousset et al., 2012; Pignon et al., 2013). This postnatal relationship between the basal and the neuroendocrine lineages is a current area of investigation, as recently it was published that the neuroendocrine lineage derives at least in part from the migratory neural crest (Szczyrba et al., 2017). An intermediate, "double-positive" (CK5+/CK8+) cell has also been reported, presumably a transition state from bipotent basal cell to differentiated luminal fate (Xue et al., 1998; Ousset et al., 2012). Basal cells divide either symmetrically (parallel to the basement membrane), generating two daughter cells with a basal cell fate, or asymmetrically (perpendicular to the basement membrane), generating a basal and a luminal daughter cell (Wang et al., 2014a). A molecular determinant of mitotic spindle orientation includes expression of Gata3, deficiency of which causes subsequent mislocalization of polarity regulator PRKCZ and mitotic spindle randomization (Shafer et al., 2017).

As the organ matures, potency of basal cells becomes restricted, and the epithelial lineages are largely considered to be self-sustained by lineage-specific progenitors (Wang et al., 2013). In both homeostasis and regeneration, a small minority of basal cells are capable of bipotency, occasionally yielding luminal cells at similar frequencies (Choi et al., 2012; Wang

et al., 2013). Furthermore, based on sequential double-labeling with thymidine analogs, it is probable that prostatic expansion in homeostasis and regeneration occurs through a generalized self-renewal of epithelial lineages, rather than an intermediate, transit-amplifying compartment (Pignon et al., 2015) (summarized in **Figure 1.6**).

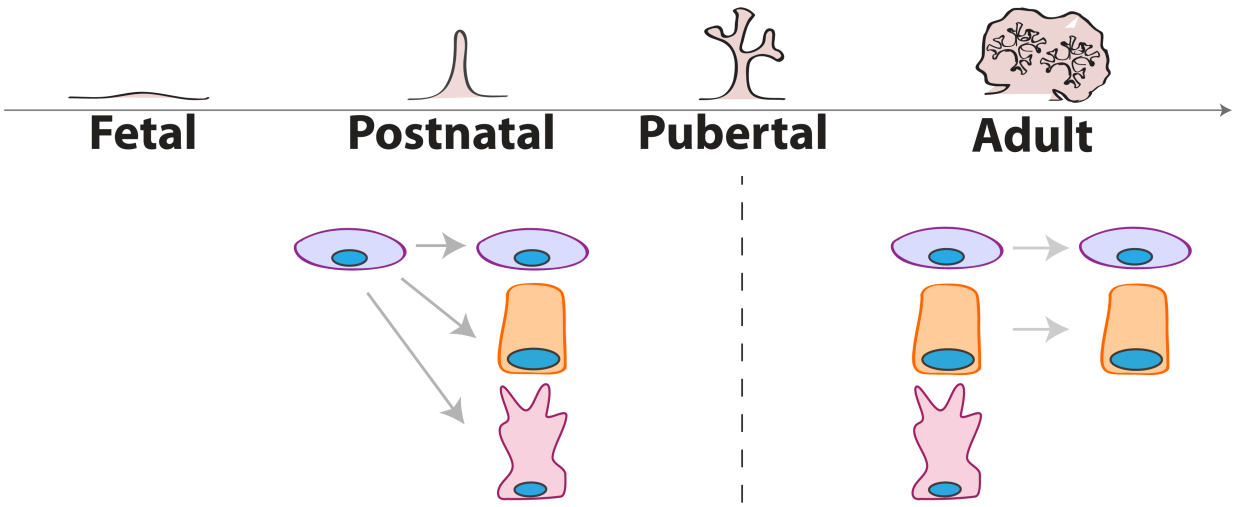

Figure 1.6: Overview of lineage relationships in the prostate epithelium. During postnatal development, it has been shown by multiple groups that the basal cell (shown in purple) serves as a multipotent progenitor cell, deriving both luminal (shown in orange) and neuroendocrine (shown in pink) cells. In contrast, it is believed that both the basal and luminal cell lineages are self-sustained via lineage-specific progenitors in adult prostatic homeostasis. The relationship, if any, to neuroendocrine cells is still mysterious

Host castration results in preferential apoptosis of luminal cells and subsequent tissue involution. Re-administration of testosterone drives luminal cell regeneration and restoration of the prostate to its original size and morphology, a process that can be repeated multiple times in rodents (Tsujimura, 2002). Lineage-tracing studies performed during regression-regeneration cycles using a basal cell-specific driver highlight the existence of rare, bipotent basal stem cells. It was reported that these cells contribute very little to luminal cell regeneration (Wang et al., 2013). Interestingly, these basal cells require expression of androgen receptor to achieve bipotentiality (Xie et al., 2017; Chua et al., 2018). New luminal cells are largely derived from remaining luminal cells that survived androgen deprivation (Liu et al., 2011; Choi et al., 2012).

Multiple lineage tracing studies have revealed the existence of rare, castration-resistant luminal cells (Wang et al., 2009; 2015; Yoo et al., 2016). The prototypical study focused on luminal cells expressing Nkx3.1, a downstream target gene of AR (Sciavolino et al., 1997) and well-known regulator of prostate epithelial differentiation (Bhatia-Gaur et al., 1999). So-called CARNs (castration-resistant Nkx3.1-expressing cells)contribute to prostatic regeneration upon reintroduction of androgen, and were shown to be able to produce both basal and luminal cells during generation (Wang et al., 2009). CARNs also appear to require AR expression to generate viable luminal progeny (Xie et al., 2017; Chua et al., 2018).

A similar lineage tracing study examined the role of Lgr5-positive cells in the adult murine prostate regeneration (Wang et al., 2015). Lgr5 expression marks both basal and luminal cells in an intact murine prostate. During the process of prostatic regeneration, it was observed that Lgr5+ basal cells were bipotent, but the majority of the Lgr5+ luminal cells were unipotent.

Specific depletion of castration-resistant Lgr5-expressing cells resulted in the generation of significantly smaller prostates, demonstrating a requirement for these cells (Wang et al., 2015).

Recently, another lineage tracing study revealed the existence of a non-overlapping population of castration-resistant luminal cells. These cells express Bmi1, a member of polycomb-repressing complex critical for maintenance of chromatin silencing (van Lohuizen et al., 1991; Lukacs et al., 2010; Michiel Sedelaar et al., 2013) and prostatic development (Lukacs et al., 2010; Arnold et al., 2011; Yoo et al., 2016). These castration-resistant Bmi1-expressing cells (so-called CARBs) are capable of self-renewal and contribute to androgen-mediated prostatic regeneration (Wang et al., 2009; Arnold et al., 2011; Yoo et al., 2016). Additionally, both CARBs and CARNs appear to serve as a cell-of-origin in a murine mouse model of prostate cancer that relies on deletion of a tumor suppressor gene, *Pten* (Srinivas et al., 2001; Wang et al., 2009; Pignon et al., 2015; Yoo et al., 2016). As of yet it is unclear whether castration-resistant Bmi1+ or Lgr5+ cells depend on nuclear AR for their survival in androgen-deficient animals.

Importantly, open questions about the biology of prostate homeostasis and regeneration remain unanswered. In the prostate epithelium, Sox2 has not previously been investigated, particularly as a potential marker of progenitor cells. Therefore, in this thesis, I use mouse models to define the role of Sox2+ cells in prostate homeostasis, regeneration, and disease. In chapter 2, I use Sox2+ cell lineage tracing analyses to identify a long-term and castration-resistant bipotent stem cell population marked by Sox2. I also examine potential molecular function of Sox2 in the prostate via chromatin immunoprecipitation studies. I find that Sox2 associates with gene loci that are separate from canonical loci found in embryonic stem cells. In chapter 3, I characterize a novel murine model of prostatic disease, benign prostatic hyperplasia, and probe potential changes in Sox2 expression. Interestingly, despite the dogma that benign

prostatic hyperplasia may result from an “embryonic reawakening” of the prostate epithelium, I documented no changes in Sox2 expression.

Taken together, my studies have begun to elucidate the role that Sox2+ cells play in prostate progenitor cell biology and function. These data will lay the groundwork necessary for new insights into prostate regeneration and tumorigenesis. In addition to filling gaps in knowledge in the field, I expect that my data will lay the groundwork for identification of novel therapeutics that can abrogate prostatic disease. The next steps will include a more formal molecular characterization of how Sox2 expression drives changes in gene expression to maintain potency in prostate epithelial cells. These findings raise additional follow-up questions about the necessity of Sox2 expression and Sox2-expressing cell populations to achieve prostate homeostasis and regeneration.

CHAPTER II

SOX2 EXPRESSION MARKS CASTRATION-RESISTANT PROGENITOR CELLS IN THE ADULT MURINE PROSTATE

Abstract

Despite intensive study, gaps remain in our understanding of prostate epithelial stem cell specification and resulting lineage relationships. Identification of defined epithelial cell populations with progenitor properties is critical for understanding prostatic development and disease. Here we show that the stem cell transcription factor Sox2 marks a population of castration-resistant basal and luminal cells. We utilize lineage tracing to demonstrate that the Sox2 lineage is capable of self-renewal and contributes to prostatic regeneration. Notably, Sox2 is expressed in persisting cells in response to castration. Sox2 ChIP-seq analysis in prostate human epithelial cells demonstrates Sox2 binding and potential regulation of both stem and non-stem cell associated Sox2 targets when compared to human embryonic stem cells. Taken together, these data implicate Sox2 as a marker and potential regulatory factor of the adult progenitor cell compartment in the prostate.

Introduction

Prostate disease, including cancer and benign prostatic hyperplasia, continues to be a significant health challenge. Insight into regulatory mechanisms of epithelial stem cell function in the prostate is essential toward our understanding of epithelium formation, homeostasis, and disease initiation, and a precise understanding of lineage specification of adult prostatic progenitor cells remains controversial. Notably, the intrinsic properties of these progenitor cells, and the critical transcription factors that regulate their behavior, may dictate clinical behaviors of prostatic disease and represent potential therapeutic targets for disease prevention and intervention.

The pseudostratified epithelium of the prostate is comprised of three cell types. Terminally differentiated, androgen-dependent luminal cells produce secretory proteins and are marked by cytokeratin (CK) 8, 18, androgen receptor (AR) (Kasper, 2008; Shen and Abate-Shen, 2010). Basal cells lie adjacent to the basement membrane and are marked by expression of cytokeratin 5, 14, and ΔNp63 (Signoretti et al., 2000). Rare neuroendocrine (NE) cells, thought to influence proliferation of the prostatic epithelium through paracrine signaling, express synaptophysin and/or chromogranin A (Szczyrba et al., 2017).

Morphogenesis and maintenance of the prostate relies upon AR-mediated paracrine signaling from the stroma. In mice, androgen-deprivation via castration causes massive and preferential apoptosis of luminal cells, whereas basal cells are largely unaffected (English et al., 1987). Subsequent prostatic atrophy can be reversed upon androgen replacement (Evans and Chandler, 1987), suggesting that there exists a pool of castration-resistant stem cells which can give rise to AR-dependent, differentiated cells (Tsujimura, 2002). Androgens can be cycled repeatedly, yielding relatively little difference in function, size, and cell composition of each resultant prostate (Isaacs, 1987).

During postnatal prostatic development basal cells appear to serve as multipotent progenitors, as they are able to yield both luminal and neuroendocrine cells (Ousset et al., 2012; Pignon et al., 2013). Controlled by mitotic spindle orientation, basal cells can divide symmetrically (parallel to the basement membrane), generating two basal daughter cells, or asymmetrically (perpendicular to the basement membrane), generating a basal and a luminal daughter cell (Wang et al., 2014a; Shafer et al., 2017). Upon organ maturation, epithelial lineages are largely considered to be self-sustained by lineage-specific progenitors (Wang et al., 2013). In both homeostasis and regeneration, a small minority of basal cells are capable of bipotency, occasionally yielding luminal cells at similar frequencies (Choi et al., 2012; Wang et al., 2013). Interestingly, these rare basal stem cells require expression of androgen receptor to achieve bipotentiality (Xie and Wang, 2017; Xie et al., 2017).

Lineage-tracing studies performed during regression-regeneration cycles using a basal cell-specific driver demonstrated that rare basal stem cells contribute very little to luminal cell regeneration (Wang et al., 2013). In contrast, new luminal cells are largely derived from remaining luminal cells that survive androgen deprivation (Liu et al., 2011; Choi et al., 2012). Multiple lineage tracing studies have revealed the existence of castration-resistant luminal cells competent for prostatic regeneration upon reintroduction of androgen (Wang et al., 2009; 2015; Yoo et al., 2016).

Key regulatory mechanisms of adult stem cell maintenance, particularly in the prostate, remain unclear. Notch and Wnt signaling are two such signaling mechanisms that drive cell fate decisions, including maintenance of stemness, cell survival, and differentiation. Both pathways are exquisitely context-dependent. Mammalian cells typically express some combination of four transmembrane receptors (NOTCH1– NOTCH4), five canonical transmembrane ligands (JAG1

and JAG2, and DLL1, DLL3 and DLL4) and ten classic downstream targets (HES1–HES7, HEY1, HEY2 and HEYL). Notch signaling initiates when a membrane-bound ligand on the sending cell binds to a receptor on the receiving cell. In general, Notch signaling activation is thought to contribute to the differentiation and fate specification processes of prostate progenitor cells(Wang et al., 2006; Valdez et al., 2012; Park et al., 2016). More recent reports have suggested that NOTCH1 specifically seems to be responsible for prostate basal cell commitment, whereas NOTCH3 is required for stepwise prostate luminal cell differentiation (Frank et al., 2017).

Notably, Notch and Wnt pathways share mechanisms of crosstalk in the prostate, but seem to have opposing roles in prostatic progenitor cell populations (Shahi et al., 2011). Canonical Wnt signaling hinges on stabilization and subsequent shuttling of β-catenin (CTNNB1) to the nucleus to activate downstream target genes. Conversely, in the absence of Wnt ligand binding, β-catenin is targeted to degradation, resulting in minimal or no activation of Wnt signaling. A proxy for Wnt signaling activation is Axin2, a scaffolding protein that serves as a negative feedback regulator of Wnt signaling (Jho et al., 2002). Evidence in adult mammary gland and intestinal epithelia suggests that Wnt signaling promotes proliferation of progenitor cells via upregulation of cell cycle-stimulating genes and concomitant downregulation of Notch (Teulière et al., 2005; Roarty and Rosen, 2010; van Amerongen et al., 2012; Horvay and Abud, 2013).

The transcription factor SOX2 (SRY [sex determining region Y]-box 2) is well-known as an stem cell factor that maintains embryonic pluripotency (Boyer et al., 2005; Takahashi and Yamanaka, 2006) and regulates developmental epithelium formation (Arnold et al., 2011). SOX2 has recently been reported as both a marker and driver of stemness in both normal and malignant

adult tissues (Juuri et al., 2012; Boumahdi et al., 2014), marking progenitor populations in multiple tissues (Ellis et al., 2004; Brazel et al., 2005; Kiernan et al., 2005; Taranova et al., 2006; Fauquier et al., 2008; Driskell et al., 2009; Que et al., 2009; Okubo et al., 2009b; Gu et al., 2016; Kempfle et al., 2016; Steevens et al., 2017). Notably, SOX2 was recently reported to promote lineage plasticity and resistance to anti-androgen therapy, a frontline strategy to treat prostate cancer (Kregel et al., 2013; Ku et al., 2017; Mu et al., 2017). We and others reported that a portion of ΔNp63-positive basal epithelial cells also express SOX2 (Kregel et al., 2013).

However, whether SOX2 marks a progenitor cell compartment competent for prostate homeostasis and regeneration in intact tissues *in vivo* has not been examined. In this study, we employ lineage tracing to show that Sox2-expressing cells contribute to homeostatic turnover in the prostate. Notably, Sox2 expression marks a castration-resistant prostate epithelial cell population that is capable of prostate regeneration. Furthermore, Sox2 overexpression seems to drive activation of Wnt signaling and concomitant downregulation of Notch receptors and ligands.

Materials and Methods

Animals

Sox2-CreER; ROSA26-lsl-EYFP mice (Arnold et al., 2011) were recreated from commercially available strains (Sox2-CreER: 017593; R26-lsl-EYFP: 006148) sold by the Jackson Laboratory (Bar Harbor, ME). Sox2-GFP mice (Ellis et al., 2004; Arnold et al., 2011) (JAX strain 017592) were purchased directly from supplier and bred in house. Mice were administered 2mg tamoxifen (Sigma, St Louis, MO) suspended in corn oil by intraperitoneal injection daily for four consecutive days. For *in utero* lineage tracing, a single pulse of 2 mg

tamoxifen with 1 mg progesterone (Sigma) was given to pregnant females at E11.5. All animal care and use was approved by the University of Chicago Institutional Animal Care and Use Committee (IACUC protocol #72294).

Animal Procedures

11-14 week old, post-pubescent C57/BL6 males were castrated as previously described (Kregel et al., 2013). Briefly, animals were first anesthetized using ketamine/xylazine. Following preparation of the surgical site, an incision was made in the scrotum. For each testicle, the testis, vas deferens, and attached testicular fat pad were pulled out of the incision and tied off. The testis, vas deferens, and fatty tissue were severed just below the surgical knot. The scrotal incision was closed with a non-absorbable Nylon suture (Med-Vet; Mettawa, IL). After castration, silastic hormone pellets containing 12.5mg testosterone (Steraloids; Newport RI) were surgically implanted to induce prostatic regeneration as previously described. Implants were used according to Sedelaar et al., whereby a 1cm implant maintains host testosterone levels at 5.3 ± 0.5 ng/mL (18.2 nM) which is similar to eugonadal adult human males (Michiel Sedelaar et al., 2013). Animals were age-matched across conditions. All efforts were made to minimize any suffering, and the mice were humanely euthanized following the experiment for purposes of histology. Prostatic regression and regeneration took place over 3 weeks each.

Histology and immunofluorescence staining

Prostates were fixed with 4% paraformaldehyde for 40min, followed by incubation in 30% sucrose for overnight and embedded in OCT. Cryosections (5uM) were stained with specified antibodies (**Table 2.1**). For formalin-fixed paraffin-embedded tissues, 5uM sections were incubated in 10mM citrate buffer (pH 6) and steamed for 15 minutes at high pressure. Slides were allowed to cool and then were blocked with 10% normal donkey serum (Sigma) with

Mouse-On-Mouse Blocking Reagent (MKB-2213, Vector Labs, Burlinggame, CA) and incubated with primary antibodies diluted in 10% normal donkey serum. Sections then were incubated with secondary antibodies labelled with Alexa Fluor 488, 594, or 647 (Jackson ImmunoResearch, Westgrove PA). Sections were counterstained with Hoechst 33342 (Thermo) and mounted with ProLong Gold Antifade reagent (Invitrogen/Molecular Probes).

Microscopy

Immunofluorescence images were visualized using a Marianas Yokogawa type spinning disk inverted confocal fluorescent microscope, controlled using SlideBook (version 6). Max projections were composed in ImageJ (version 1.46r), each image is scaled to its normalization timepoint for each lobe. Automated cell counting was done by setting a binary threshold, using a water shed segmentation and particle counting algorithm. Each field was manually confirmed.

Cell Lines and Primary Cultures

Non-malignant epithelial cultures were established from fresh human prostate tissues acquired from surgical specimens as previously described (Chen et al., 2012). These tissues were acquired under an expedited protocol approved by the University of Chicago Institutional Review Board (IRB). Tissue samples were managed by the University of Chicago Human Tissue Resource Center core facility; the need for patient consent was waived as acquired samples were de-identified. 4mm biopsy punches of non-tumor tissue were taken from prostate and seminal vesicle tissues of patients undergoing radical prostatectomy; half of this tissue was fixed and analyzed by a pathologist to confirm the absence of tumor. Dissociation of prostate tissue and growth of epithelial cells has been previously described (Gao et al., 2001; Vander Griend et al., 2008) and the same methods were used to establish prostate (PrEC) cultures. Cultures were grown using Keratinoctye Serum-Free Defined media supplemented with growth factors (GFs)

(standard K-SFM, Invitrogen Life Technologies) and can be cultured up to 8 passages before notable cellular senescence (Uzgare et al., 2003; Uzgare and Isaacs, 2004). For our experiments, all cultures were analyzed at or before their fourth passage. The human WA01(H1) embryonic stem cell line was acquired via WiCell (Madison, WI) and cultured using the feeder-independent protocol using mTeSR1 media (Stem Cell Technologies; Vancouver, B.C.). ES cells were used within ten passages of thawing (Kregel et al., 2013).

RNA Isolation and Quantitative Real-Time RT-PCR

Total RNA was extracted using the RNeasy Mini Kit and on-column DNase I digestion (QIAGEN). cDNA synthesis was performed using the SuperScript® III First-Strand Synthesis SuperMix for qRT-PCR kit (Life Technologies). For the PCR Arrays, RT^2 qPCR Master Mix (SA Biosciences) was combined with either the Human Wnt RT^2 Profiler™ PCR Arrays (Cat# PAHS-043ZA-2, SA Biosciences) or the Human Notch RT^2 Profiler™ PCR Arrays (Cat# PAHS-059ZA-2, SA Biosciences) were used to examine the transcripts of 84 key genes involved in each pathway. Arrays were performed with biological replicates in triplicate for each condition. The RT^2 Profiler™ PCR Array Data Analysis software was used to assess average change in threshold cycle (ΔCT) values for each of the samples relative to vehicle control ($\Delta\Delta$CT), determine standard error and obtain p-values via student's t-test.

ChIP and RNA Sequencing

PrEC and WA01 cells were treated as described as described above. DNA and associated proteins were crosslinked with 1% formaldehyde, and lysates were sonicated and immunoprecipitated as described previously (Kregel et al., 2013). ChIP experiments were conducted using the ChIP Assay Kit and the manufacturer's protocol (EMD Millipore). A polyclonal goat anti-SOX2 mAb (P48431, R&D Systems), or a goat IgG control, were used for

immunoprecipitation. Eluted ChIP DNA was purified using the PCR Purification Kit (Qiagen). ChIP Sequencing libraries were generated using the Kapa Low-throughput Library Preparation Kit (Kapa Biosystems, cat. No. KK8230) Total RNA was isolated using the 'RNeasy Mini' kit (Qiagen) following the manufacturer's instructions. Quality of extracted RNA was evaluated using a 2200 TapeStation system (Agilent). Samples with a RIN score ≥ 7 were selected for making libraries. RNA Sequencing libraries were built using the 'Stranded mRNA-Seq' kit for Illumina platforms (KAPA) with OligodT magnetic beads to enrich for mRNA species. Libraries were run on a 2200 TapeStation system (Agilent) to confirm fragment size, and then quantified by qPCR using the Library Quantification kit (KAPA). Sequencing was done on a HiSeq 2000 sequencing system (Illumina) as 50bp, single-end runs.

Bioinformatic Analyses of Sequencing Data

ChIPseq Peak and Region Analysis: All ChIP-seq reads were analyzed using the FastQC tool suite (http://www.bioinformatics.babraham.ac.uk/projects/fastqc/). Low quality and adapter sequences were trimmed using Trimmomatic (Bolger et al., 2014). The trimmed reads were then aligned to the reference genome GRCh38 using BWA (Li and Durbin, 2009) and the resulting alignments were sorted and converted to BAM format using Samtools (http://www.htslib.org/doc/samtools.html). Duplicate reads were subsequently removed with Picard tools (http://broadinstitute.github.io/picard/). Two methods, MACS2 (Feng et al., 2012) and Q (Hansen et al., 2015), were used for peak detection for SOX2 IP data. Peaks detected by Q which had a quality score >35 and also overlapped a peak detected by MACS2 were used for further analysis.

RNAseq Differential Expression: All RNA-seq reads were analyzed using the FastQC tool suite. Low quality and adapter sequences were trimmed using trimmomatic (Bolger et al.,

2014). The trimmed reads were then aligned to the reference genome GRCh38 using STAR (star) and the resulting alignments were sorted and converted to BAM format using Samtools. Duplicate reads were subsequently removed with Picard tools. Gene and transcript-level expression was quantified using RSEM(Li and Dewey, 2011)) followed by differential expression analysis with the EBSeq package (Leng et al., 2013).

Transcription Factor Motif Analysis: SOX2 peak regions that passed earlier selection criteria were then expanded to a uniform range of 250bp around the summit in order to submit the targeted sequences for motif analysis using MEME Suite (*9*). In addition, FIMO (Grant et al., 2011) was employed to scan for all JASPAR (vertebrates 2016) (Mathelier et al., 2016) transcription factor motifs. In the set of SOX2 peaks where a canonical SOX2 motif was discovered, SpaMo was used to infer potential binding partners.

Statistical Analysis

Statistics for all mouse experiments were analyzed as indicated in figure legends. All experiments were performed with at least three animals in each experiment. Data are displayed as mean ± SEM. n is the number of biological replicates unless otherwise specified.

Antibodies	Source	Identifier
Chicken polyclonal anti-GFP (ab13970)	Abcam	AB_300798
Rabbit polyclonal anti-CK5 (905501)	Biolegend	AB_2565050
Rabbit monoclonal anti-CK8+18 (ab53280)	Abcam	AB_869901
Mouse monoclonal anti-p63 clone 4a4 (PTA-6626)	ATCC	
Rabbit monoclonal anti-Ki67 clone SP6 (ab16667)	Abcam	AB_302459
Goat polyclonal anti-Sox2 (AF2018)	R&D Systems	AB_355110
Mouse monoclonal anti-Bmi1 (ab14389)	Abcam	AB_2065390
Rabbit polyclonal anti-Androgen Receptor (ab133273)	Abcam	AB_11156085
Rabbit polyclonal anti-Pax2 (ab79389)	Abcam	AB_1603338
Alexa Fluor® 594 AffiniPure $F(ab')_2$ Fragment Donkey Anti-Goat IgG (H+L) (705-586-147)	Jackson ImmunoResearch	AB_2340434
Alexa Fluor® 594-AffiniPure Donkey Anti-Mouse IgG (H+L) (715-585-150)	Jackson ImmunoResearch	AB_2340854
Alexa Fluor® 594-AffiniPure F(ab')2 Fragment Donkey Anti-Rabbit IgG (H+L) (711-586-152)	Jackson ImmunoResearch	AB_2340622
Alexa Fluor® 488 AffiniPure $F(ab')_2$ Fragment Donkey Anti-Chicken IgY (IgG) (H+L) (703-546-155)	Jackson ImmunoResearch	AB_2340376
Alexa Fluor® 488 AffiniPure $F(ab')_2$ Fragment Donkey Anti-Rabbit IgG (H+L) (711-546-152)	Jackson ImmunoResearch	AB_2340619
Alexa Fluor® 488 AffiniPure $F(ab')_2$ Fragment Donkey Anti-Mouse IgG (H+L) (715-546-150)	Jackson ImmunoResearch	AB_2340849
Alexa Fluor® 647 AffiniPure Donkey Anti-Mouse IgG (H+L) (715-605-150)	Jackson ImmunoResearch	AB_2340862

Table 2.1 Antibodies used in this study

Results

Embryonic Sox2+ cells can give rise to adult Sox2+ cells as well as basal and luminal cells

Sox2 has been shown to play an important role in the fetal development of multiple tissues, including the nervous system (Bylund et al., 2003; Graham et al., 2003; Ellis et al., 2004), anterior foregut endoderm and derivatives (Que et al., 2007), retina (Taranova et al., 2006), lens epithelium (Kamachi et al., 1998), taste bud (Okubo et al., 2009a), inner ear (Kiernan et al., 2005), as well as stomach epithelium, lung, and testes (Arnold et al., 2011). Thus, we initially sought to determine whether Sox2 is specifically expressed during embryonic formation of the urogenital sinus, the anlagen tissue of the prostate. We first used IHC to evaluate Sox2 expression in embryos at E12.5, coincident with the formation of the urogenital sinus epithelium (Staack et al., 2003b; Georgas et al., 2015; Toivanen and Shen, 2017). We noted prominent expression of Sox2 specifically in the urogenital sinus epithelium (**Figure 2.1, 2.2A**). Notably, the mesoderm-derived Wolffian duct, which derives the mature seminal vesicle tissue, did not contain cells with any detectable Sox2 expression (**Figure 2.1)**. Additionally, we observed persistence of Sox2 expression in the developing prostate epithelium through postnatal day 5 (**Figure 2.1**).

Since Sox2-positive cells are detectable at the earliest stages of prostate development, we sought to investigate whether such Sox2-expressing urogenital sinus epithelial cells yielded basal and/or luminal cells during and after prostatic development. Thus we adapted a previously published genetic lineage tracing approach to fate-map the Sox2 lineage in the prostate (**Figure 2.2B**) (Arnold et al., 2011). Briefly, a tamoxifen (TAM)-inducible Cre allele (CreERT2) was knocked into one allele of the endogenous Sox2 locus; these mice are thus heterozygous for Sox2 expression, with one allele driving CreERT2. It should be noted that such mice are

phenotypically normal (Arnold et al., 2011). These mice were subsequently crossed with a homozygous ROSA26-YFP (yellow fluorescent protein) reporter mouse (Srinivas et al., 2001).

Upon administration of tamoxifen, Sox2-expressing cells and their resultant progeny permanently express YFP. To fate-map fetal Sox2+ cells, we injected pregnant females carrying Sox2-CreER; ROSA26-lsl-EYFP (hereafter Sox2-LT) embryos with tamoxifen and progesterone at E12.5. We investigated the distribution of YFP at E17.5, when the urogenital sinus epithelium begins to bud into the surrounding urogenital sinus mesenchyme (Staack et al., 2003a; Georgas et al., 2015; Toivanen and Shen, 2017). After the formation of prostatic buds, the epithelium undergoes extensive proximal-distal outgrowth and branching morphogenesis in a proximal-distal wave (Sugimura et al., 1986). YFP expression was observed in plastic double-positive CK8+/p63+ cells as well as more-differentiated single-positive CK8+ luminal and single-positive p63+ basal cells (**Figure 2.2C**).

We then sought to investigate whether embryonic Sox2+ cells serve as precursors for Sox2-expressing cells in the adult murine prostate. Post-pubescent males were sacrificed at 9 weeks of age and evaluated for YFP expression in all three lobes of the prostate. We noted that while Sox2-expressing basal cells also co-expressed YFP, this was not always the case (**Figure 2.2D**). We cannot completely discount a partial Cre efficiency as a result of inefficient tamoxifen treatment (approximately 26%, **Figure 2.4A and 2.4B.**). These data indicate that the Sox2 lineage may not be statically established during embryogenesis. A co-stain with Ki67, a marker of proliferation, demonstrates that Sox-expressing cells are often Ki67-negative, providing evidence that these cells do not actively divide in the adult prostate. Notably, embryonic Sox2-expressing cells in the UGS are capable of giving rise to both CK8+ luminal and p63+ basal cells in the adult prostate (**Figure 2.2E**). These studies demonstrate that embryonic Sox2+ cells give

rise to adult Sox2+ cells, and can also generate Sox2-negative luminal cells, indicating that Sox2 expression is lost upon terminal differentiation.

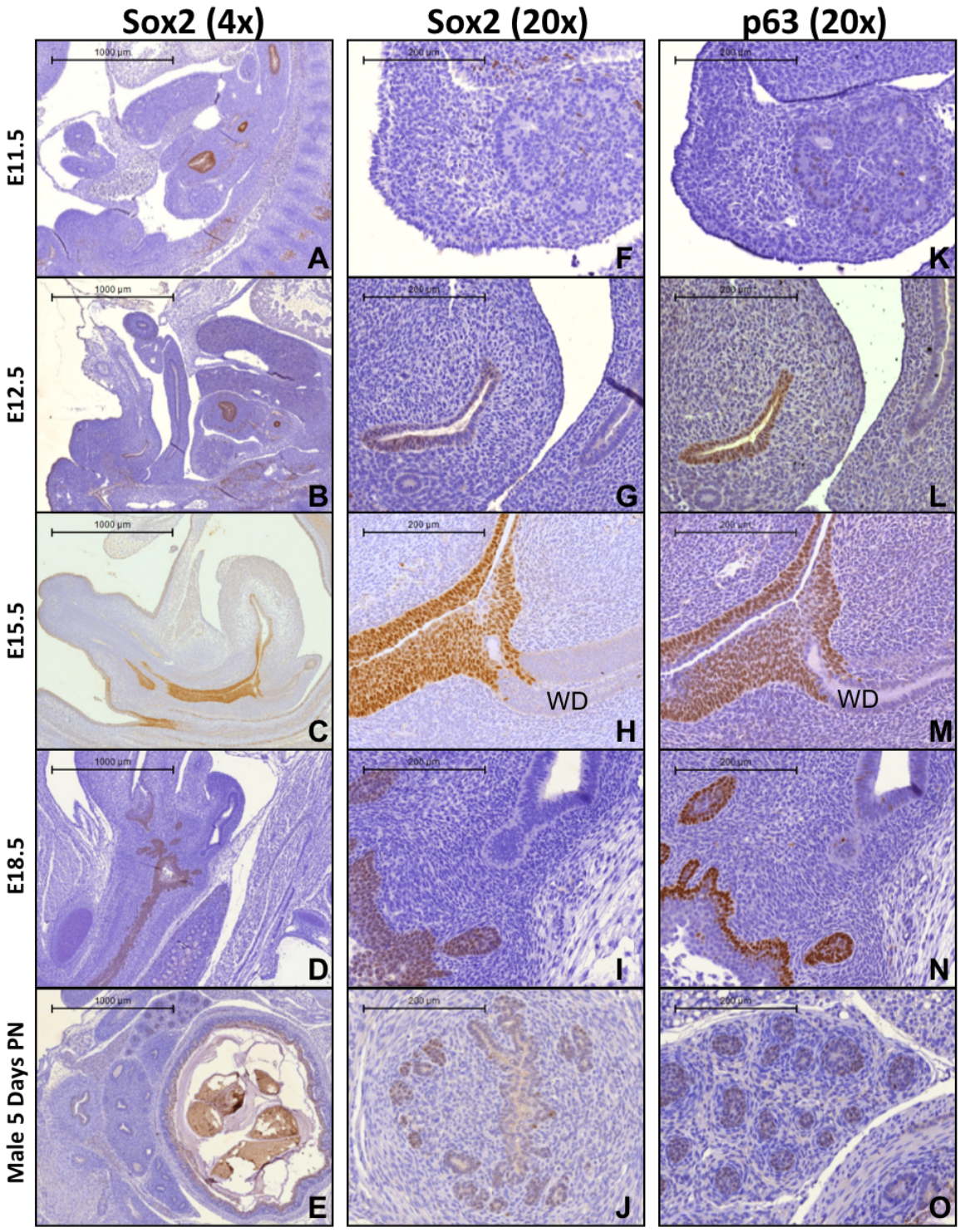

Figure 2.1: Sox2 expression specifically marks endodermal structures and persists into postnatal development of the prostate. (a-e) Representative immunohistochemistry of Sox2 in the urogenital sinus epithelium (UGSE) of murine embryos through development. Black scale bar, 1000um. (f-j) Immunohistochemistry of Sox2 in the UGSE of murine embryos through development. Black scale bar, 200um. WD, Wolffian duct. (k-o) Immunohistochemistry of basal cell marker p63 in the UGSE of murine embryos through development. Black scale bar, 200um. WD, Wolffian duct.

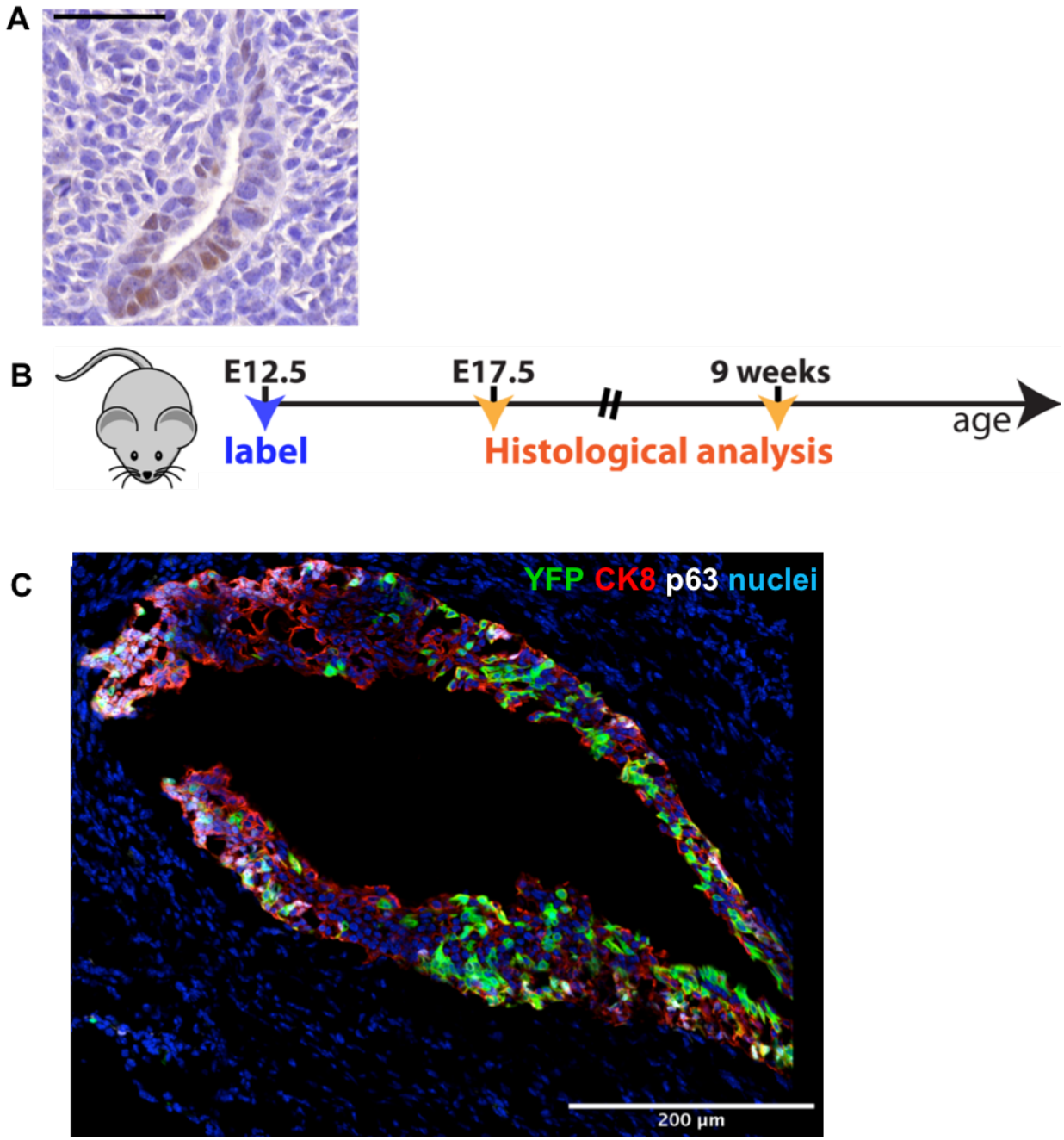

Figure 2.2: Embryonic Sox2+ cells can give rise to adult Sox2+ cells as well as basal and luminal cells. a) Representative immunohistochemistry of Sox2 in the urogenital sinus epithelium (UGSE) of E12.5 embryos. Black scale bar, 50um. (b) Scheme for labeling embryos *in utero*. (c) Representative immunofluorescent (IF) staining shows co-localization of YFP with basal cell marker p63 and luminal cell marker CK8) in the UGSE of E17.5 embryo (montage images of sagittal sections). Scale bar, 200um.

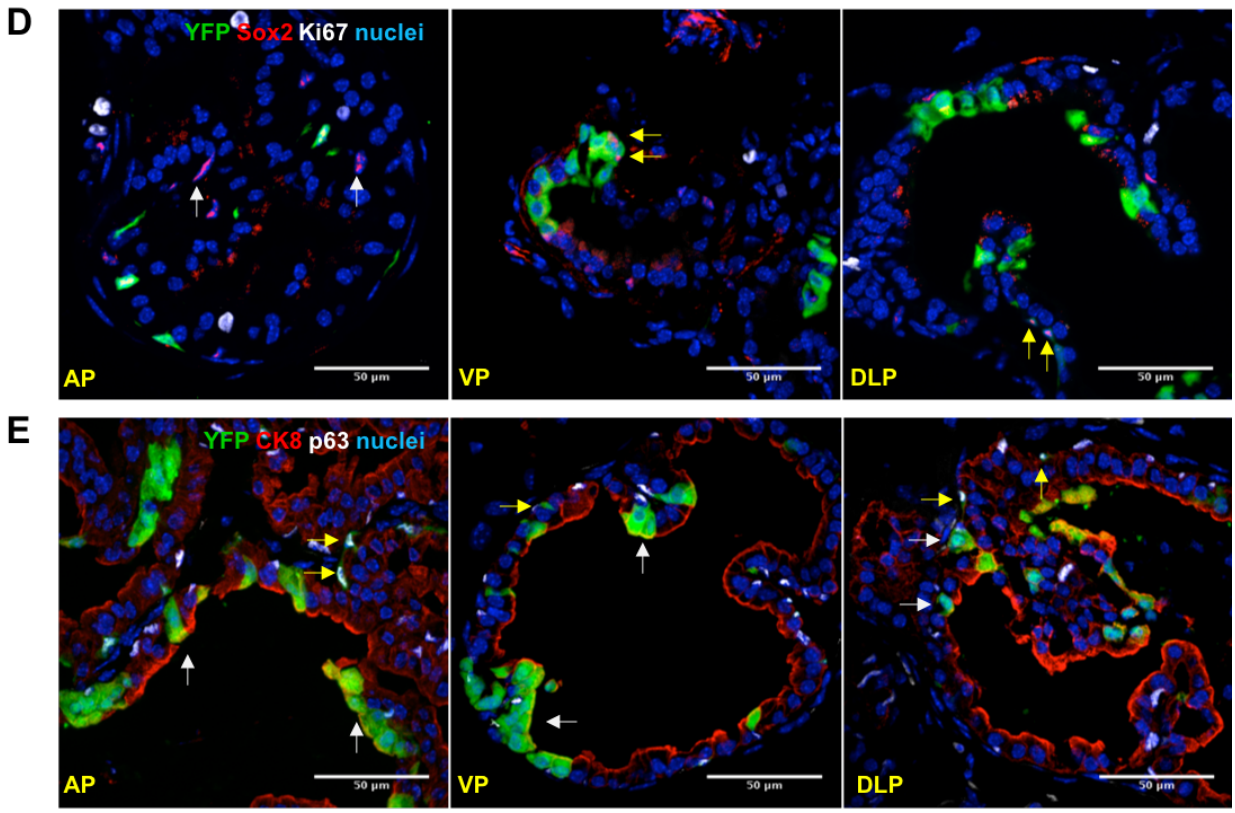

Figure 2.2 continued: (d) IF staining shows co-localization of YFP with Sox2 and Ki67 in post-pubescent murine prostate. Yellow arrows: Sox2+ cells positive for YFP. White arrows: Sox2+ cells negative for YFP. (e) IF staining shows co-localization of YFP with p63 and CK8 in post-pubescent murine prostate. Yellow arrows: YFP+ cells positive for basal cell markers. White arrows: YFP+ cells positive for luminal cell markers. Scale bar, 50um. AP, anterior prostate; VP, ventral prostate; DLP, dorsolateral prostate.

Sox2 is largely expressed in the proximal adult murine prostate

Previous studies have suggested that prostate epithelial cell progenitor cell populations reside in the proximal prostatic region, adjacent to the urethra (Tsujimura, 2002; Goto et al., 2006). Thus, we next sought to investigate the location, distribution, and cell-type expression of adult Sox2+ cells in the post-pubescent murine prostate. Cre activity was induced by tamoxifen treatment within hormonally intact adult male Sox2-LT mice for 4 days, 24 hours later prostates were harvested and examined for YFP (**Figure 2.2A**) (Arnold et al., 2011). We divided the adult prostate gland into proximal, intermediate and distal thirds and quantified the percentage of Sox2+ cells in each location. Examination of the prostates of tamoxifen-treated mice revealed that YFP marked 2.5% of cells in the proximal region of the prostate as compared to 0.2% of cells in the more distal parts of the gland (**Figure 2.2B, 2.2C**). These data demonstrate that the majority of Sox2-expressing cells localized to the proximal region of the gland.

Considering previous reports of heterogeneity within adult epithelial lineages (Kwon et al., 1AD; Goldstein et al., 2008; Wang et al., 2013; Chua et al., 2014b; Kwon et al., 2015; Ceder et al., 2017; Chua et al., 2018; Zhang et al., 2018), we co-stained for endogenous Sox2 with basal (CK5) and luminal (CK8) markers. We observed Sox2 expression in basal cells within proximal and distal regions of all three lobes of the prostate. Interestingly, Sox2 only marked luminal cells within proximal, but not distal, regions, especially within the ventral and dorsolateral lobes, (**Figure 2.2D**, n = 6 mice). Taken together these data suggest that Sox2 expression may differentiate between the more plastic proximal cells and the more restricted distal cells, particularly in the luminal lineage.

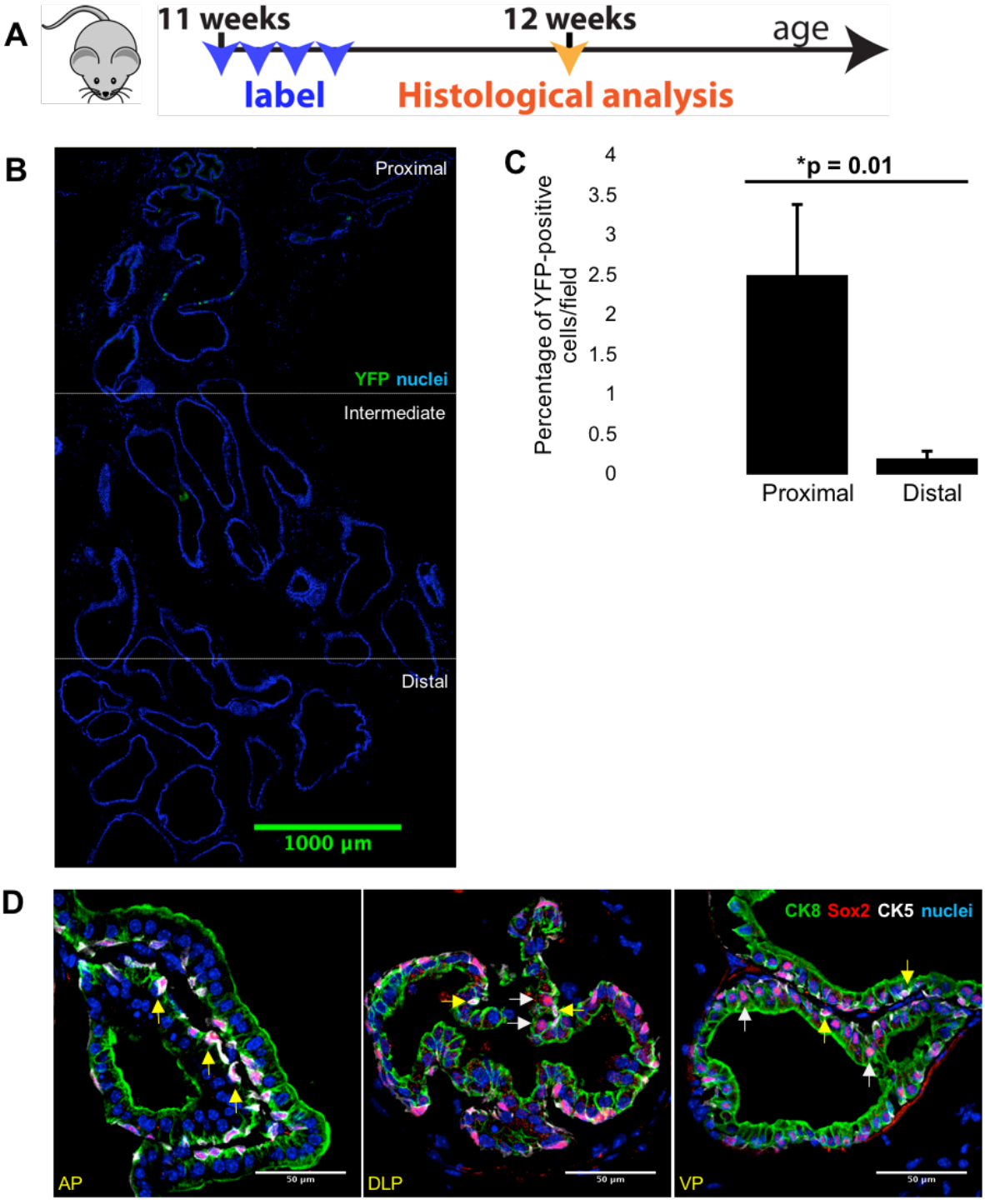

Figure 2.3: Sox2 is predominantly expressed in the proximal adult murine prostate. (a) Scheme for labelling Sox2+ cells in the adult mouse prostate. (b) YFP expression (green) in adult mouse prostate 24 hours after last tamoxifen pulse. Scale bar, 1000um. (c) Quantitation of YFP+ cells in proximal and distal prostates of anterior prostate (n = 3 mice). Data represent the mean±SEM, two-tailed Student's t-test. *p=0.01. (d) IF staining shows colocalization of Sox2 with CK8 and CK5. Yellow arrows: Sox2+ cells positive for basal cell markers. White arrows: Sox2+ cells positive for luminal cell markers. Scale bar, 50um. AP, anterior prostate; VP, ventral prostate; DLP, dorsolateral prostate.

Sox2+ cells contribute to homeostatic turnover in the adult murine prostate

Two major criteria of adult stem cells include the capability to self-renew and give rise to multiple lineages. To determine whether the prostatic Sox2+ lineage is capable of longevity and potency in epithelial homeostasis, Sox2-LT mice were pulsed with tamoxifen and then chased for extended periods of time (2, 6, and 12 months). We conducted co-immunofluorescence for YFP, as well as basal cell-specific p63 and luminal cell-specific CK8, to fate-map Sox2+ cells in adult prostatic homeostasis. Analyses of murine prostates immediately after the four consecutive administrations of tamoxifen yielded the appearance of individual dispersed YFP+ cells (**Figure 2.3**, far left panel, n =3 mice per timepoint). Such YFP-positive cells persist to the 2, 6, and 12-month time points, demonstrating the longevity of Sox2+ cells. At 12 months post-pulse, YFP+ clonal patches of CK8+ luminal cells emerge, suggesting that Sox2+ cells contribute to epithelial homeostasis (**Figure 2.3**, far right panel). These results suggest that Sox2 marks both basal and luminal cells that are capable of self-renewal.

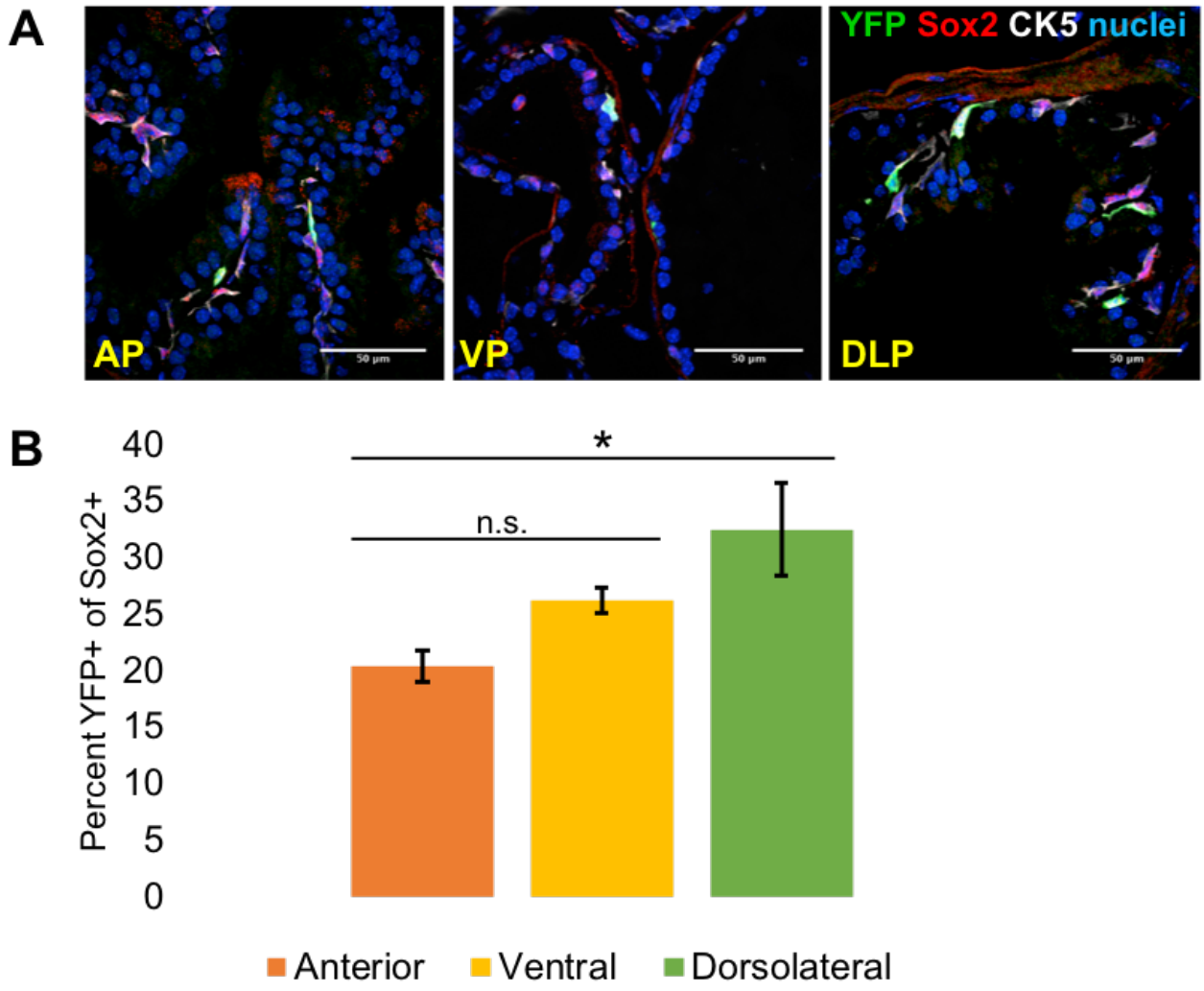

Figure 2.4 Sox2+ cells contribute to homeostatic turnover in the adult murine prostate: (a) Representative immunofluorescent (IF) staining shows co-localization of YFP with basal cell marker CK5 and Sox2 in adult murine prostate (n = 6 mice). Scale bar 50um. (b) Quantitation of proportion of YFP+ cells over Sox2+ in each lobe of murine prostate (n = 3-6 mice each). Data represent the mean±SEM., one way ANOVA. *p=0.001; n.s. non-significant. Scale bar, 50um. AP, anterior prostate; VP, ventral prostate; DLP, dorsolateral prostate.

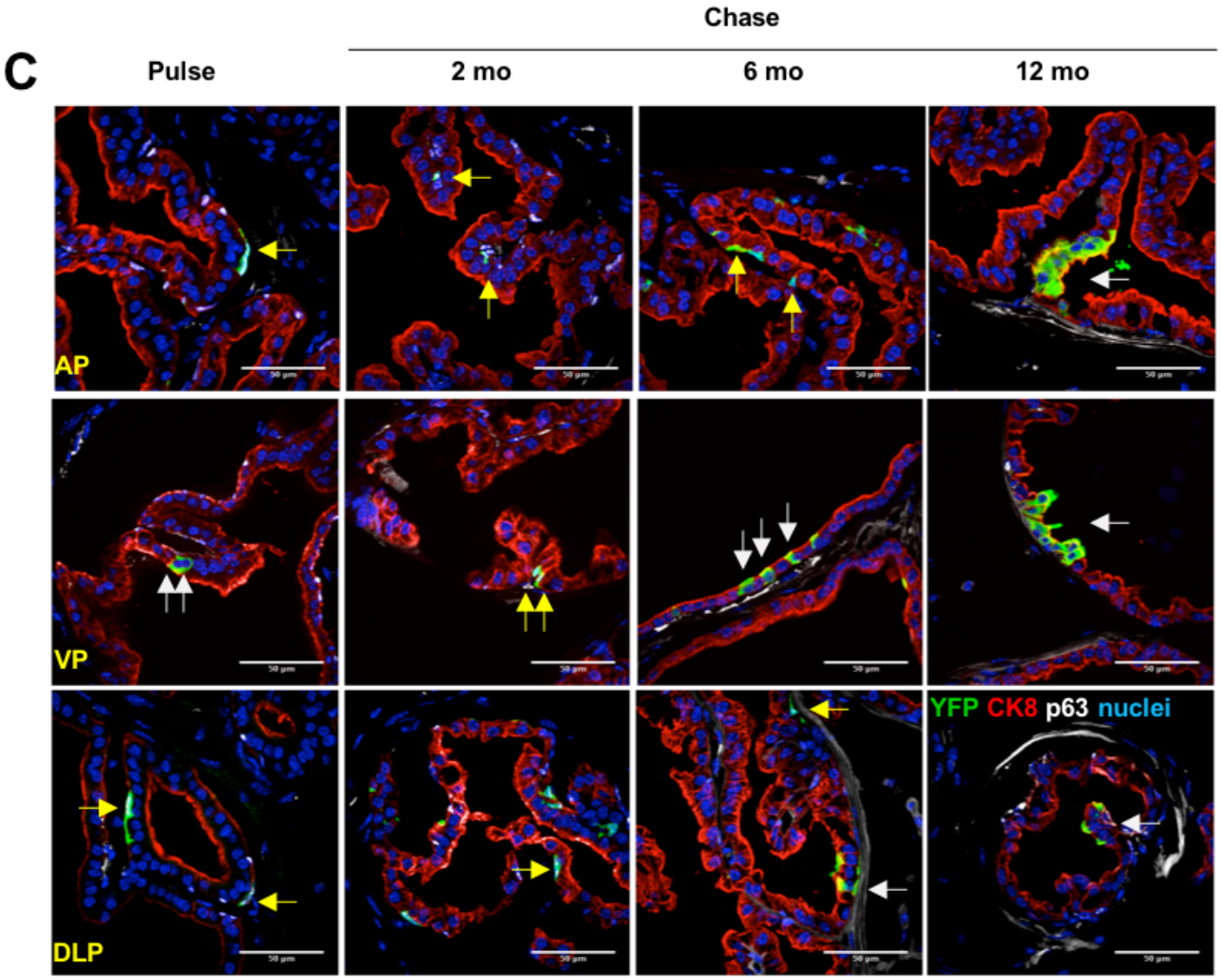

Figure 2.4 continued: (c) IF staining shows colocalization of YFP (green) with either CK8 or p63. Yellow arrows: YFP+ cells positive for basal cell markers. White arrows: YFP+ cells positive for luminal cell markers. Scale bar, 50um. AP, anterior prostate; VP, ventral prostate; DLP, dorsolateral prostate.

Sox2+ cells are castration-resistant and contribute to prostatic regeneration

A hallmark of *bona fide* prostate progenitor cells is the ability to persist during castration and contribute to epithelial regeneration after testosterone administration. To determine the castration-resistance of Sox2+ cells, we pulse labeled Sox2-LT mice and induced two cycles of castration and testosterone-induced regeneration (**Figure 2.4A**, n = 3 mice per timepoint). We then quantified proportion of YFP+ cells at each time point, as well as the percentage of YFP+ cells that were either luminal (CK8) or basal (p63) (**Figure 2.4B and 2.4C**). At the pulse time point, a total of 1.82% of cells were YFP+, 87% of which were p63+ basal cells and 13% of which were CK8+ luminal cells (**Figure 2.4B and 2.4C**). After host castration, we observed a significant enrichment of YFP+ cells, totaling 2.75% in the regressed prostate (60% basal, 40% luminal, $p<0.05$)**.** The percentage of YFP-labeled cells grew significantly upon restoration of testosterone, from 2.75% in the regressed prostate to 3.85% in the regenerated prostate (66% basal, 34% luminal, $p<0.05$). A second castration reduced YFP+ cells from 3.85% in regenerated prostates back to 2.87% (78% basal, 22% luminal), similar to the first regression. Taken together these results indicate that Sox2-expressing cells in the intact murine prostate are castration-resistant, and contribute to prostatic regeneration upon testosterone supplementation.

We and others have previously demonstrated that Sox2 expression is sufficient to promote both *in vivo* castration resistance as well as *in vitro* resistance to the anti-androgen Enzalutamide, and that androgen-mediated signaling influences Sox2 expression (Kregel et al., 2013; Ku et al., 2017; Mu et al., 2017). Thus, we sought to determine whether Sox2 is expressed in persisting, castration-resistant cells in the context of nonmalignant regeneration. Indeed, some persisting cells in the regressed prostate express Sox2 but not YFP, suggesting that persisting cells may upregulate Sox2 *de novo* in response to castration (**Figure 2.4E**). Interestingly,

persisting cells also express nuclear AR, sometimes, but not always, in concert with Sox2 and/or YFP. Taken together, these results indicate that the mechanisms of specification of a Sox2+ castration-resistant lineage may not be AR-dependent, in contrast to castration-resistant Nkx3.1-expressing cells (CARNs) (Xie and Wang, 2017; Xie et al., 2017; Chua et al., 2018).

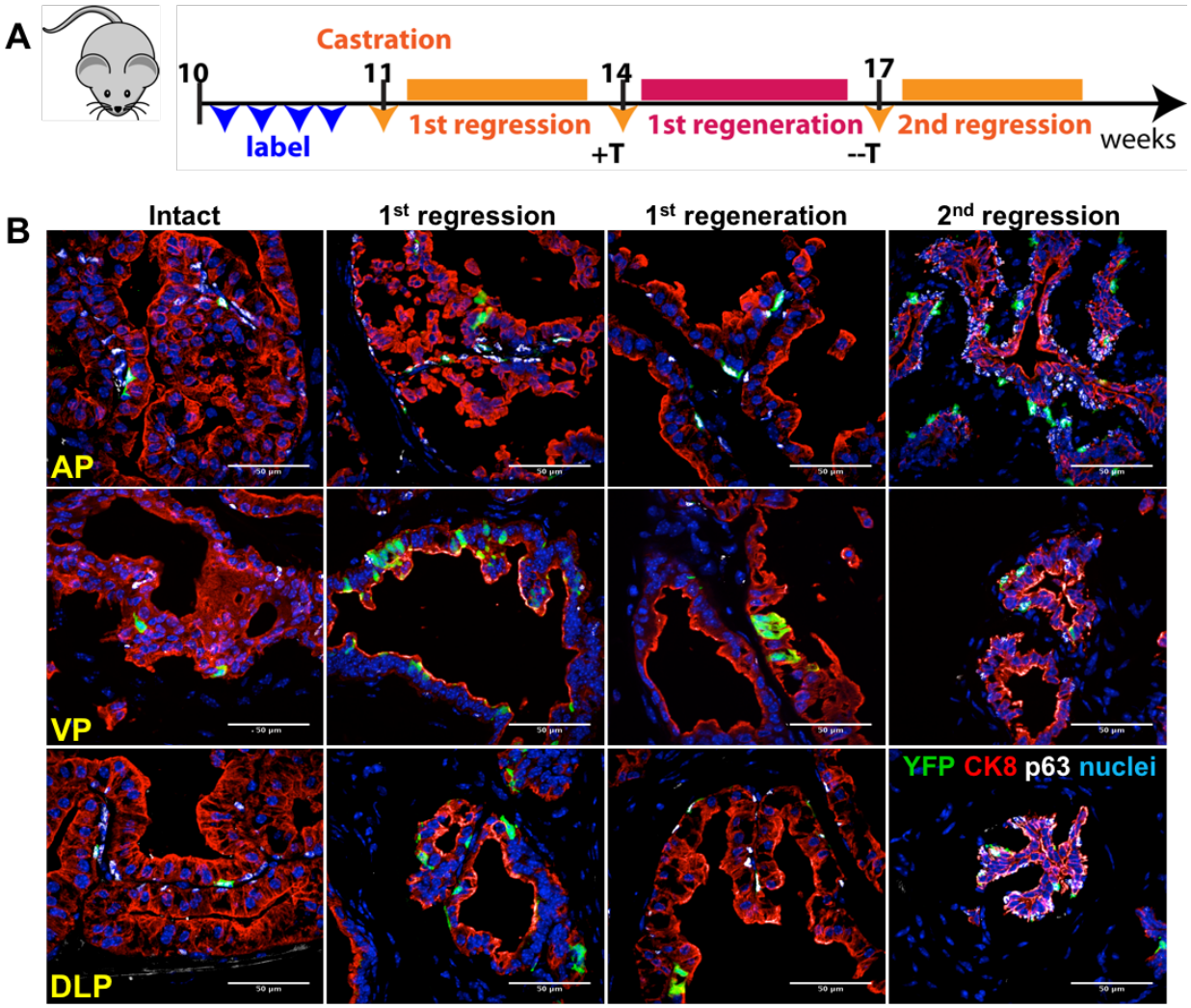

Figure 2.5: Sox2+ cells are castration-resistant and contribute to prostatic regeneration. (a) Scheme for Sox2 lineage marking during serial prostate regression and regeneration. (b) Immunofluorescence staining to assess YFP+ luminal cells that co-express CK8 (white arrows) or YFP+ basal cells that co-express p63 (yellow arrows) after serial prostate regeneration. AP, anterior prostate; VP, ventral prostate; DLP, dorsolateral prostate. Scale bar, 50um.

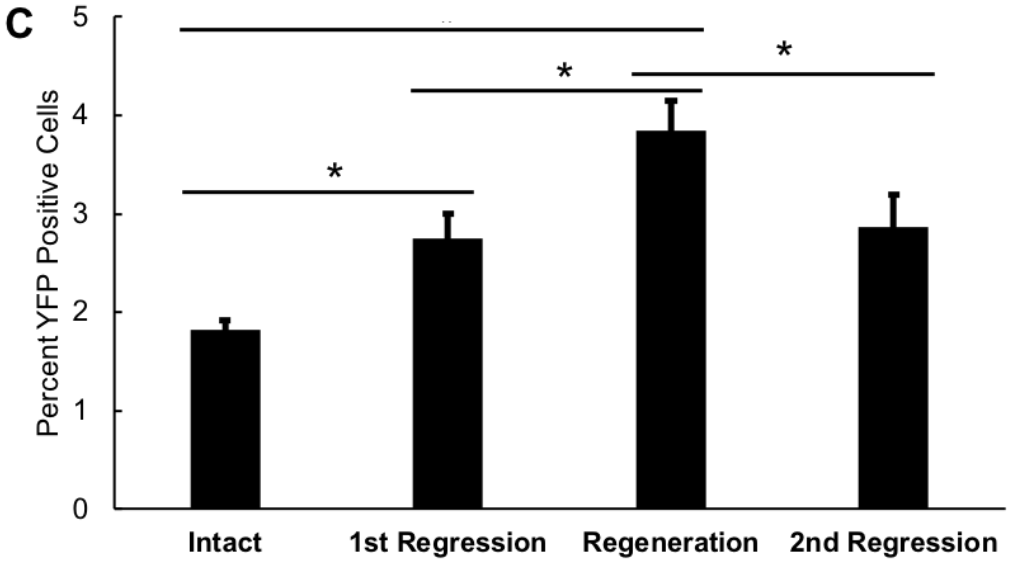

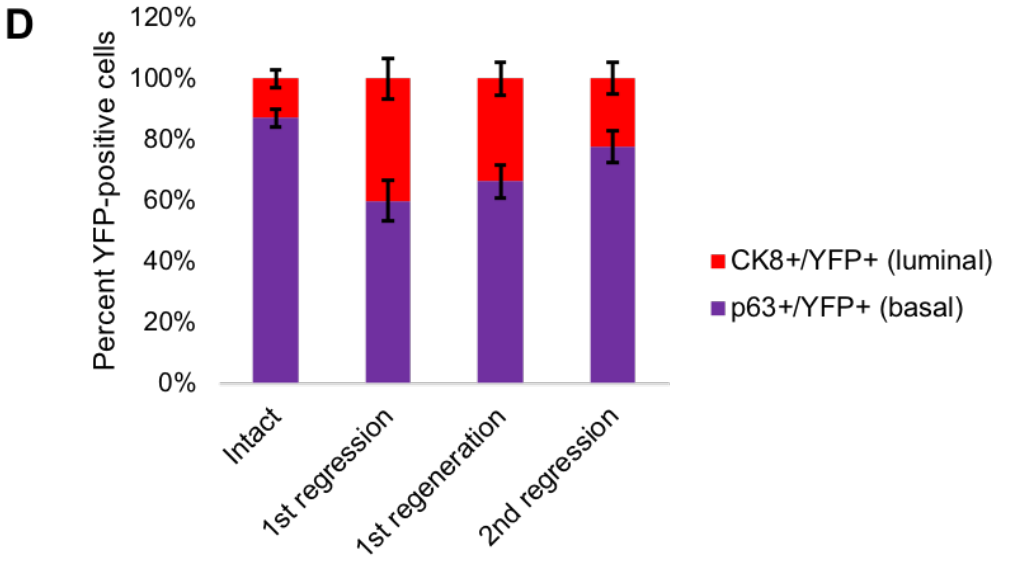

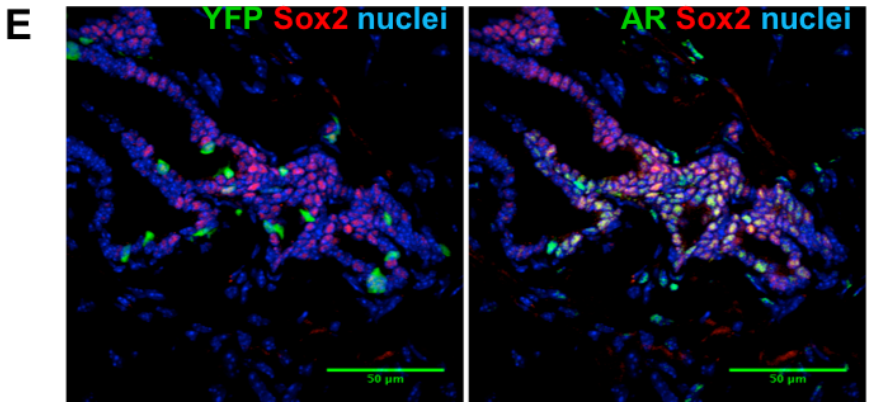

Figure 2.5 continued: (c) Graph showing percentage of total YFP+ cells in intact, castrated or regenerated prostates over all lobes. Data represent the mean±SEM. *P<0.05, Tukey's Honest Significant Difference test.

Figure 2.5 continued: (d) Graph showing percentage of YFP+ cells co-expressing luminal or basal markers in intact, castrated or regenerated prostates. (e) IF staining shows colocalization of YFP (green) and Sox2 (red) or AR (green) and Sox2 (red) in regressed dorsolateral prostate. Scale bar, 50um.

Castration-resistant Sox2+ cells have regenerative capacity *in vivo*

Our observation that Sox2 expression may be upregulated *de novo* in castration-resistant luminal epithelial cells led us to investigate the fate of such cells during prostatic regeneration. To do this, we first castrated a cohort of Sox2-LT mice, allowed three weeks for full prostatic involution, labelled Sox2-expressing cells by tamoxifen treatment, and then induced two cycles of prostate regeneration by treating mice with testosterone (**Figure 2.5A**, n = 3 mice per timepoint). We noted YFP labeling of a total of 2.7% of remaining cells (44% CK8+, 56% p63+ basal). Notably, the fraction of CK8+ cells that were YFP-labeled after castration increased threefold as compared to an intact prostate, indicating upregulation of Sox2 in response to castration (**Figure 2.5B and 2.5C**). Administration of testosterone significantly increased YFP-labeled cells to 4.7% (58% CK8+, 42% p63+), and clonal patches of CK8+ luminal cells begin to emerge. These data indicate that castration-resistant cells expressing Sox2 are capable of self-renewal and contribute to prostatic regeneration. The overall fraction of YFP+ cells did not significantly increase between regeneration cycles (5.06% as a result of the second regeneration versus 4.36% in the first regeneration), indicating that while castration-resistant Sox2-exprressing cells can regenerate epithelial cells following castration, progeny produced from these cells remain sensitive to castration.

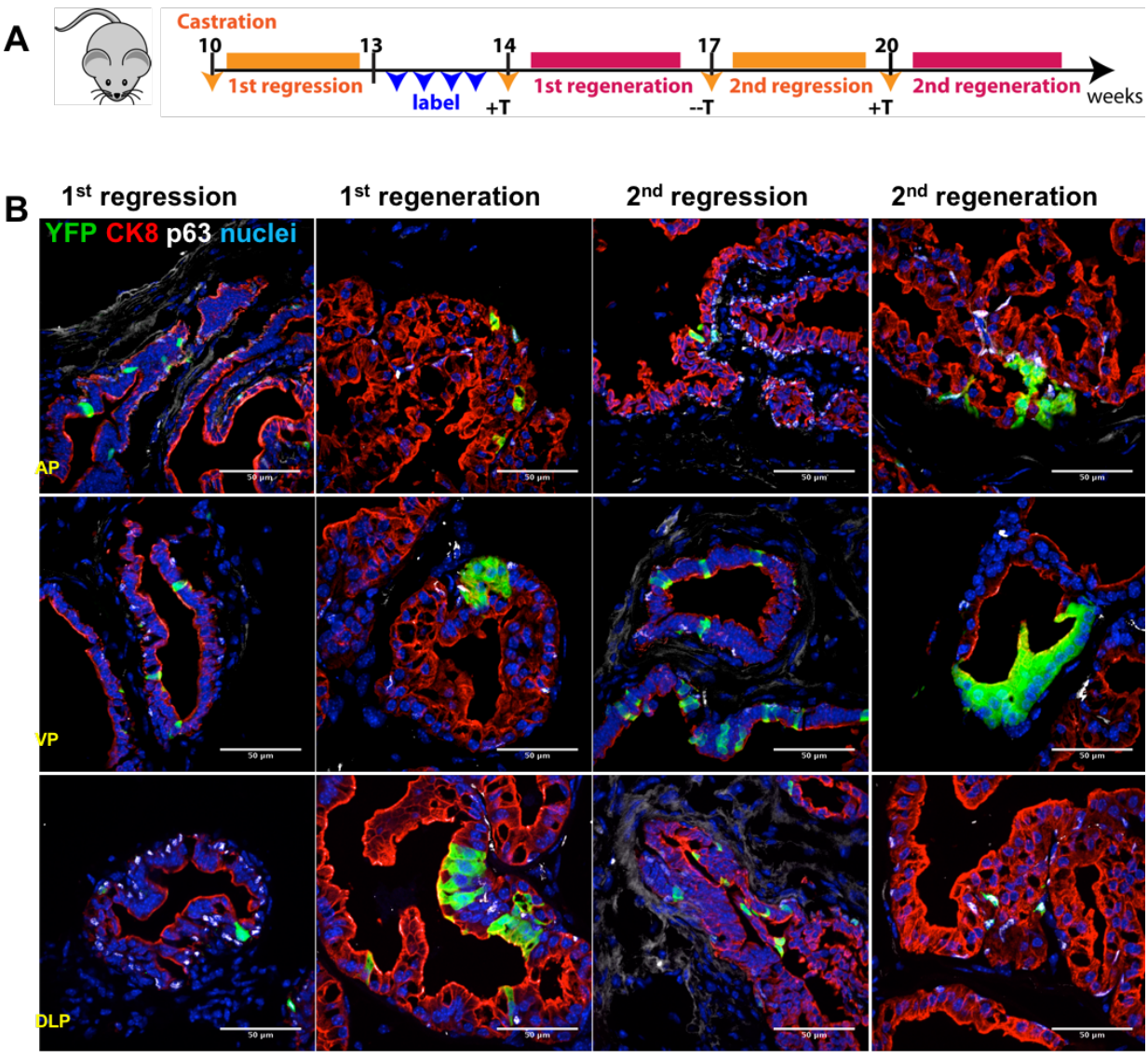

Figure 2.6: Castration-resistant Sox2+ cells have regenerative capacity *in vivo.* (a) Scheme for Sox2 lineage marking during serial prostate regression and regeneration. (b) Immunofluorescence staining to assess YFP+ luminal cells that co-express CK8 (white arrows) or YFP+ basal cells that co-express p63 (yellow arrows) after serial prostate regeneration. Scale bar, 50um. AP, anterior prostate; VP, ventral prostate; DLP, dorsolateral prostate. Scale bar, 50um.

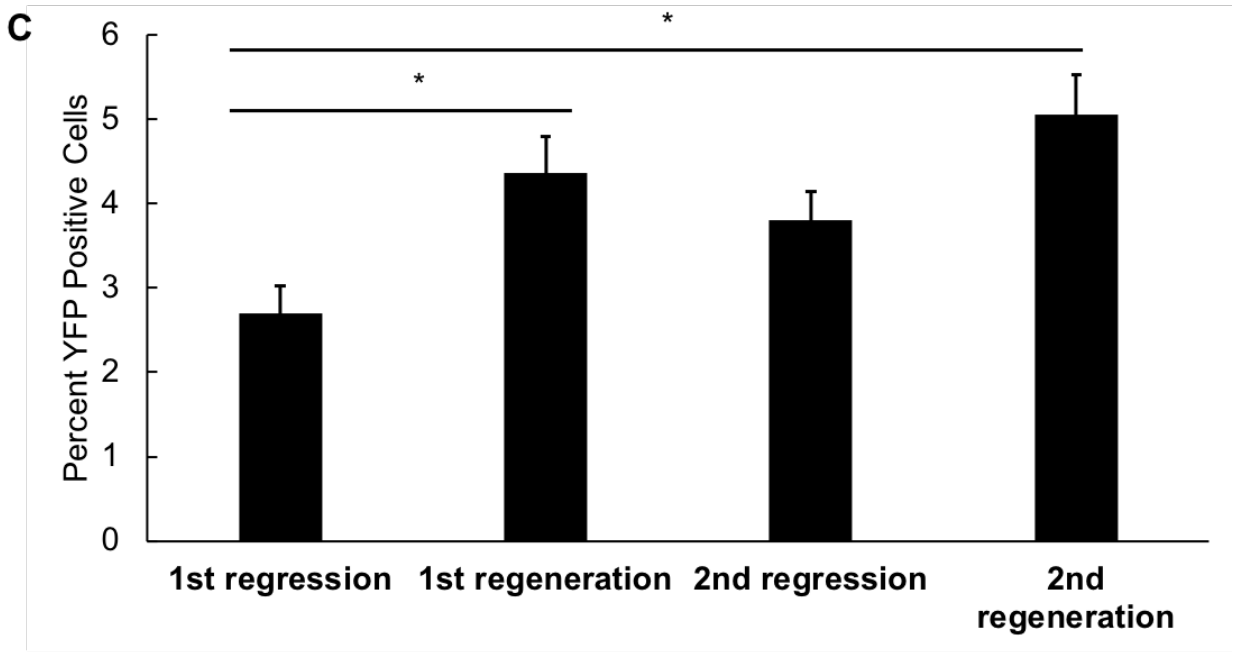

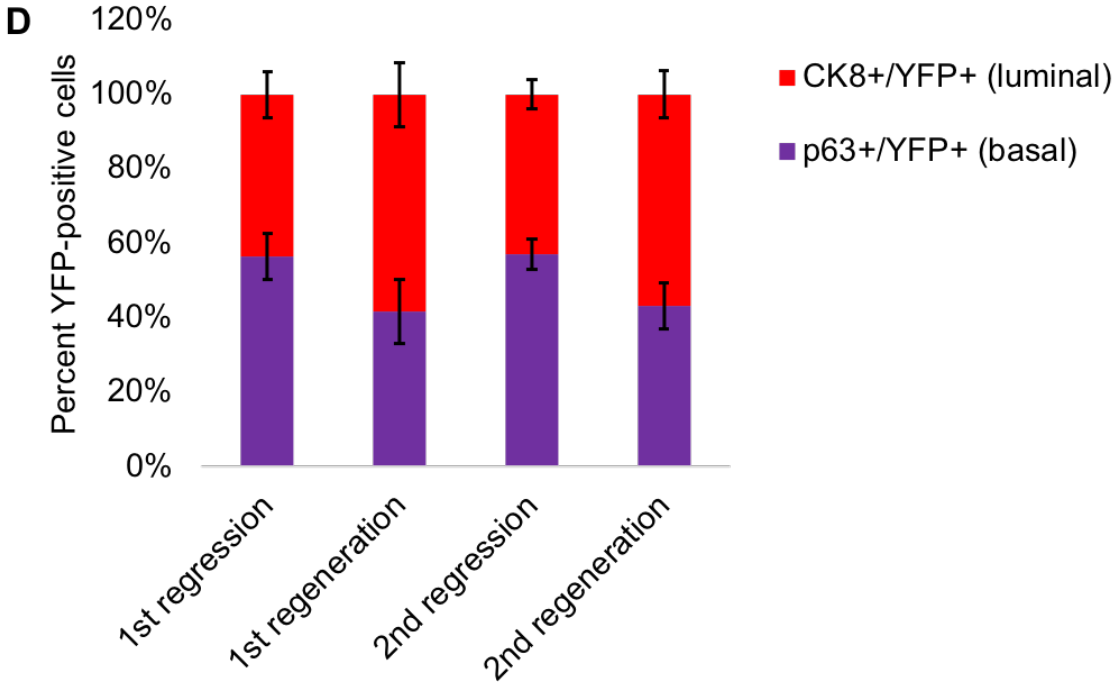

Figure 2.6 continued: (c) Graph showing percentage of total YFP+ cells in intact, castrated or regenerated prostates over all lobes. Data represent the mean±SEM. *P<0.05, Tukey's Honest Significant Difference test. (d) Graph showing percentage of YFP+ cells co-expressing luminal or basal markers in intact, castrated or regenerated prostates.

Sox2 regulates distinct genes in adult prostate epithelial cells as compared to human embryonic cells

Previous studies have documented cell-specific gene targets, binding partners, and co-factors for Sox2 in other adult tissues (Kondoh and Kamachi, 2010; Sarkar and Hochedlinger, 2013). Whether Sox2 is a driver of stemness in adult prostate cells remains unknown. Moreover, it is also unclear whether Sox2 binds a set of similar clientele genes in adult prostatic progenitor cells as compared to canonical targets in embryonic stem cells (Boyer et al., 2005). To more mechanistically understand functions of Sox2 in prostate epithelial cells (PrECs), we conducted chromatin immunoprecipitation and next-generation sequencing (ChIP-Seq) alongside paired RNA-seq to identify SOX2-bound loci in PrECs (Kregel et al., 2013; Vander Griend et al., 2014).

These analyses revealed SOX2 binding within 5000bp of 2547 RNA species, 1799 of which were protein coding (**Figure 2.7A**). Analyses using parallel SOX2 ChIP-Seq and RNA-Seq of human embryonic stem cells (hESCs) demonstrate that 1243 (69%) of SOX2-bound genes in PrECs are shared with hESCs (**Figure 2.7B**). To gain some insight into the pathways that SOX2 potentially regulates in PrECs, we conducted Ingenuity Pathway Analyses (IPA) of shared and PrEC-unique targets. These analyses highlighted marked PrEC-specific differences in Wnt and Notch signaling. To validate *in silico* analyses, we stably overexpressed Sox2 in hTERT-immortalized PrECs, which do not endogenously express Sox2. We then used quantitative PCR-based profiler arrays to more holistically investigate Wnt and Notch pathways in Sox2-sufficient PrECs as compared to Sox2-deficient PrECs (**Figure 2.7C and Figure 2.7D**).

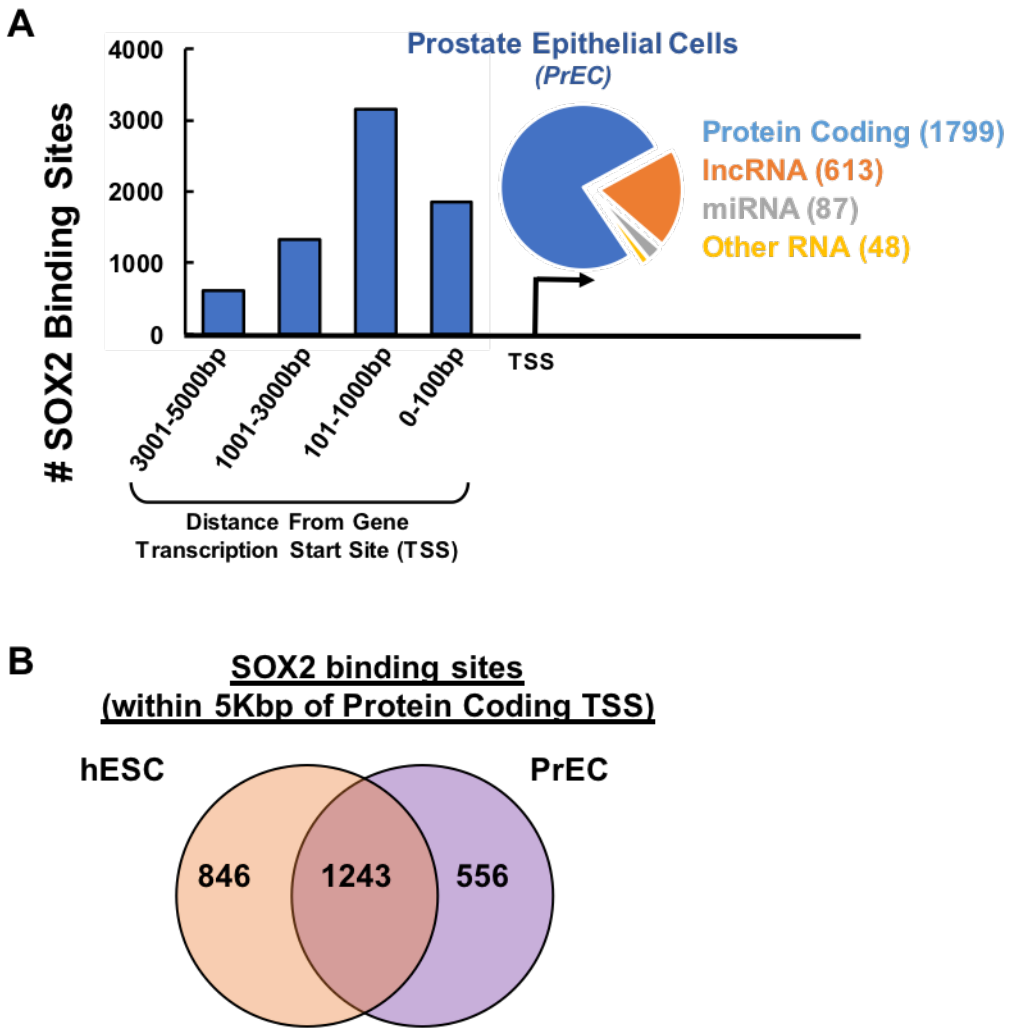

Figure 2.7 Sox2 ChIP-seq in human prostate epithelial cells (PrECs) reveals both stem and non-stem cell associated targets. (a) Sox2 peak regions within 5000 bp of putative transcription start sites (TSS) were prioritized. Sox2 binding is enriched 100bp-1000bp upstream of TSS. Of all binding sites, 1799 were protein coding genes. (b) Of the 1799 protein coding loci, 1243 genes were found to be shared between the two cell lines. Notably, 556 protein coding genes were found to be expressed specifically in PrECs but not found in human embryonic stem cells (hESCs).

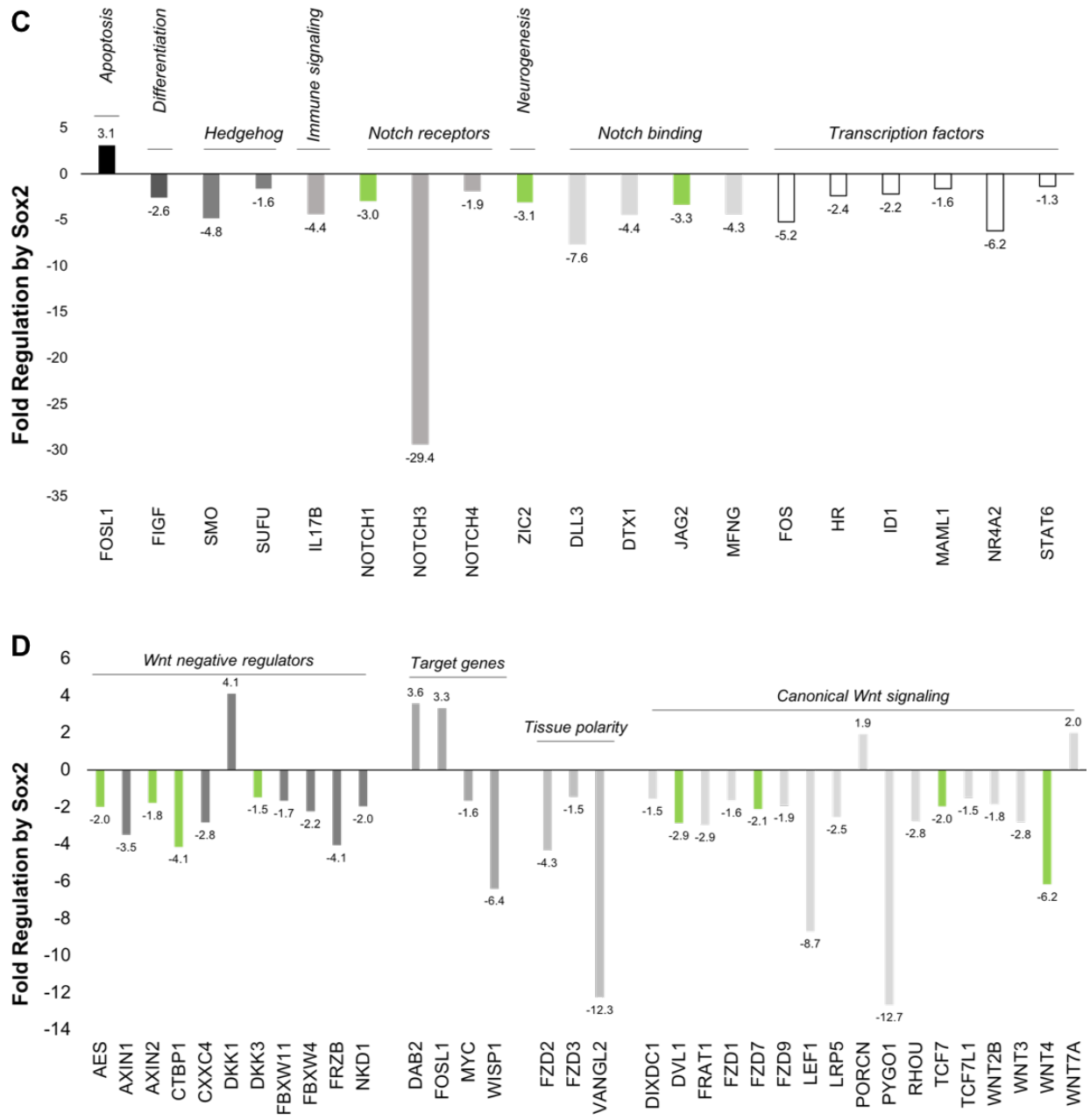

Figure 2.7 continued: (c) Notch pathway genes significantly up- or down-regulated in Sox2-overexpressing PrECs as compared to parental controls. Green bars represent Sox2-target genes in PrECs enriched in the Sox2 ChIP-seq. (d) Wnt pathway genes significantly ($p < 0.05$) up- or down-regulated in Sox2-overexpressing PrECs as compared to parental controls. Green bars represent Sox2-target genes in PrECs enriched in the Sox2 ChIP-seq. Gene enrichment calculations performed using QIAGEN online tools. $p < 0.05$, Student's t-test.

Gene	AVG dCT		2^-dCt		Fold Change	p-value	fold regulation
	Sox2	par	2^-dCt	par	Sox2/par	Sox2/par	Sox2/par
ADAM10	-1.3	-0.93	2.4538	1.9075	1.29	0.221	1.29
ADAM17	0.21	0.51	0.8615	0.6998	1.23	0.416	1.23
AES	-0.94	-1.4	1.9207	2.6299	0.73	0.165	-1.37
AXIN1	2.14	2.07	0.2261	0.2379	0.95	0.732	-1.05
B2M	-2.02	-1.52	4.0418	2.8712	1.41	0.192	1.41
CBL	1.6	2.29	0.3295	0.2042	1.61	0.232	1.61
CCND1	-1.35	-1.14	2.5521	2.2064	1.16	0.328	1.16
CCNE1	3.93	3.14	0.0655	0.1130	0.58	0.089	-1.73
CD44	-2.96	-2.89	7.7902	7.4041	1.05	0.649	1.05
CDKN1A	-2.99	-2.19	7.9173	4.5683	1.73	0.208	1.73
CFLAR	2.06	2.13	0.2395	0.2277	1.05	0.612	1.05
CHUK	2.81	2.96	0.1421	0.1281	1.11	0.290	1.11
CTNNB1	-0.11	-0.15	1.0780	1.1083	0.97	0.825	-1.03
DLL1	3.63	3.82	0.0807	0.0709	1.14	0.380	1.14
DLL4	7.36	8.7	0.0061	0.0024	2.53	0.130	2.53
EP300	0.85	1.15	0.5541	0.4501	1.23	0.363	1.23
ERBB2	2.83	5.45	0.1401	0.0228	6.15	0.456	6.15
FZD2	4.59	3.49	0.0416	0.0887	0.47	0.165	-2.13
FZD4	4.83	4.86	0.0352	0.0344	1.02	0.767	1.02
FZD7	5.96	5.44	0.0160	0.0231	0.69	0.070	-1.44
GAPDH	-5.64	-5.52	49.6940	45.7278	1.09	0.292	1.09
GLI1	8.32	7.46	0.0031	0.0057	0.55	0.184	-1.82
GSK3B	-1.28	-0.44	2.4312	1.3582	1.79	0.190	1.79
HDAC1	0.22	0.2	0.8556	0.8675	0.99	0.902	-1.01
HES1	0.1	0.68	0.9320	0.6220	1.5	0.549	1.5
HES5	11.99	13.15	0.0002	0.0001	2.23	0.162	2.23
HEY1	5.11	5.2	0.0289	0.0271	1.06	0.486	1.06
HEY2	10.9	10.21	0.0005	0.0008	0.62	0.058	-1.61
HEYL	13.74	13.66	0.0001	0.0001	0.94	0.814	-1.06
HOXB4	13.65	13.66	0.0001	0.0001	1	0.941	1
HPRT1	2.01	1.52	0.2474	0.3483	0.71	0.282	-1.41
IFNG	13.74	13.66	0.0001	0.0001	0.94	0.814	-1.06
IL2RA	13.74	13.66	0.0001	0.0001	0.94	0.814	-1.06
JAG1	-2.24	-1.76	4.7294	3.3753	1.4	0.303	1.4

Table 2.2 Notch pathway genes non-significantly changed in response to Sox2 overexpression

Gene	AVG dCT		2^-dCt		Fold change	p-value	Fold regulation
	Sox2	par	2^-dCt	par	Sox2/par	Sox2/par	Sox2/par
KRT1	13.74	13.66	0.0001	0.0001	0.94	0.814	-1.06
LFNG	7.69	5.44	0.0048	0.0230	0.21	0.063	-4.73
LMO2	8.26	8.58	0.0033	0.0026	1.25	0.288	1.25
LOR	13.74	13.66	0.0001	0.0001	0.94	0.814	-1.06
MAML2	3.51	4.07	0.0875	0.0596	1.47	0.110	1.47
MMP7	11.1	13.66	0.0005	0.0001	5.88	0.114	5.88
NCOR2	0.39	0.24	0.7605	0.8438	0.9	0.517	-1.11
NCSTN	0.5	0.48	0.7047	0.7162	0.98	0.831	-1.02
NEURL1	7.88	8.28	0.0042	0.0032	1.32	0.344	1.32
NFKB1	1.47	2.23	0.3606	0.2124	1.7	0.212	1.7
NFKB2	1.11	2.39	0.4638	0.1901	2.44	0.150	2.44
NOTCH2	0.93	0.94	0.5255	0.5218	1.01	0.837	1.01
NOTCH2NL	1.02	0.84	0.4937	0.5567	0.89	0.950	-1.13
NUMB	0.9	1	0.5365	0.4994	1.07	0.620	1.07
PAX5	13.58	13.18	0.0001	0.0001	0.76	0.375	-1.32
POFUT1	2.78	2.26	0.1451	0.2085	0.7	0.096	-1.44
PPARG	7.24	6.77	0.0066	0.0092	0.72	0.076	-1.39
PSEN1	0.76	1.15	0.5885	0.4501	1.31	0.349	1.31
PSEN2	3.18	3.25	0.1102	0.1047	1.05	0.685	1.05
PSENEN	2.13	2.63	0.2282	0.1614	1.41	0.289	1.41
PTCRA	12.87	13.19	0.0001	0.0001	1.25	0.590	1.25
RBPJL	10.76	10.02	0.0006	0.0010	0.6	0.375	-1.67
RFNG	1.86	1.4	0.2758	0.3776	0.73	0.582	-1.37
RUNX1	0.35	0.84	0.7819	0.5567	1.4	0.316	1.4
SEL1L	0.28	1.06	0.8245	0.4780	1.73	0.175	1.73
SH2D1A	13.29	13.66	0.0001	0.0001	1.29	0.357	1.29
SHH	13.48	13.54	0.0001	0.0001	1.04	0.706	1.04
SNW1	-0.27	0.2	1.2016	0.8675	1.39	0.197	1.39
STIL	3.38	2.93	0.0959	0.1311	0.73	0.388	-1.37
TLE1	2.03	2	0.2451	0.2503	0.98	0.961	-1.02
WISP1	11.98	10.68	0.0002	0.0006	0.41	0.165	-2.45
WNT11	13.37	13.46	0.0001	0.0001	1.07	0.635	1.07

Table 2.2 continued

Gene symbol	AVG dCT		2^-dCt		Fold Change	p-value	fold regulation
	Sox2	par	2^-dCt	par	Sox2/par	Sox2/par	Sox2/par
APC	10.06	9.8	0.0009	0.0011	0.84	0.122	-1.19
BCL9	9.97	9.09	0.0010	0.0018	0.54	0.155	-1.84
BTRC	7.91	7.97	0.0042	0.0040	1.04	0.998	1.04
CCND1	3.22	3.9	0.1076	0.0672	1.6	0.092	1.6
CCND2	2.78	3.16	0.1459	0.1120	1.3	0.357	1.3
CSNK1A1	3.29	3.9	0.1020	0.0669	1.53	0.395	1.53
CSNK2A1	3.44	3.24	0.0921	0.1057	0.87	0.353	-1.15
CTNNB1	5.01	4.69	0.0310	0.0389	0.8	0.298	-1.26
CTNNBIP1	7.62	7.51	0.0051	0.0055	0.93	0.618	-1.08
DAAM1	5.68	5.78	0.0195	0.0182	1.07	0.524	1.07
DVL2	5.54	5.16	0.0215	0.0279	0.77	0.180	-1.3
EP300	6.01	5.96	0.0155	0.0161	0.97	0.809	-1.04
FGF4	18.31	18.07	0.0000	0.0000	0.85	0.103	-1.18
FOXN1	18.25	16.49	0.0000	0.0000	0.29	0.066	-3.4
FZD1	9.18	8.48	0.0017	0.0028	0.62	0.052	-1.63
FZD4	9.18	9.52	0.0017	0.0014	1.26	0.183	1.26
FZD5	10.1	9.6	0.0009	0.0013	0.71	0.349	-1.42
FZD6	5.52	5.52	0.0218	0.0218	1	0.982	1
FZD8	11.38	10.95	0.0004	0.0005	0.74	0.229	-1.35
GAPDH	-1.36	-1.19	2.5669	2.2886	1.12	0.173	1.12
GSK3A	5.72	5.21	0.0190	0.0270	0.7	0.113	-1.42

Table 2.3 Wnt pathway genes non-significantly changed in response to Sox2 overexpression.

Gene symbol	AVG dCT		2^-dCt		Fold Change	p-value	fold regulation
	Sox2	par	2^-dCt	par	Sox2/par	Sox2/par	Sox2/par
GSK3B	4.3	4.61	0.0509	0.0409	1.24	0.630	1.24
JUN	6.82	7.37	0.0089	0.0060	1.47	0.317	1.47
KREMEN1	8.49	8.54	0.0028	0.0027	1.04	0.986	1.04
LRP6	7.22	7.37	0.0067	0.0060	1.11	0.958	1.11
MAPK8	7.11	7.63	0.0073	0.0051	1.43	0.264	1.43
MMP7	17.31	18.07	0.0000	0.0000	1.69	0.353	1.69
NFATC1	18.12	16.5	0.0000	0.0000	0.33	0.065	-3.08
NLK	6.61	6.9	0.0102	0.0084	1.22	0.231	1.22
PITX2	18.31	18.07	0.0000	0.0000	0.85	0.103	-1.18
PPARD	6.43	6.49	0.0116	0.0112	1.04	0.884	1.04
RHOA	2.01	2.14	0.2488	0.2276	1.09	0.306	1.09
RUVBL1	4.08	4.29	0.0593	0.0513	1.16	0.182	1.16
SFRP1	8.53	8.45	0.0027	0.0029	0.95	0.696	-1.06
SFRP4	18.31	18.07	0.0000	0.0000	0.85	0.103	-1.18
SOX17	17.01	16.8	0.0000	0.0000	0.86	0.865	-1.16
TLE1	6.77	6.61	0.0092	0.0103	0.89	0.426	-1.12
WIF1	18.27	17.3	0.0000	0.0000	0.51	0.078	-1.96
WNT1	18.31	18.07	0.0000	0.0000	0.85	0.103	-1.18
WNT10A	17.07	15.99	0.0000	0.0000	0.47	0.172	-2.12
WNT11	17.63	16.49	0.0000	0.0000	0.46	0.178	-2.2
WNT16	18.31	18.07	0.0000	0.0000	0.85	0.103	-1.18
WNT2	18.2	18.07	0.0000	0.0000	0.92	0.486	-1.09
WNT3A	18.2	16.82	0.0000	0.0000	0.38	0.125	-2.6
WNT5B	10.69	10.18	0.0006	0.0009	0.7	0.173	-1.43
WNT6	18.31	17.03	0.0000	0.0000	0.41	0.083	-2.43
WNT7B	10.51	9.84	0.0007	0.0011	0.63	0.072	-1.59
WNT8A	18.31	17.88	0.0000	0.0000	0.74	0.184	-1.35
WNT9A	9.97	10.27	0.0010	0.0008	1.23	0.415	1.23

Table 2.3 continued

Interestingly, overexpression of Sox2 drives downregulation of three of four NOTCH transmembrane receptors (NOTCH1, 3, and 4), as well as some canonical ligands (JAG2, DLL3, DTX1, and MFNG). Although NOTCH1 is a target gene of Sox2, NOTCH3 is significantly more downregulated in response to an increase in Sox2 (**Figure 2.7C**). Taken together, these results suggest that Sox2 overexpression downregulates upstream components of Notch signaling, perhaps to limit differentiation of prostate basal cells. Furthermore, overexpression of Sox2 in PrECs seems to drive downregulation of negative regulators of Wnt (**Figure 2.7D**), several of which are Sox2 target genes in PrECs (AES, AXIN2, CTBP1, and DKK3). However, downstream actors of canonical Wnt signaling also appear to be downregulated upon overexpression of Sox2.

Discussion

Here we present experimental evidence of a Sox2-positive, castration-resistant epithelial population that contributes to prostatic regeneration. Persisting luminal cells appear to upregulate Sox2 in response to castration, and were also shown to contribute to prostatic regeneration. These data are also in accordance with previous data from our lab demonstrating that exogenous overexpression of Sox2 is sufficient to drive castration-resistance in a hormone-sensitive prostate cancer cell line (Kregel et al., 2013). These data demonstrate that Sox2-expressing luminal cells are intrinsically castration-resistant. Bioinformatic analyses indicate that Sox2 binds a distinct, non-overlapping set of genes in prostate epithelial cells as compared to more canonical clientele genes in embryonic stem cells. Specifically, Sox2 overexpression appears to inhibit Notch signaling, perhaps by activating Wnt signaling.

Previous reports have demonstrated that prostate basal and luminal lineages are largely self-sustained (Choi et al., 2012). Our data are in accordance with this paradigm, and do not

discount the rare bipotent basal stem cell. However, we cannot completely exclude the possibility that rare YFP-labelled basal and luminal cells capable of multipotency exist. Indeed, Cre efficiency was expectantly low (Arnold et al., 2011), perhaps reflecting low activity of the Sox2 promoter during epithelial homeostasis.

Notably, Sox2 appears to mark castration-resistant basal and luminal epithelial cells, as evidenced by YFP signal and endogenous Sox2 staining post-castration. These data are in direct opposition to previous reports in which Sox2-expressing luminal cells are not found in p63-null epithelial grafts in a urogenital sinus recombination assay, indicating that Sox2-positive luminal cells are progeny of p63+ basal cells (Wang et al., 2014a). This tissue grafting assay may not be an ideal recapitulation of the adult murine prostate *in vivo,* and likely reflects an embryonic or postnatal developmental phase (Wang et al., 2013).

In addition to our work, multiple lineage tracing studies have revealed the existence of rare, castration-resistant luminal cells that contribute to prostatic regeneration (Wang et al., 2009; 2015; Yoo et al., 2016). Interestingly, two of these populations, castration-resistant cells expressing either Nkx3.1 (CARNs) or Bmi1 (CARBs), were shown to be distinct, non-overlapping populations (Yoo et al., 2016). Recent work has hypothesized that CARNs are specified in an androgen-dependent manner, as maintenance of viable daughter cells requires AR (Xie and Wang, 2017; Xie et al., 2017; Chua et al., 2018). Previous data from our lab showing the repressive relationship between AR and Sox2 (Kregel et al., 2013) suggest that castration-resistant Sox2-expressing cells are probably not specified in an androgen-dependent manner. However, this hypothesis remains to be explicitly tested, and whether the castration-resistant Sox2-lineage overlaps with either Bmi1, Nkx3.1, or Lgr5 is unclear. Future work should address underpinning mechanisms of how these progenitor cells are specified. In particular, more work is

necessary to fully understand the relationship between Sox2 and AR in a normal, nonmalignant context.

Similarly, gene profiler arrays were done in immortalized PrEC cultures, most of whose constituent cells are of the basal lineage. Therefore, luminal and neuroendocrine cell lineages are underrepresented in these particular studies. Although we have discovered novel Sox2 target genes in prostate basal cells, particularly in the Notch and Wnt signaling pathways, it is clear that more work should be done to understand how Sox2 expression influences these pathways *in vivo*. Characterizing the expression profiles of Wnt and Notch pathways, particularly in Sox2-positive luminal cells, would be beneficial to our understanding of adult progenitor cell biology in prostate homeostasis and regeneration.

Multiple reports detailing distinct markers of castration-resistant luminal cells beg the question of whether prostatic regeneration can be achieved via facultative progenitors that receive signals from their surrounding niche. These progenitors, perhaps specified based on localization within a niche, could potentially exist alongside pre-determined and static progenitor populations. Future studies examining the molecular differences between these populations may shed light on this hypothesis. Indeed, whether the Sox2-expressing lineage is required for prostatic homeostasis and regeneration is unknown.

Major questions that remain in the field center on the origin of castration-resistant prostate cancer, and the underpinning mechanisms of how castration-resistance dictates disease course, and/or is acquired as a result of treatment resistance. Several recent lineage tracing studies indicate that while it is possible for both basal and luminal cells to serve as the cells of origin for prostate cancer, luminal cells appear to be more sensitive to malignant transformation (Wang et al., 2014b). Our group and others have begun to establish the potential link between

Sox2 expression and prostate cancer biology, specifically how tumor cells may escape frontline, luminal cell-specific therapeutics that target AR (Kregel et al., 2013; Jiang et al., 2017; Kar et al., 2017; Ku et al., 2017; Mu et al., 2017). Further studies, particularly whether castration-resistant Sox2-expressing cells are more prone to oncogenic transformation, are required to understand how Sox2 expression in tumorigenic cells may alter natural history of the disease.

As expression of SOX2 in human prostate cancer might indicate a phenotypic switch of the cancer cells, it is crucial to understand resultant changes in gene expression throughout tumor initiation and progress as a result of an upregulation of SOX2. Interestingly, SOX2 appears to fulfill a tumor suppressor function in gastric tumors driven by canonical Wnt signal activation (Sarkar et al., 2016). In murine models of skin squamous cell carcinoma (Boumahdi et al., 2014) and medulloblastoma (Vanner et al., 2014), lineage ablation of Sox2-expressing cells abrogated tumor initiation and lead to tumor regression. In contrast, the Sox2 lineage was found to be dispensable for initiation, growth, and metastasis of melanoma (Schaefer et al., 2017). Taken together these findings highlight the criticality of context-dependent signaling concerning Sox2 in relation to its function and cellular lineage. SOX2 itself does not represent a highly druggable target protein: as a transcription factor, it is difficult to design highly specific small-molecule inhibitors to its active site that are also targeted to only cancer cells of interest (Fontaine, 2015). From the perspective of therapeutic design, it is possible that some clientele genes of SOX2 represent highly druggable targets. Understanding the signaling mechanisms that control prostatic progenitor cell pools is a prerequisite to discerning molecular pathways that play key roles in prostate development and disease. These studies may identify novel targets and lay the groundwork for clinical risk stratification and personalized treatment of prostatic disease.

CHAPTER III

MAGNETIC RESONANCE IMAGING AND MOLECULAR CHARACTERIZATION OF A HORMONE-MEDIATED MURINE MODEL OF PROSTATE ENLARGEMENT AND BLADDER OUTLET OBSTRUCTION

Abstract

Urinary complications resulting from benign prostatic hyperplasia (BPH) and bladder outlet obstruction (BOO) continue to be a serious health problem. Novel animal model systems and imaging approaches are needed to understand the mechanisms of disease initiation, and to develop novel therapies for BPH. Long-term administration of both estradiol (E) and testosterone (T) in mice can result in prostatic enlargement and recapitulate several clinical components of lower urinary tract symptoms (LUTS). Here we utilize longitudinal magnetic resonance imaging (MRI) and histologic analyses to quantify changes in prostatic volume, urethral volume, and genitourinary vascularization over time in response to estradiol-induced prostatic enlargement. Our data demonstrate significant prostatic enlargement by 12 weeks post-treatment, with no detectable immune infiltrate by macrophages, T- or B-cell populations. Importantly, the percentage of cell death as measured by TUNEL was significantly decreased in the prostatic epithelium of treated animals as compared to controls. We found no significant change in prostate cell proliferation in treated mice when compared to controls. These studies highlight the utility of MRI to quantify changes in prostatic and urethral volumes over time. In conjunction with histological analyses, this approach has the high potential to enable mechanistic studies of initiation and progression of clinically relevant LUTS. Additionally, this model is tractable for investigation and testing of therapeutic interventions to ameliorate or potentially reverse prostatic enlargement.

Introduction

Benign prostatic hyperplasia (BPH), or prostatic enlargement, is the pathophysiological process by which the prostate gland undergoes a second, abnormal growth phase that worsens with age (McNeal, 1978; Isaacs, 1987). At least 50% of men between the ages of 50 and 60 show pathologic signs of BPH, and by age 90 the incidence of clinical BPH increases to 90% (McVary, 2003; Izumi et al., 2014). Lesions removed at prostatectomy indicate that the process of BPH may be initiated even before the patient is 30 years old (Berry et al.).

Surrounding the urethra as it passes through the prostate, the transition zone is the site of nearly all clinically-significant BPH (McNeal, 1978; 1981). As a result of prostatic hyperplasia, patients can experience bladder outlet obstruction (BOO) and subsequent lower urinary tract symptoms (LUTS), both of which worsen with age. LUTS can include urinary retention, nocturia, weak stream, dribbling, pain and frequent daytime urination. These symptoms represent substantial quality of life challenges and significant co-morbidities (Izumi et al., 2014). While successful in some patients, some front-line treatments for BPH patients can result in significant financial and physiological burdens, and ultimately lose efficacy (Isaacs, 2008). As the success of these therapies can be short-lived, other factors may be involved in BPH pathogenesis. Currently, there is a paucity of animal models to test molecular and physiologic hypotheses pertaining to the initiation and progression of BPH. This gap in knowledge represents a hurdle in our progress toward developing more effective therapies to treat BPH.

It has long been hypothesized that BPH can result from aberrant stem cell activation and subsequent hyper-proliferation, an “embryonic reawakening” (McNeal, 1978; Isaacs, 1987). Lack of sufficient *in vivo* models, however, has made this hypothesis difficult to test directly (Notara and Ahmed, 2012; Prajapati et al., 2013). Foundational studies done in canines demonstrate that treatment with a combination of androgen- and estrogen-receptor agonists could

induce prostatic hyperplasia (DeKlerk et al., 1979). Moreover, the pathology of the hormonally induced hyperplasia was not fundamentally different than the spontaneous hyperplasia found in older Beagles (DeKlerk et al., 1979).

The transcription factor Sox2 (SRY [sex determining region Y]-box 2) has been recently shown to be expressed in BPH nodules of human patients (Bae et al., 2010; Yu et al., 2014). Sox2 is well-known as an embryonic stem cell factor that maintains pluripotency and regulates epithelium formation in fetal development (Arnold et al., 2011; Sarkar and Hochedlinger, 2013). Considering these data together, we therefore wanted to more closely investigate Sox2 expression and any changes in the Sox2+ prostatic epithelial cell lineages as a result of hormonal dysregulation.

Recently, it has been shown that long-term administration of both estradiol (E) and testosterone (T) using slow-release implants in mice can induce bladder obstruction and model key components of prostatic hyperplasia (Nicholson et al., 2012). Hormonal dysregulation results in urinary tract complications consistent with clinical BOO in men, including bladder enlargement and increase in bladder smooth muscle and collagen (Nicholson et al., 2015). Moreover, as a result of T+E treatment, mice displayed a significant decrease in the size of the prostatic urethral lumen, increased prostate mass, and increased number of prostatic ducts associated with the prostatic urethra (Nicholson et al., 2012). A follow-up study by the same group established estrogen receptor alpha (ERα) as a key mediator of BOO/BPH pathophysiology in this model, mimicking the hormonal milieu found in aging men (Nicholson et al., 2015). While these data are novel and compelling, the original group harvested tissue from their mice at defined time points, potentially independent of clinical presentation, and were not able to fully capture the natural history of this model. Adapting a method to utilize imaging

analyses of these mice over time would allow us to efficiently quantify changes in prostate and urethra volume over time and measure changes in response to therapy.

Clinically, magnetic resonance imaging (MRI) has frequently been used to evaluate prostatic disease as it provides a relatively high spatial resolution as well as soft tissue contrast (Kwak et al., 2015; Guneyli et al., 2016). Notably, multi-parametric MRI – T2-weighted (T2W) MRI, diffusion-weighted MRI (DWI), dynamic contrast-enhanced (DCE) MRI, and MR spectroscopy – is capable of identifying prostate cancers with high sensitivity (Turkbey et al., 2011). MRI can potentially be used to estimate zone-specific prostatic volume, detect enlarged zones, and approximate stromal/glandular ratio (Schiebler et al., 1989; Grossfeld and Coakley, 2000; Visschere et al., 2016).

Here we investigate the utility of MRI with histological analyses to quantify changes in prostate volume and cellular composition following hormone-induced BOO and prostatic enlargement. In our hands, we can recapitulate previously reported estradiol-mediated urethral thickening and bladder outlet obstruction in mice. Moreover, we find that MR imaging is a powerful tool with which to longitudinally monitor prostatic enlargement and genitourinary vascularization. Interestingly, in this mouse model, we demonstrate that Sox2 expression was no longer confined to the basal cell compartment at 10 weeks of treatment in the dorsal lobe of mice treated with T+E as compared to T controls.

Materials and Methods

Animals

All animal care and use was approved by the University of Chicago Institutional Animal Care and Use Committee (IACUC protocol #72294). 11 week old, post-pubescent C57/BL6 males were castrated as previously described (Kregel et al., 2013). Briefly, animals were first

anesthetized using ketamine/xylazine. Following preparation of the surgical site, an incision was made in the scrotum. For each testicle, the testis, vas deferens, and attached testicular fat pad were pulled out of the incision and tied off. The testis, vas deferens, and fatty tissue were severed just below the surgical knot. The scrotal incision was closed with a non-absorbable Nylon suture (Med-Vet; Mettawa, IL). After castration, silastic hormone pellets containing a blend of 11.25mg testosterone and 1.25mg estradiol (Sigma; St. Louis, MO) were surgically implanted to induce hormonal dysregulation as previously described (Nicholson et al., 2012; 2015). Control mice were implanted with a 12.5-mg/pellet/mouse testosterone pellet. Implants were used according to Sedelaar et al., whereby a 1cm implant maintains host testosterone levels at 5.3 ± 0.5 ng/mL (18.2 nM) which is similar to eugonadal adult human males (Michiel Sedelaar et al., 2013). Animals were age-matched across conditions. Isoflurane anesthesia was used in all *in vivo* imaging studies of mice, all efforts were made to minimize any suffering, and the mice were humanely euthanized following the experiment for purposes of histology. Mice treated with T+E who became moribund were sacrificed humanely and censured accordingly.

Magnetic Resonance Imaging and Analysis

A 9.4 Tesla small animal scanner (Bruker, Billerica, MA) with 11.6 cm inner diameter and actively shielded gradient coils (maximum constant gradient strength for all axes: 230 mT/m) was used to acquire MR images (Mustafi et al., 2015). The mouse was placed supine on an animal holder and inserted into a 30-mm-diameter quadrature mouse volume coil (Bruker, Billerica, MA). Multi-slice Rapid Acquisition with Relaxation Enhancement (RARE) T2-weighted images with fat suppression were acquired with the following parameters: $TR/TE_{effective}$=4000/20 ms and 8000/40 ms, field-of-view (FOV) = 25.6 mm x 25.6 mm, matrix size=256^2, slice thickness=0.5 mm, RARE factor=4, number of averages = 2 with 47 slices in the

axial plane. For time-of-flight (TOF) angiography, a flow compensated, T1-weighted sequence with a short TR and thin slices was used to maximize inflow effects and depict flowing blood as a bright signal. Parameters for TOF were: $TR/TE_{effective}$=10/3 ms, flip angle = 60°, FOV = 25.6 mm x 25.6 mm, matrix size = 256 x 256, slice thickness = 0.5 mm, number of averages = 4 with 47 slices. In-plane resolution for TOF was 100 microns as in T2-weighted images. The acquisitions time for each slice was 10.2 s and the total acquisition time for this TOF sequence was 8 minutes.

An integrated software program, Amira (FEI Visualization Sciences Group, Burlington, MA), was used to measure the volumes of prostate and urethra, and to create three-dimensional images. By orienting the *in vivo* MR images and the *ex vivo* MR and histology images in the same direction, MRI was accurately correlated with histopathology. Regions-of-interest (the prostate and the urethra) were labeled on each slice of each week of T2-weighted images. To measure blood volume, the 5 center slices of prostate were identified on the T2-weighted images acquired in weeks 10 and 12 post-treatment. The corresponding TOF images were used to measure and label the blood volumes in those five center slices. Volume was calculated from the total number of pixels in each region-of-interest multiplied by voxel volume (.005 mm^3). Volumes were calculated for all mice for each week before the mouse was sacrificed. Mann Whitney U test were performed for statistical analysis. A p-value <0.05 was considered significant.

Preparation of Mouse Urogenital Glands for Ex Vivo MRI and Histology

Following *in vivo* MRI studies, urogenital glands, including prostate, seminal vesicles, bladder, and penis, were excised from the mouse body and placed in 10% formalin for two weeks for tissue fixation. Prior to *ex vivo* imaging the tissue sample was removed from the

formalin, rinsed daily with phosphate buffered saline (PBS, Fisher Scientific, Waltam, MA) for 3 days, and then placed between two layers of pathology foam. Immediately prior to imaging the tissue was washed twice with fomblin (Solvay Solexis, West Deptford, NJ) and then saturated with fresh fomblin. The sample was folded in plastic wrap and placed in the MRI coil for imaging. Fomblin is an oily, fluorinated polymer with no MRI signal that is used to keep the tissue moist while imaging in order to minimize susceptibility gradients. Following *ex vivo* MRI, the sample was removed from the wrap, washed thoroughly in PBS, and put in a histology cassette in ethanol. Because the *ex vivo* tissue and the H&E-stained tissue were scanned in the same orientation, the *ex vivo* MR images bridged the gap between *in vivo* MRI and histology to facilitate accurate correlation (Mustafi et al., 2015). The same 9.4T scanner was used to acquire *ex vivo* MR images, with the tissue being held in an eight-leg, low-pass, half-open birdcage coil (length=3 cm, width=3 cm, height=2 cm) that was built in the lab. *Ex vivo* three-dimensional images were acquired with a T_2-weighted sequence with fat suppression and with $TR/TE_{effective}$=4000/20 ms, FOV=25.6 mm x 25.6 mm x 8 mm, matrix size=384 x 384 x 120, isotropic resolution=67 microns, and with an average of 5.

Immunohistochemistry and Image Acquisition

Five-micrometer thick sections were first baked and rehydrated using a series of xylene and ethanol gradients. Antigen retrieval was performed by heating slides with a steamer in 10mM citrate buffer (pH 6) for 20 minutes. Sections were blocked and incubated with primary antibodies for 1-2 hours at room temperature. Antibodies were used as follows: p63 clone 4a4 (ATCC), Ki67 (cat. No. RM-9106S, Thermo Scientific), CD3 (cat. No. Ab16669, Abcam), F4/80 (cat. No. MCA497GA, abD Serotec), CD31 (cat. No. ab28364, Abcam), and B220 (cat. No. 553085, BD). Additional markers include Sox2 (cat. No. AF2018, R&D Systems), cytokeratin 5 (cat. No. 905501, BioLegend), cytokeratin8+18 (cat. No. ab668, Abcam). Following TBS wash,

the antigen-antibody binding was detected with Envision+System (DAKO, K4001, K4002, K4003) and DAB+Chromogen (DAKO, K3468). Tissue sections were briefly immersed in hematoxylin for counterstaining and were cover-slipped. Histology and immunohistochemistry images were acquired on the Scanscope XT (Aperio). An average of 5-10 fields per mouse at each time point (n = 2-5 mice) were traced and subsequently analyzed. Positive nuclei were quantified using a Nuclear Stain or Positive Pixel algorithm in ImageScope, optimized on control slides.

Results

Estradiol-mediated hormonal dysregulation induces prostatic enlargement as detected by MRI

Post-pubescent male mice were castrated and surgically implanted with subcutaneous, silastic implants containing testosterone alone (T-control), or a combination of testosterone and estradiol (T+E) (Nicholson et al., 2012). We evaluated mice from both the control and experimental arms using MRI at 2-4 week intervals post-implantation and then sacrificed accordingly for histologic analyses (**Figure 3.1 panel A**). Figure 1 illustrates an increase in overall prostate volume when measured longitudinally via MRI. We observed a significant increase in prostate volume of mice treated with T+E as compared to T controls; this increase in volume was statistically significant at 12 weeks post-hormone implantation (**Figures 3.1B and C**). Serial analyses of prostate volume over time demonstrated that the prostatic volume of mice in the T+E group showed approximately a 2-fold change in prostate volume ($p = 0.01$) as compared to the control group, whereas control mice showed no overall significant change over time (**Figures 3.1C and D**).

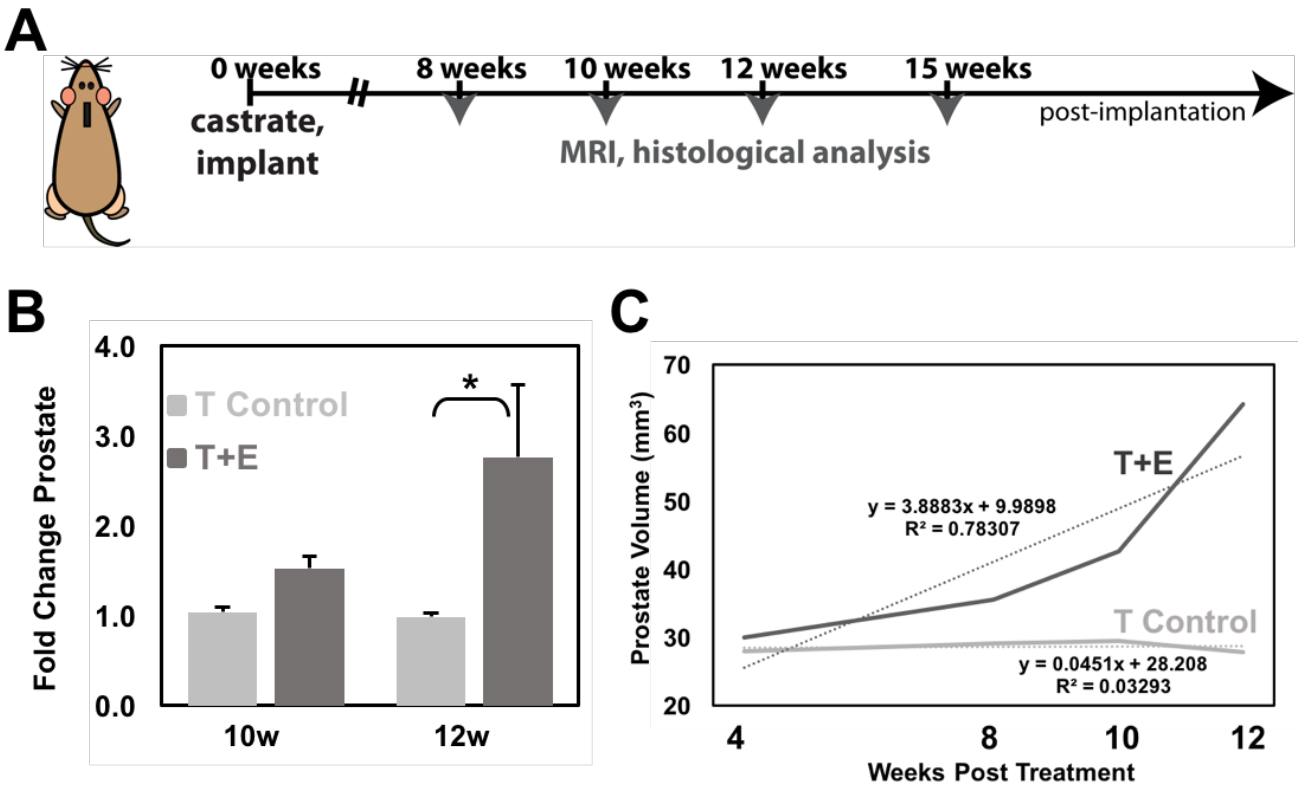

Figure 3.1: Longitudinal magnetic resonance imaging (MRI) analyses of prostatic enlargement in mice treated with combined testosterone (T) and estradiol (E). A: Schematic of experimental approach, whereby 10-week–old male C57BL6 mice were castrated and given a s.c. silastic implant containing either testosterone alone (T control) or a 10:1 ratio of testosterone and estradiol (T+E). At 8, 10, 12, and 15 weeks after castration, mice were imaged and tissues were obtained for histological analyses. **B:** Quantification of prostate volume by MRI demonstrates a significant increase in prostatic volume beginning at 12 weeks after treatment. **C:** Longitudinal analyses demonstrate an approximate doubling of prostatic volume in the T+E condition as compared to the T-control condition. The dotted lines represent a best-fit curve for each of the cohorts.

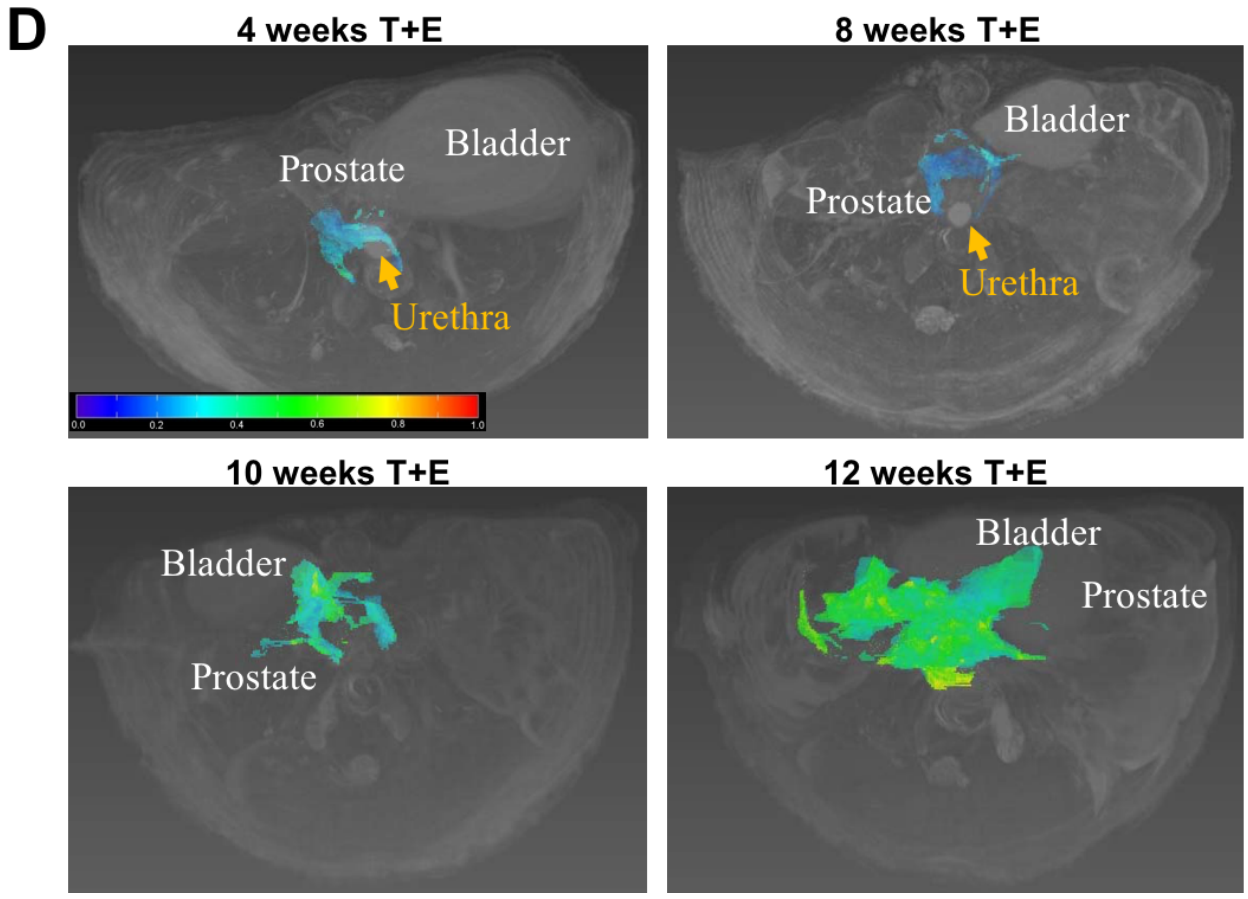

Figure 3.1 continued: D: Representative MR images illustrating changes in prostate volume as a function of time in mice treated with T+E. The prostate volume is indicated in color—a color bar is shown for the hyperintense prostate lesion on T2-weighted images; other anatomical sites (bladder and urethra) are also noted. The heat map correlates to fluid density, where red is more intense and blue is less intense. $*P < 0.05$.

Prostate Enlargement is Associated with Decreased Urethral Volume and Increased Blood Vessel Volume

To further characterize the prostatic enlargement associated with T+E treatment, we also utilized MRI to measure prostate blood volumes and prostatic urethra volume. Although we noted some variability among mice, quantification of prostatic urethral volume demonstrated a significant reduction in volume at 12 weeks post-hormone treatment ($p = 0.02$, **Figure 3.2 panel A**). Multiple mice exhibited a distended urethra as a result of T+E treatment (**Figure 3.2B**). We observed urine retention in the bladders of multiple mice after the 12-week treatment time point. Prostate blood volumes were measured using TOF (time-of-flight) angiography, and mice treated with T+E had an average blood volume of 15.3 mm^3, while the average blood volume of the T-control treated mice was 9.2 mm^3 ($p = 0.01$, **Figures 3.2C and D**). This increase in blood volumes was corroborated by immunohistochemistry staining of CD31, an endothelial cell marker, and was observed even at the 10-week time point prior to notable prostatic enlargement (**Figure 3.2E**).

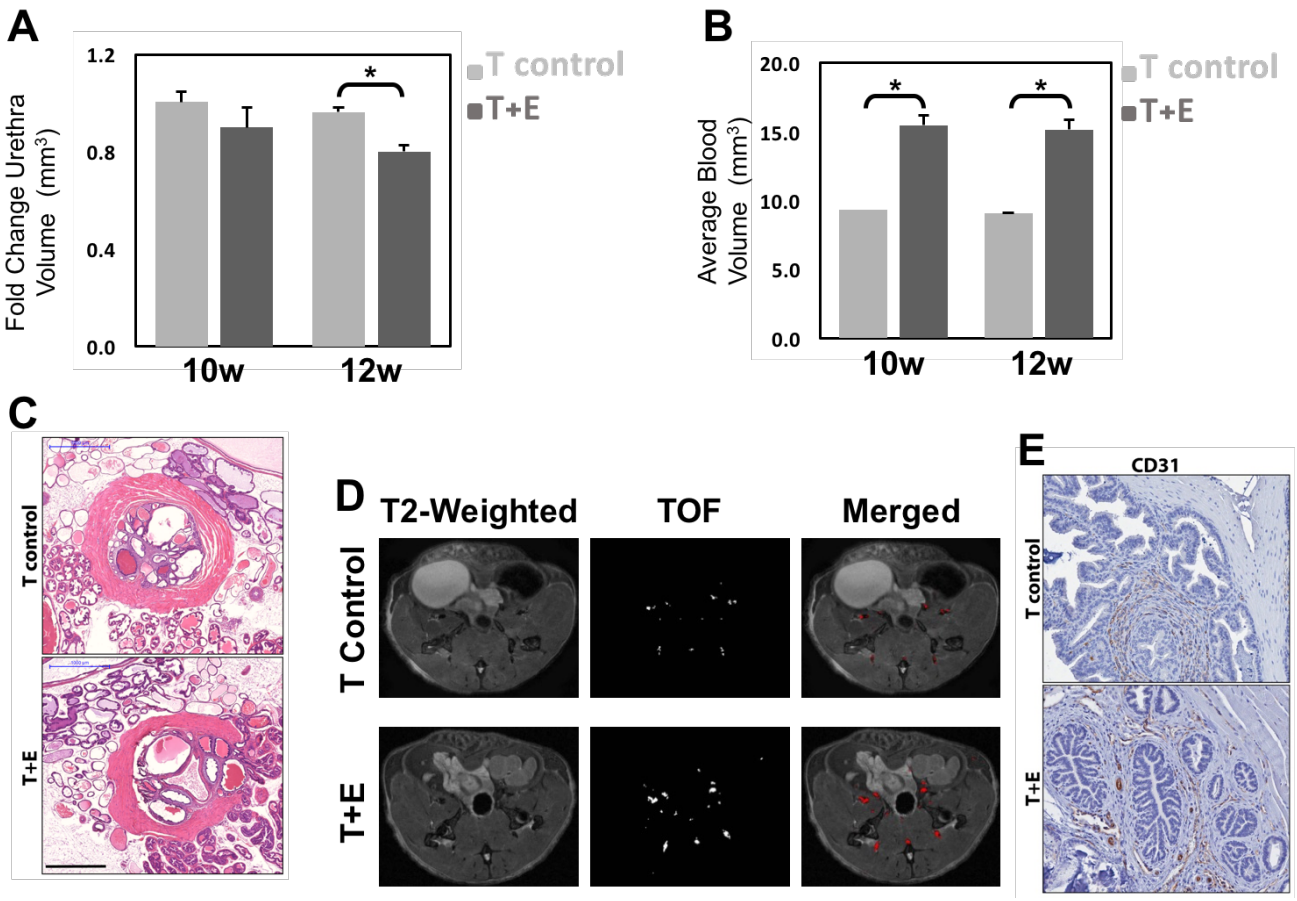

Figure 3.2: Urethral volume decreases and prostate blood vessel volume increases in mice with enlarged prostates. A: Quantification of prostatic urethral volume from magnetic resonance imaging demonstrates a significant decrease on prostatic enlargement. **B:** Quantification of prostatic blood vessel volume demonstrates a significant increase in blood vessel volume before significant prostatic enlargement at 12 weeks. **C:** Hematoxylin and eosin staining of representative urethral sections at 15 weeks after treatment in both the testosterone and estradiol (T+E) and T-treated cohorts of mice reveals a narrowed urethral lumen. **D:** T2-weighted and time-of-flight (TOF) images illustrating changes in blood vessel volume in the T+E mice as compared to the testosterone alone (T-control) mice at 12 weeks. **E:** CD31 immunohistochemical staining reveals an increase in endothelial cells in prostatic glands in T+E treated mice as compared to T controls. $^{*}P < 0.05$. Scale bars = 200 μm (**C**). Original magnification: ×2 (**C**); ×20 (**E**).

Analyses of enlarged prostates reveals predominantly normal histology

In order to capture more high-resolution analyses of prostatic volume and determine whether certain prostatic lobes were disproportionally impacted by the T+E treatment, we conducted *ex vivo* MRI (**Figure 3.3**). This figure illustrates that *in vivo* MRI images can be precisely correlated with *ex vivo* histology images. Histologic analysis of enlarged prostate glands (T+E) showed predominantly normal histology with rare foci of epithelial hyperplasia with mild nuclear atypia in the dorsal prostate (Shappell et al., 2004). Such changes are comparable to what is observed in mice 1-2 years of age, even though our oldest mouse was 26 weeks at the 15-week post-treatment time point. Stromal thickness and inflammatory cell infiltrate was similar to T-control group and not above the background level expected in untreated mice.

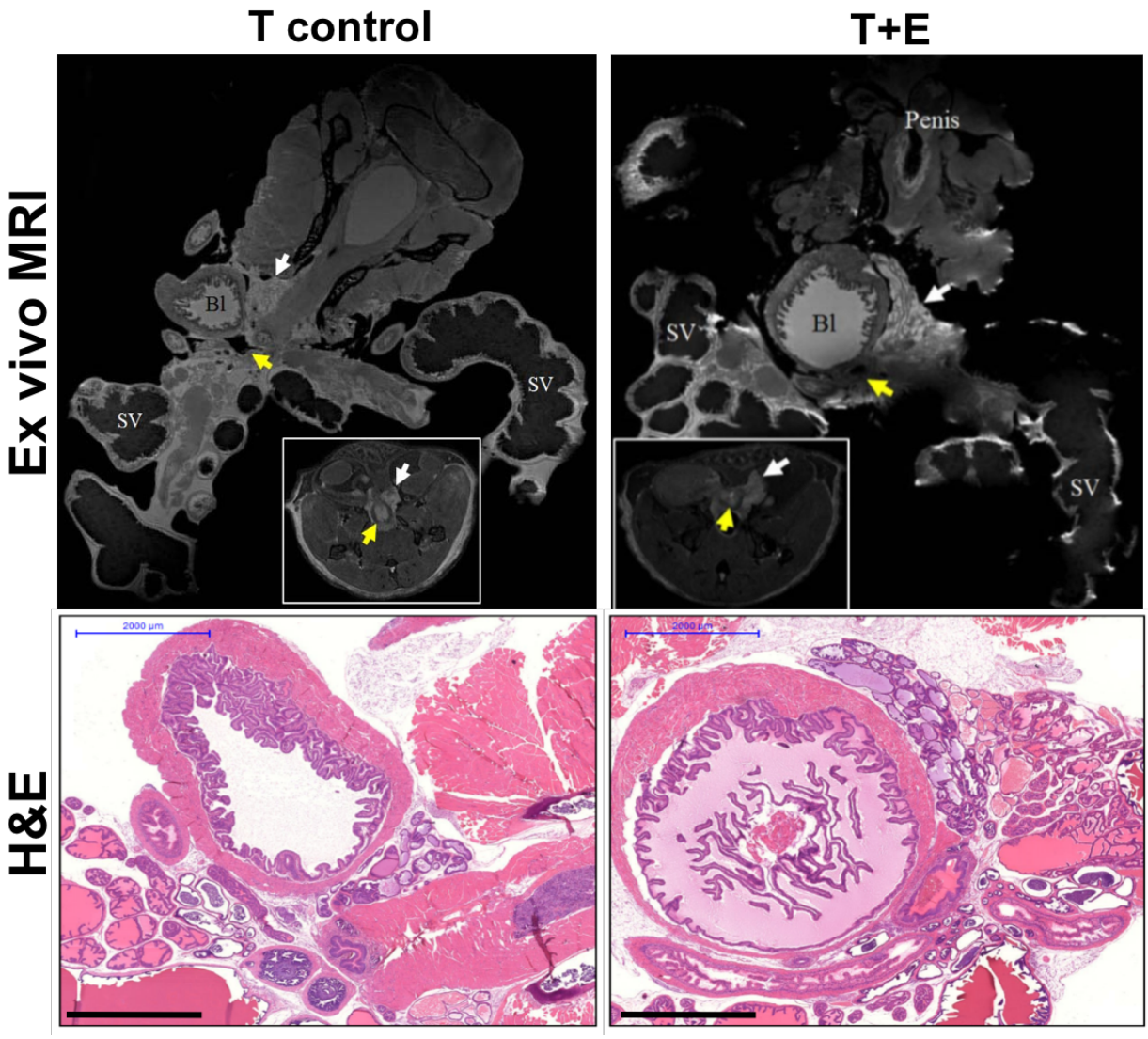

Figure 3.3: Ex vivo magnetic resonance imaging (MRI) and histological analyses of prostatic enlargement. Top row: High-resolution MRIs of prostates removed from the animal at the experimental end point. **Insets:** Invivo images of prostate before removal and *ex vivo* imaging. **White arrows** indicate the prostate, whereas the **yellow arrows** indicate the urethral opening. **Bottom row**: Hematoxylin and eosin (H&E) staining of prostates imaged *ex vivo*. Scale bars = 2000 µm (**bottom row**). Original magnification: ×8 (**top row**); ×1 (**insets**). Bl, bladder; SV, seminal vesicle.

Prostatic inflammatory infiltrate is not altered as a result of estradiol treatment

Given the increased blood vessel density during prostatic enlargement we investigated whether there was an increased prostatic inflammatory infiltrate in the T+E treated mice, and whether such an increased in immune cell infiltration might be an underpinning mechanism of prostatic enlargement. Analyses of H&E sections did not reveal any overt immune cell infiltrates in the T+E condition when compared to the T-control condition. Immunohistochemical staining and quantification of macrophages (F4/80), T-cells (CD3), and B-cells (B220) document no significant changes in cell populations within enlarged prostates (**Figure 3.4**). These data do not support a mechanism of inflammation-induced enlargement, but do not preclude the possibility that differential behavior of the immune cells present, or other populations, may contribute to prostatic enlargement. It is also possible that the time points assessed were not optimized for the detection of maximal immune cell infiltrate.

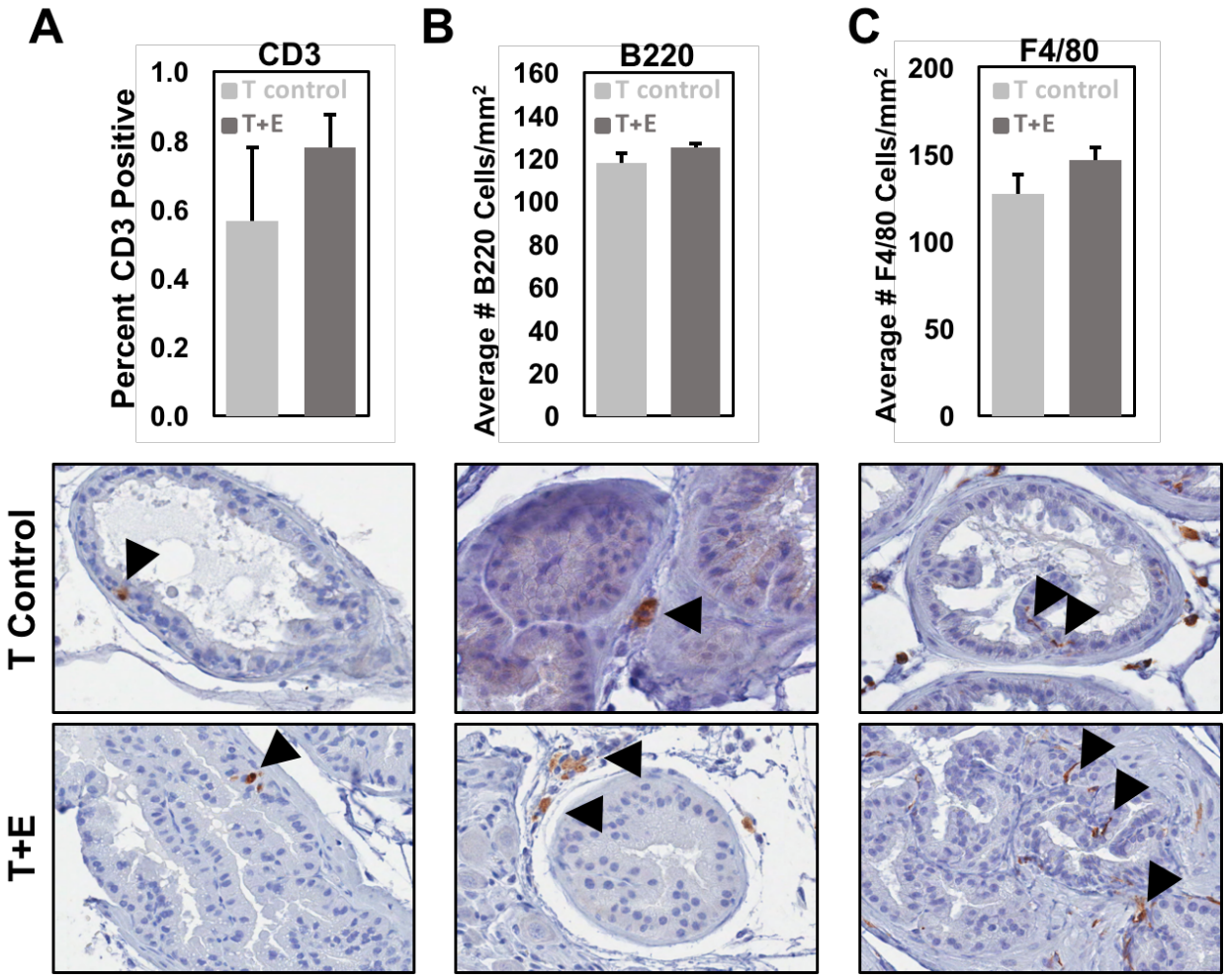

Figure 3.4 Quantification of immune infiltrates into enlarged versus control prostates. To measure changes in immune cell populations after prostatic enlargement, we stained and quantified the presence of T cells via CD3 (**A**), B cells via B220 (**B**), and macrophages via F4/80 (**C**). Data from 12- and 15-week time points, after significant prostatic enlargement, were combined for increased statistical power. We observed no statistically significant change in T-cell, B-cell, or macrophage populations on prostatic enlargement. Representative images of immunostaining are shown, each from the dorsal lobe. **Arrowheads** represent positive cells for immunohistochemical stain of corresponding markers. Original magnification, ×40 (**A–C**). T control, testosterone alone; T+E, testosterone and estradiol.

Decreased cellular death, but not increased cellular proliferation, contributes to prostatic enlargement

The observed lack of robust epithelial hyperplasia, stromal hyperplasia, or immune cell infiltrates during prostatic doubling led us to investigate whether there were significant changes in cell proliferation or death during prostatic enlargement. Tissues at 12 and 15-week time points were stained for the proliferation marker Ki-67 or using a Terminal deoxynucleotidyl transferase (TdT) dUTP Nick-End Labeling (TUNEL) assay to detect dying cells. Quantification of staining across all prostatic lobes demonstrated no significant differences in the percentage of Ki-67 positive cells between T-control vs. T+E treated conditions (**Figure 3.5 panel A**). In addition, we tested whether a different population of cells, such as luminal epithelial cells, was proliferating in response to T+E treatment. We thus conducted co-immunofluorescent staining of Ki-67 along with a luminal cell-restricted cytokeratin (CK8) and a basal cell-restricted cytokeratin (CK5). Comparison of T-control vs. T+E treated mice document that Ki-67 expression was detected in both luminal and basal epithelial cells but was not different between T-control vs. T+E conditions (**Figure 3.5B**). Detection and quantitation of cell death by TUNEL, however, demonstrated that the percentage of dying cells decreased dramatically in T+E treated mice compared to T-control mice (**Figure 3.5C**). These data demonstrate that decreased cellular death, but likely not increased cellular proliferation, in the T+E treatment condition contributes, at least in part, to prostatic enlargement.

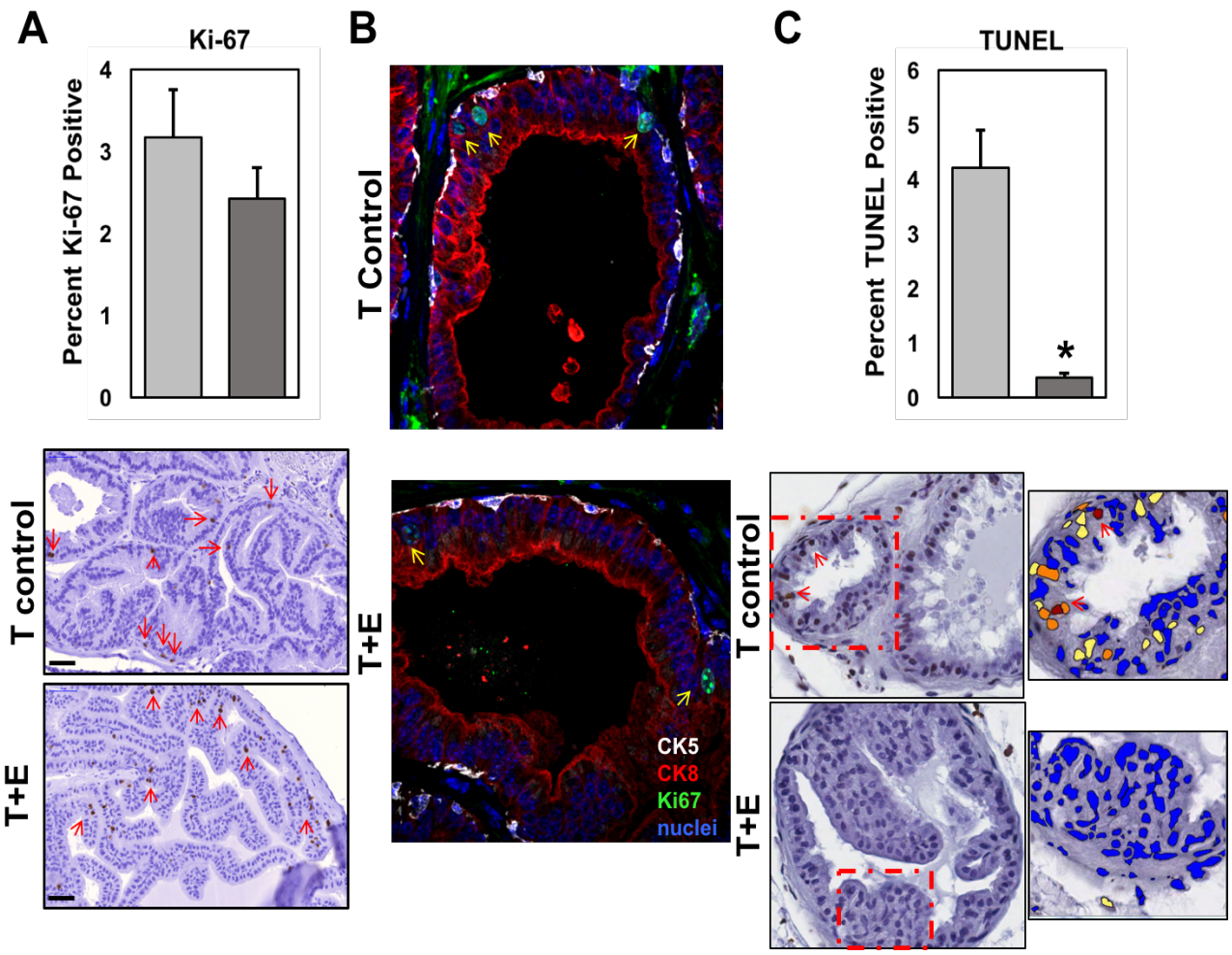

Figure 3.5: Decreased cell death, but not increased cell proliferation, is associated with prostatic enlargement. A: Quantification of Ki-67 positivity, used herein as an indicator of proliferation, demonstrates no significant increase in the percentage of proliferating cells in the testosterone and estradiol (T+E) cohort of mice. Data from 12- and 15-week time points were combined for increased statistical power (5 to 10 fields quantified per mouse). Representative images of Ki-67 immunostaining (each from the dorsal lobe) are shown. **Red arrows** denote Ki-67^{+} cells. **B:** Immunofluorescence analyses of Ki-67 positivity (green) in both CK5-positive basal epithelial cells (white) and CK8-positive luminal epithelial cells (red) demonstrate no change in the population of epithelial cells undergoing cell proliferation in the T+E versus testosterone alone (T-control) mice. Nuclei are counterstained with DAPI in blue. **Yellow arrows** denote Ki-67^{+} cells. Representative images of immunostaining are shown. **C:** Quantification of cell death using terminal deoxynucleotidyl transferase dUTP nick-end labeling (TUNEL) staining via immunohistochemistry (5 to 10 fields quantified per mouse) demonstrates a significant reduction in cell death on prostatic enlargement. eSlide Manager software version 12.1.0.5029 (Aperio) was used to count positive cells using a Positive Nuclear Algorithm optimized on test and control slides (**dotted boxes** shown at higher magnification in the **right panels**). Representative images of immunostaining are shown. Blue cells are negative for TUNEL, yellow cells are 1+ positivity, orange cells are 2+ positivity, and maroon cells are 3+ positivity (**red arrows** denote 3+ TUNEL^{+} cell nuclei). n = 4 mice (**A**); n = 2 mice (**C**). $^{*}P < 0.05$ versus T control. Original magnification, ×40 (**A–C**).

Sox2 is not upregulated as a result of estradiol treatment

We and others have previously shown that expression of the pluripotency factor Sox2 can potentiate pro-survival intercellular signaling in prostate cells (Jia et al., 2011; Lin et al., 2012; Li et al., 2014; Kar et al., 2017). Given that we observed significantly decreased cellular death in estradiol-treated mice, we wondered if we would see a concomitant change in Sox2 expression. Interestingly, we do not find a significant upregulation of Sox2 in human BPH nodules as compared to adjacent normal transition zone (**Figure 3.6**).

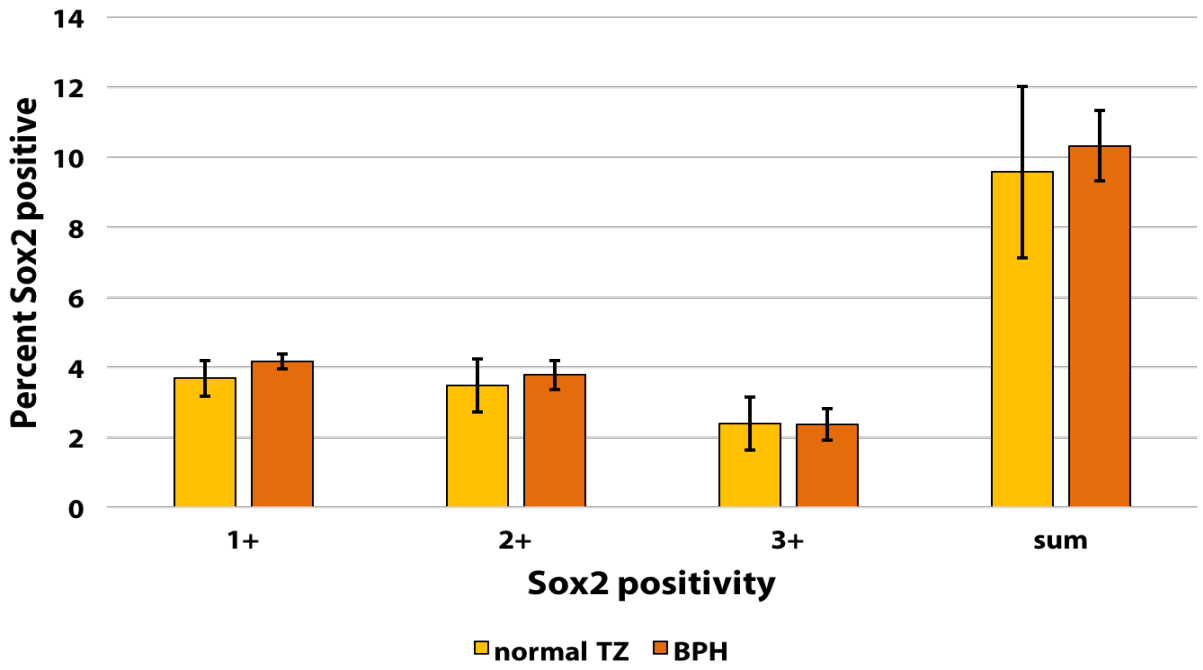

Figure 3.6: Sox2 is not significantly upregulated in human BPH tissue as compared to adjacent normal tissue. Quantification via immunohistochemistry stain (5 to 10 fields quantified per patient, n= 6 patients) demonstrates no significant differences in Sox2 expression in BPH epithelial nodules (orange bars) as compared to normal adjacent transition zone (yellow bars). eSlide Manager software version 12.1.0.5029 (Aperio) was used to count positive cells using a Positive Nuclear Algorithm optimized on test and control slides.

Discussion

Here we demonstrate that long-term treatment of mice with testosterone and estradiol induces a significant increase in prostatic volume with a concomitant decrease in urethral volume. We utilize MR imaging in conjunction with histological analyses to investigate the mechanistic underpinnings of progression of hormone-induced LUTS in a recently established mouse model (Nicholson et al., 2012; 2015). *In vivo* MR imaging was particularly useful in longitudinal quantification of prostatic and urethral volumes (**Figures 3.1B, 3.1C, 3.2A**). *Ex vivo* MR scans provided a high-resolution image of increased prostatic cellularity after 15 weeks of hormonal treatment. Using histological analyses we did not observe overt epithelial or stromal hyperplasia or immune infiltrate by B- or T-cells in prostates of T+E treated animals as compared to controls. However, there was a significant reduction in TUNEL-positive prostatic epithelial cells in the T+E treated cohort at 15 weeks post treatment.

Foundational studies on the effects of steroid hormones on canine prostate growth have documented that estrogen treatment significantly augments androgen effects, inducing a 4-fold increase in total canine prostate weight and DNA content (Walsh and Wilson, 1976; DeKlerk et al., 1979; Coffey and Walsh, 1990). Furthermore, treatment of a castrated dog with estrogens in conjunction with testosterone results in either normal glandular growth, or, if used in tandem with dihydrotesterone, glandular hyperplasia. Taken together, these data indicate that changing ratios of androgens and estrogens, such as in the aging process, might promote abnormal prostatic growth (DeKlerk et al., 1979; Coffey and Walsh, 1990). Indeed, dogs and primates are the only mammals known to spontaneously develop symptomatic BPH. This pathophysiology has been attributed to encapsulation of the prostate by fascial layers, enabling urethral obstruction to occur as a consequence of increased prostatic tissue mass (Nicholson et al., 2012; 2015).

Despite fundamental differences in prostate anatomy, the effects of hormone-mediated prostatic growth have been recapitulated in studies done using rodents. Low doses of estrogen given to pre-pubescent male rats sensitize the adult prostate to testosterone-mediated growth as measured by ventral prostate wet weight (Coffey, 2001). More recently, it was reported that long-term treatment of mice with testosterone and estradiol induces glandular prostatic growth, bladder outlet obstruction, and voiding dysfunction in male mice (Nicholson et al., 2012; 2015). Specifically, estradiol treatment of mice caused morphological changes in the proximal urethra, an increased number of periurethral prostatic ducts, and narrowing of the urethal lumen. It has been postulated that an increase in the prostate tissue encapsulated within the thick rhabdosphincter in mice may result in restriction of urinary flow, analogous to BOO found in men due to BPH (Nicholson et al., 2015).

Using MR angiography, we noted an increase in blood volumes surrounding the prostate, indicating more genitourinary vascularization as a result of estradiol treatment (Figure 2D-E). Interestingly, microvessel density surrounding epithelial and stromal BPH nodules is enhanced relative to adjacent normal tissue and is elevated in prostates from men with symptomatic BPH, particularly those who have failed surgical treatment (Deering et al., 1995; Kojima et al., 1997; Foley and Bailey, 2000; Sun et al., 2010). Therefore, it may be therapeutically beneficial to reduce prostatic blood flow in men with symptomatic BPH, a notion supported by early-stage clinical studies (Carnevale et al., 2010). Indeed, Finasteride significantly reduces prostate microvessel density in men, most potently in sub-epithelial stroma where blood vessels course in close apposition to urethra urothelium (Marshall and Narayan, 1993; Hochberg et al., 2002; Pareek et al., 2003; Donohue et al., 2005; Lekas et al., 2006; Sutton et al., 2006). How microvessel density increases in response to the hormonal milieu found in human BPH is

unclear. Studies by other labs indicate that new vascular development may occur via a mechanism involving hyperplasia and focal hypoxia (Sampson et al., 2008).

While an increase in blood volumes suggested potential infiltration of inflammatory cells, we found no change in distribution of immune cells within the prostate as a result of T+E treatment. The bulk of (>90%) immune cells found within the stroma and epithelium of human prostate are T-lymphocytes, particularly cytotoxic CD8+ (De Nunzio et al., 2016). Typically, periglandular areas of the prostate are infiltrated by cytotoxic T-lymphocytes (CD8+), whereas the fibromuscular stroma contains lymphoid aggregates composed of 50% B-cells surrounded by CD4+ T-cells. Additionally, macrophages are present in small populations (De Nunzio et al., 2016). We saw no difference in the number or distribution of the pan T-cell marker CD3 in the murine prostate. Further, using the macrophage marker F4/80 as well as the B-cell marker B220, we did not determine a large contribution by either population to prostatic enlargement.

Conversely, human BPH tissue contains infiltrates of T-lymphocytes, B-lymphocytes, and macrophages. These cells are found to be chronically activated and coordinate cytokine release (IL-2, IFN-γ, and TGF-ß) that may drive fibromuscular growth in BPH (Kramer et al., 2002). Furthermore, various pro-inflammatory cytokines have been discovered to be upregulated in BPH tissue, particularly IL-15 in stromal cells, IL-17 in infiltrating T cells, IFN-γ in basal and stromal cells, and IL-8 in epithelial cells (Briganti, 2009). We cannot exclude the possibility that immune infiltrate occurred transiently and/or out of phase with our time points (either earlier or later in the treatment time course). Future experiments at additional time points are necessary to determine estradiol-mediated impact of various immune cell populations and cytokine signaling to LUTS pathogenesis in this model.

Notably, we detected a significant increase in Sox2 in the luminal cell compartment in dorsolateral lobes of prostates of mice treated with estradiol as compared to controls. This is in contrast to our data showing that Sox2 is chiefly expressed in the basal cell compartment of the dorsolateral lobe of the murine prostate under normal conditions (Chapter 2). These data indicate that Sox2 may be playing a role in the survival of these cells as a result of hormonal dysregulation. Interestingly, we did not see a similar upregulation of Sox2 in the epithelium of BPH nodules from human patients as compared to normal adjacent transition zone epithelium. It is possible that the time points of human tissue examined (after disease onset) were not optimal, if SOX2 upregulation occurs prior or closer to initiation of the disease. Future experiments are required to dissect the underpinning mechanisms of how Sox2 might be driving these processes, perhaps by preventing apoptosis, promoting cell survival, or potentially contributing to a more de-differentiated cellular phenotype. Specifically, it will be interesting to examine potential changes in SOX2 expression pre- and post- 5-alpha-reductase inhibitor treatment, considered a frontline therapy for human BPH.

Interestingly, estradiol treatment of mice did not seem to significantly spur cellular hyperplasia based on Ki67 staining. Instead, estradiol treatment was protective against cell death, as evidenced by TUNEL staining, coincident with volumetric changes in the prostate and urethral lumen. Longitudinal MR imaging revealed a significantly increased rate of prostatic enlargement in between 10 and 12 weeks of estradiol treatment based on the changing slope of the curve (**Figure 3.1B**). We speculate this may be due to the continued accumulation of actively dividing epithelial cells exceeding our detection threshold. This is not completely surprising, as historical canine studies have also reported that in established BPH the abnormal size of the aged prostate is maintained by a decrease in the rate of cell death, as opposed to an increase in the rate

of cell replication (Coffey and Walsh, 1990). It is likely that the pathophysiologic response of the prostatic epithelial and stromal compartments to estradiol treatment depends on additional variables, including dosage, timing of exposure, and presence of androgens.

Overall, the hormonal dysregulation of this mouse model recapitulates several features of the clinical presentation of human LUTS. In accordance with the seminal publications describing this model, we observed an increase in prostatic volume, as well as a concomitant decrease in prostatic urethral volume. At the timepoints we evaluated, we did not observe canonical hyperplasia of prostatic stroma or epithelium, as is highly prevalent in BPH patients. Moreover, we did not observe overt immune infiltrate at experimental timepoints. However, we cannot exclude the possibility that immune infiltrate or epithelial proliferation occurred at other time points not evaluated via histology or MRI. Additionally, we cannot exclude the possibility of a mouse-strain specific immune response. Future experiments are needed to more thoroughly investigate underpinning mechanisms of initiation and progression of LUTS in this mouse model.

This model is technically tractable as it does not require an invasive surgery and can be used in conjunction with transgenic animals. Therefore, future work can utilize this model to more specifically dissect the roles of relevant proteins and pathways in the development of BOO and BPH. Furthermore, these studies illustrate the high impact of longitudinal MRI analyses to quantify changes in prostate and urethral volume over time. Such an approach has the high potential to enable 1) investigations of novel therapeutic approaches to ameliorate BPH; 2) mechanistic studies of factors contributing to either initiation or progression of BPH; and 3) an increased understanding of the role of estrogenic hormones in regulating prostatic volume.

CHAPTER IV

DISCUSSION, CONCLUSIONS AND FUTURE DIRECTIONS

Overall, my work has begun to define the contributions of Sox2+ cells to the homeostasis of prostate epithelium in physiological (Chapter 2) and pathophysiological (Chapter 3) contexts. In Chapter 2 I utilize a genetic lineage approach in order to follow the Sox2+ population in the prostate throughout development, adult homeostasis, and regeneration. In Chapter 3 I characterize a novel murine model of bladder outlet obstruction (BOO) and begin to interrogate the model for changes in expression of Sox2. These data fill an existing gap in knowledge in the field of prostate stem cell biology and thus, may lay the groundwork to identify novel therapeutics that can abrogate progression of prostatic disease by targeting a putative epithelial progenitor population. Below, I review and interpret my results, highlighting implications of these findings (summarized in **Figure 4.1**). Further, I propose future research directions that address open questions in the field as well as follow-up questions that have emerged from my research.

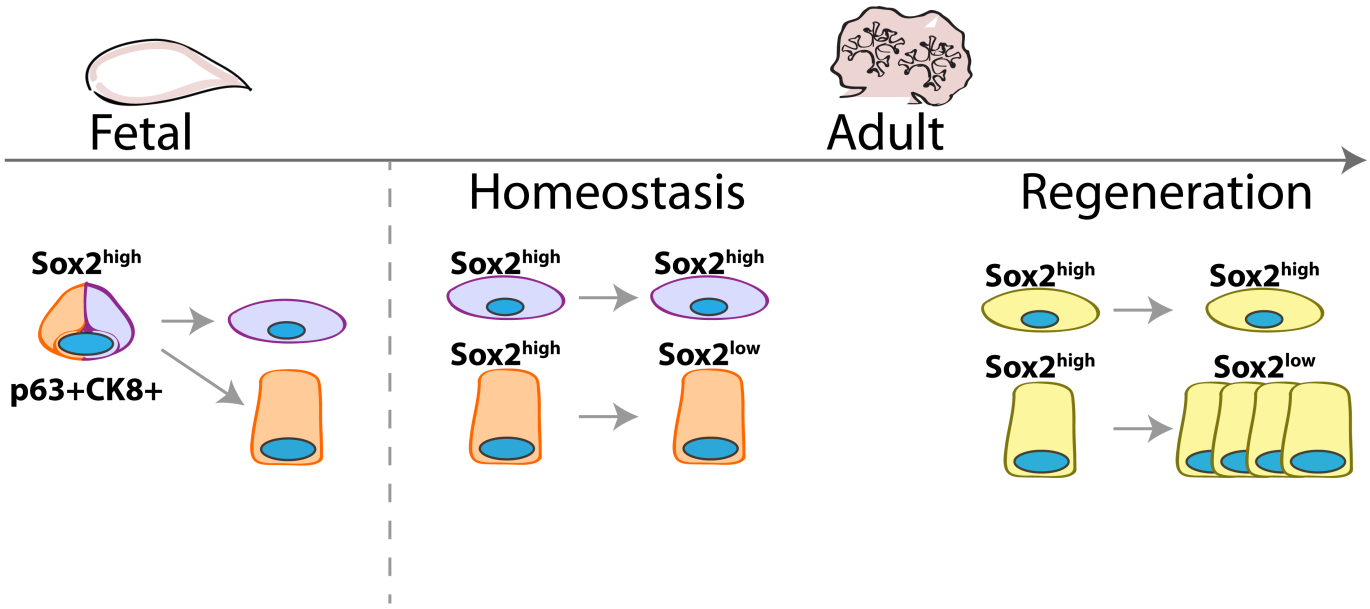

Figure 4.1: Proposed roles of Sox2+ lineage in prostate development, homeostasis, and regeneration. We have observed robust Sox2 expression throughout embryonic and postnatal development of the urogenital sinus, the anlagen tissue of the adult prostate. Using genetic lineage tracing we have shown that embryonic Sox2+ cells can give rise to adult CK8+ luminal and p63+ basal cells. Additionally, embryonic Sox2+ cells do not necessarily give rise to adult Sox2+ cells. In adult homeostasis, we have demonstrated that Sox2-expressing basal and luminal cells can give rise to daughter cells. This is particularly interesting in the luminal cell lineage, as only proximal, but not distal, luminal cells of the ventral and dorsolateral prostate lobes expressed Sox2. We note a population of Sox2-expressing castration-resistant basal and luminal cells that, throughout multiple cycles of regeneration, are able to contribute to prostatic regeneration. Pulsing Sox2-expressing cells in an already castrated animal yielded markedly more YFP+ cells, indicating that remaining cells can upregulate Sox2 *de novo* in response to castration. Finally, we seek to determine molecular parameters for how Sox2 may be controlling a progenitor cell compartment in the adult murine prostate. Using ChIP-seq with paired RNAseq, we find Sox2 binds distinct gene targets in adult prostate epithelial cells as compared to canonical targets in human embryonic stem cells.

In short, the majority of prostatic regeneration is derived from the self-renewal of persisting, castration-resistant luminal cells (Liu et al., 2011; Choi et al., 2012; Wang et al., 2014a). Historically it has been suspected that proximal, but not distal, luminal cells are capable of self-renewal (Tsujimura, 2002; Goto et al., 2006). Our work here establishes that proximal, but not distal, luminal cells express Sox2. Castration-resistant Sox2-expressing cells contribute significantly to prostatic regeneration. Considering both historical and current published data, we submit that Sox2 may be a marker with which to distinguish proximal-to-distal heterogeneity in the luminal cell lineage. Moreover, we use chromatin immunoprecipitation and sequencing to examine more mechanistic functions of Sox2-mediated signaling in adult prostate epithelial cells. These results are in comparison to canonical Sox2 gene targets and co-factors in human embryonic stem cells. Interestingly, we observe overlap of Sox2 targets between the two cell types, as well as the emergence of a distinct, non-overlapping set of genes regulated by Sox2 specifically in adult prostate epithelial cells.

Although we observed that castration-resistant Sox2-expressing cells contribute to prostatic regeneration, the small percentage of YFP+ cells in multiple rounds of castration-regeneration hints at the existence of multiple progenitor pools. This is not entirely surprising, as recent exciting reports have highlighted populations marked by Nkx3.1, Lgr5, and Bmi1 (suggesting either multiple drivers of stemness, or that multiple populations are capable of contributing to glandular regeneration, or perhaps both). Taken altogether these results are in accordance with other results suggesting a more stochastic replacement model of epithelial homeostasis, and highlight the hypothesis that prostate stem cell relationships may not be hierarchical (Pignon et al., 2015).

These data serve as an exciting launch pad for further lines of inquiry. Importantly, whether Sox2 expression itself is required for stem-like qualities of progenitor cells in the adult prostate, including self-renewal and potency. Indeed, it remains unclear whether Sox2 expression and/or the Sox2-positive lineage is strictly required for prostatic regeneration. Taken together these data would begin to address the over-arching question of whether Sox2 is a passenger or a driver of stemness in adult prostate epithelial cells. We also seek to understand which, if any, signals from the microenvironment are tuning Sox2 levels throughout prostatic regeneration. In other words, what are the underpinning mechanisms of specification of castration-resistant populations? Are distinct castration-resistant populations determined via different mechanisms, and if so, is that a parameter that is clinically relevant in prostatic disease?

To test more directly whether Sox2 is a driver of stemness, future experiments will investigate whether Sox2 expression is required for prostatic regeneration. To generate basal- and luminal- Sox2 knockout mice, homozygous $Sox2^{fl/fl}$ mice will be mated with animals expressing tamoxifen-inducible Cre recombinase from either a basal specific driver (CK5-CreERT2) or a luminal specific driver (CK8-CreERT2). Adult CK5CreErT2; $Sox2^{fl/fl}$ mice will be administered tamoxifen to induce Cre-mediated excision of Sox2 specifically in basal cells; CK8CreERT2;$Sox2^{fl/fl}$ for Sox2 deletion in luminal cells. Pregnant dams can be given tamoxifen *in utero* at or after E11.5 to examine effects of Sox2 deletion on prostatic bud morphogenesis and canalization. Significant changes of proximal-distal distribution of lineage-specific cytokeratins (for example, if no co-labeling of CK5 and CK8 is observed) would be consistent with the hypothesis that Sox2 expression is required to maintain plasticity in the proximal urogenital sinus. Androgen cycling to induce prostatic regression and regeneration will be done in animals pre- and post-tamoxifen administration. We hypothesize that Sox2 deletion,

particularly in the luminal cells, in a castrated animal would significantly impact testosterone-mediated prostatic regeneration. Based on presence of other progenitor populations, we speculate that prostatic regeneration would still occur. These results would indicate that Sox2 expression is a driver of stemness, and is required for the process of prostatic regeneration. Systemic effects of Sox2 deletion may preclude us from studying these mice for longer periods of time. Alternatively, we can also engraft Sox2-deficient ($Sox2^{fl/fl}$ or Sox2-knockdown) epithelial cells into a urogenital sinus recombination assay and evaluate graft composition, size, and prostate-specific marker expression. This tissue grafting assay would more closely reflect the context of postnatal prostatic development.

To determine whether Sox2+ cells are required for prostatic regeneration, future studies will utilize genetic ablation. Cre-inducible diphtheria toxin receptor (DTR) transgenic mice (iDTR), in which Cre-mediated excision of a STOP cassette renders cells sensitive to diphtheria toxin (DT), can be used in conjunction with promoter-specific Cre (Buch et al., 2005). In our case, we seek to understand necessity and sufficiency of Sox2+ cells to the process of prostatic regeneration. Castrated Sox2Cre;iDTR mice with fully regressed prostates can be supplemented with testosterone, concurrent with administration of DT, to interrogate whether Sox2+ cells are required for prostatic regeneration. Based on my data that demonstrates that persisting luminal cells upregulate Sox2 in response to castration (Chapter 2), we would expect a wave of DT-mediated apoptosis and a significant delay in prostatic regeneration, if any were to occur. In the event that Sox2 were a passenger rather than a driver of stemness, the progenitor cell compartment may be incidentally ablated in this experimental design. Due to this caveat, more mechanistic studies are required to formally determine how Sox2 may be conferring stemlike capabilities in adult progenitors.

Castration appears to lift AR-mediated repression of Sox2, particularly in castration-resistant luminal cells. However, especially in the *in vivo* context, unanswered questions remain concerning upstream control of Sox2 expression. One parallel mechanism by which Sox2 expression may be tuned in androgen-deficient animals is TGF-β signaling. In castrated animals, the expression of this cytokine and its cognate receptors is increased (Kyprianou and T, 1988a; 1988b; 1989). The thick bank of smooth muscle enveloping the proximal prostate produces high levels of TGF-β (Nemeth and Lee, 1996; Nemeth et al., 1997). Additionally, pSMAD2 and pSMAD3 are differentially regulated by androgens in proximal cells as compared to distal (Salm et al., 2005). These findings suggest that TGF-β signaling can be differentially regulated by androgens along the proximal-distal ductal axis (summarized in **Figure 4.2**). It has been hypothesized that TGF-β signaling can maintain the dormancy of stem cells in the proximal region of prostatic ducts in androgen-replete animals (Salm et al., 2005). While it has been shown that TGF-α can upregulate Sox2 in prostate cancer cell lines, (Lin et al., 2012) the relationship between TGF-β and Sox2 in normal prostate epithelium remains unclear. Interestingly, TGF-β stimulation upregulates Sox2 in a time-dependent manner in human melanoma cells (Weina et al., 2016). Taken together, it is possible that the TGF-β pathway is a potential upstream mechanism by which Sox2 expression is sustained along a proximal-distal axis in the androgen-deficient prostate. Furthermore, it is critical to understand the context-dependent expression of Sox2 target genes, especially within the Wnt and Notch signaling pathways, as TGF-β signaling changes (as in the context of castration). Indeed, Notch signaling has been shown to confer sensitivity and orchestrate positive feedback to TGF-β signaling via upregulation of many TGF-β signaling pathway components (Klüppel and Wrana, 2005; Valdez et al., 2012).

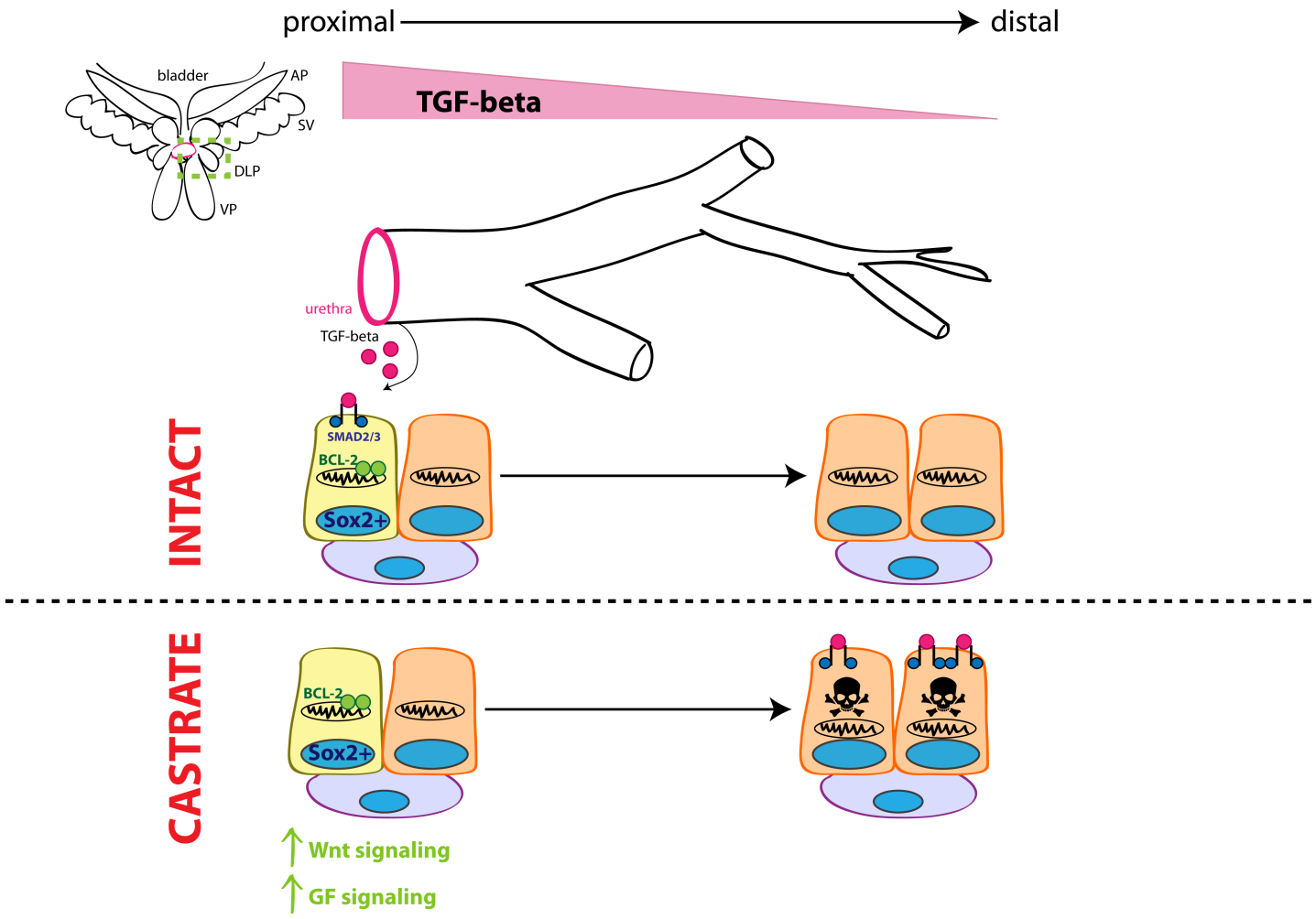

Figure 4.2: TGF-β signaling represents a prototypical mechanism of regulation of heterogeneity along the proximal-distal ductal axis. In androgen-replete animals, proximal cells respond to TGF-β signaling, which is derived at least in part from adjacent, urethral smooth muscle. Proximal cells also sustain expression of Bcl-2, specifically protecting them from apoptosis. In contrast, distal cells do not appear to express components and mediators of the TGF-β signaling pathway or Bcl-2. During castration, TGF-β signaling increases distally. Distal cells seem to be more sensitive to the increase in TGF-β, as they upregulate expression of TGFB receptor II (TGFBRII) as well as expression of SMAD 2/3, primary signal transducers of TGF-β signaling. The increased signaling distally results in the apoptosis of cells in this region, resulting in prostate involution. Interestingly, the upregulation of TGF-β in the context of androgen ablation may antagonize stromal Wnt expression, promoting prostate regression. At the same time, TGF-β signaling decreases proximally, perhaps "priming" progenitors in this niche to respond to mitogenic growth factors. Concomitantly, proximal cells downregulate TGFBRII and SMAD 2/3, becoming less sensitive to TGF-β signaling. Our data suggests that proximal cells, particularly of the luminal lineage, upregulate Sox2, perhaps in response to lack of androgen or TGF-β signaling. Our ChIP-seq data reveals that some Wnt-regulated genes are also Sox2-target genes. Further, overexpression of Sox2 in prostate epithelial cells results in subsequent overexpression of Bcl-2 at the RNA and protein levels. Taken together, upregulation of Sox2 may be upstream of Bcl-2 overexpression or Wnt signaling.

In general, specification mechanisms for progenitor cell populations in prostatic regeneration remain incompletely understood, particularly in the luminal lineage. A persisting luminal population, castration-resistant Nkx3.1-expressing cells (CARNs), have recently been shown to derive their Nkx3.1 expression from cell-autonomous androgen receptor (AR) expression (Xie and Wang, 2017; Xie et al., 2017). Interestingly, CARNs themselves do not require AR expression for their viability or proliferation, but do require AR expression in order to produce viable daughter progeny (Xie et al., 2017; Chua et al., 2018). Therefore, it has been hypothesized that after castration, residual androgen, perhaps secreted from the adrenal glands, specify CARNs in a facultative manner depending on niche localization (Xie and Wang, 2017).

In the case of CARN specification, it is clear that AR signaling is upstream of Nkx3.1 expression (Xie and Wang, 2017). More recently, castration-resistant Bmi1-expressing cells (CARBs) were discovered, and shown to be non-overlapping with the CARN population (Yoo et al., 2016). It would be reasonable to speculate that these two populations could result from two different specification mechanisms. Indeed, recently it was reported that Bmi1 binds AR and subsequently prevents MDM2-mediated AR protein degradation, resulting in sustained AR signaling (Zhu et al., 2018). Although this study was done using prostate cancer cells, it is possible that AR is downstream of Bmi1 in a nonmalignant context. While this relationship has yet to be explicitly tested in the setting of non-malignant castration-resistance, it highlights a potentially different specification mechanism than upstream AR signaling.

Taken together, these data represent an exciting avenue of further inquiry. Previous data from our lab, indicating a repressive relationship between AR and Sox2 (Kregel et al., 2013), suggest that castration-resistant Sox2-expressing cells are probably not specified in an androgen-dependent manner. However, this hypothesis remains to be explicitly tested, and whether the

castration-resistant Sox2-lineage overlaps with other castration-resistant lineages (e.g., expressing Bmi1, Nkx3.1, or Lgr5), potentially specified in an androgen-dependent manner, has not been established.

In general, luminal cells strongly depend on AR for survival, which is why removal of host androgen through castration results in preferential apoptosis of luminal cells. One mechanism for persistence of castration-resistant luminal cells is AR-mediated: either AR is activated by residual androgen signaling (in the case of CARNs) or AR can be upregulated *de novo* (perhaps in the case of CARBs). Intriguingly, there may also be preliminary evidence for a non-AR mechanism, in which another signaling pathway can substitute or compensate for loss of AR. Specifically, in the context of data presented here, this compensatory mechanism would ideally share clientele genes with AR, and importantly, be upregulated by Sox2.

A potential candidate that may substitute for AR is the glucocorticoid receptor (GR). The DNA-binding domains (DBDs) of class I steroid receptors, a family that includes AR and GR, are highly conserved (Narayanan et al., 2015). At least in hormone-responsive prostate cancer cell lines, about half of the AR cistrome overlaps that of the GR, meaning that the glucocorticoid–GR complex is capable of regulating many genes in the AR pathway (Sahu et al., 2011). In prostate cancer cells treated with enzalutamide to block AR, increased GR expression was observed. Moreover, glucocorticoid-GR complexes can promote enzalutamide resistance (Narayanan et al., 2015). Specifically, our group and others have shown that GR and AR can both activate anti-apoptotic genes (Isikbay et al., 2014; Claessens et al., 2017). The bulk of this work has been done in prostate cancer cell lines and murine xenograft mouse models – mechanisms by which GR signaling might potentiate cellular survival in the context of non-malignant castration-resistance is unclear. In our Sox2 ChIP-seq experiment, we observe that GR

is indeed a Sox2-target gene in adult prostate epithelial cells. The relationship between Sox2 and GR, especially in promotion of castration-resistance, has yet to be explored *in vivo*, in either a malignant or normal context. Future experiments may seek to treat castrated mice with novel nonsteroidal and highly selective GR modulators, CORT118335 and CORT108297, to see if the viability or regenerative capacity of persisting cells is altered (Kach et al., 2017). Inducing regression-regeneration of a prostate epithelial-specific GR knockout mouse (Zhao et al., 2014) may shed light on whether regenerative capability of persisting castration-resistant cells is blunted due to absence of this compensatory mechanism.

Persisting luminal cells may also rely on other Sox2-mediated compensatory mechanisms to overcome AR withdrawal in a castrate host. Although it is not strictly a symmetrical comparison, we used lentivirus to overexpress Sox2 in immortalized PrECs and characterize resulting changes in Wnt and Notch signaling pathways. Importantly, immortalized PrECs are a model of prostate basal cells, as luminal cells are not represented in these *in vitro* cultures.

Striking changes in Notch pathway components indicated severe downregulation of Notch transmembrane receptors and multiple canonical Notch ligands, indicating that Sox2-expressing basal cells are protected from Notch-induced differentiation. Concomitantly, overexpression of Sox2 also drove downregulation of negative Wnt regulators, indicating that Wnt signaling was at least partly activated as a result of Sox2 expression. At least in osteoblasts, Sox2 can suppress differentiation through disruption of Wnt signaling, either on the transcriptional or posttranscriptional level. APC and GSK3beta, two strong negative regulators of the Wnt pathway, are also reported to be Sox2 target genes (Seo et al., 2011). Strikingly, Bmi1 is shown to be a crucial mediator of Sox2 function in this context. Inactivation of Sox2 results in concomitant downregulation of Bmi1. Moreover, constitutive expression of Bmi1 can

compensate for loss of Sox2 in terms of self-renewal capabilities, and does not affect differentiation (Seo et al., 2011). Our Sox2 ChIP-seq reveals Bmi1 is a Sox2 target gene in both human embryonic stem cells and adult prostate epithelial cells. It is possible that some Sox2-expressing castration-resistant cells also upregulate Bmi1, which may or may not result in downstream expression of AR. Additionally, based on these data, we would hypothesize that Sox2-expressing castration-resistant cells may overlap, at least partly, with CARBs, and not CARNs.

Intriguingly, many of the genes in either the Notch or Wnt pathways were downregulated upon overexpression of Sox2 in PrECs. These results may be surprising on the surface, given that Sox2 possesses a trans-activating domain. Importantly, Sox proteins largely achieve their gene regulatory functions by forming complexes with co-factors (Kamachi and Kondoh, 2013). Binding of a single Sox protein alone to DNA does not, in itself, result in transcriptional activation or repression. Therefore, Sox2 can elicit transcriptional activation or repression depending on the co-factor recruited by the Sox2-partner factor complex (Kamachi et al., 2000; 2001; Kondoh and Kamachi, 2010). The trend of downregulation in both the Notch and Wnt pathways may suggest that a co-repressor is preferentially recruited to these target genes by Sox2. Previous proteomics studies have identified NcoR/SMRT co-repressors (Ncor1/2, nuclear receptor co- repressors 1/2) and NuRD co-repressor complexes as strongly interacting co-factors of Sox2 (Engelen et al., 2011). These data may provide insight for investigation of co-repressors recruited by Sox2 in PrECs.

In short, it is possible that persisting castration-resistant luminal cells can utilize residual androgen and/or upregulate AR in response to castration through non-androgen means, in the case of CARNs and CARBs, respectively. Additionally, we hypothesize that the Sox2-expressing

castration-resistant cells may also substitute GR for AR, and/or compensate for loss of AR with other pathways to ensure their survival. Potential, facultative methods by which castration-resistant cells may persist are summarized in **Figure 4.3**. Understanding molecular differences between specification events of castration-resistant populations is clinically relevant, especially in light of data suggesting a relationship between prognosis and cell-of-origin (Lee and Shen, 2015; Zhao et al., 2017).

Recently, lineage tracing data from adult human prostates have supported the existence of an overlapping progenitor pool for both basal and luminal cells (Moad et al., 2017). These multipotent basal stem cells self-renew to yield bipotent basal progenitors, which then migrate in cohesive streams along the proximal-distal axis of ducts. As they migrate along the ductal network, basal progenitors derive luminal cells to support tissue homeostasis. Lineage relationships in the adult human prostate appear to be more hierarchical and thus are in contrast to data gathered from murine lineage tracing cohorts. Importantly, the multipotent basal cells were reported to express Delta Like Non-Canonical Notch Ligand 1 (DLK1), a “dead” ligand to Notch. These data highlight a potential role for Notch signaling in adult epithelial stem cell biology.

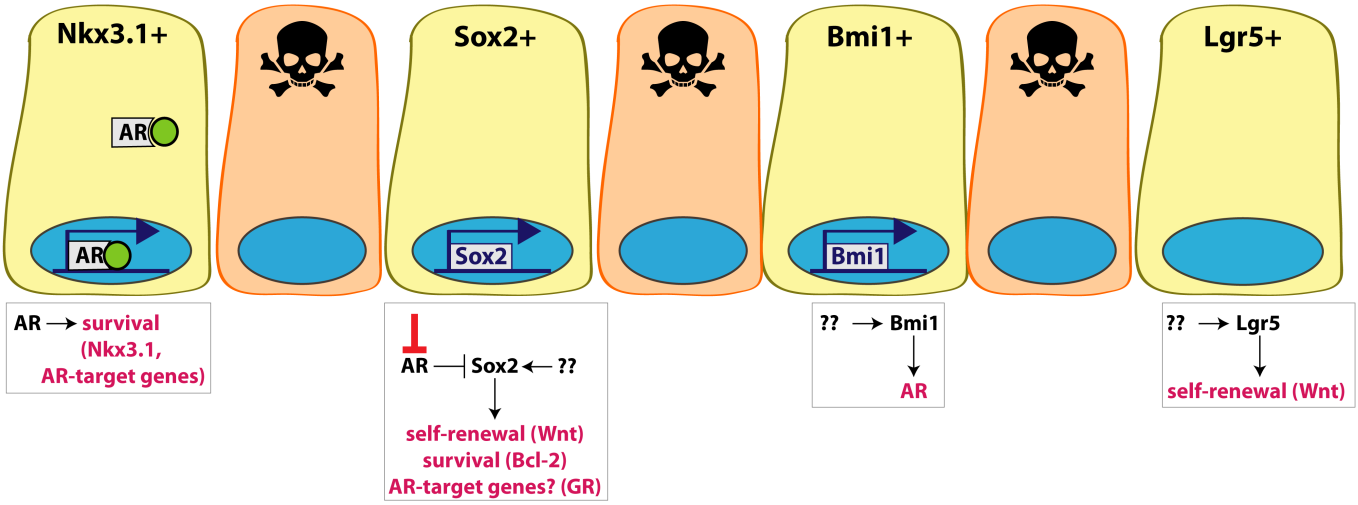

Figure 4.3: A unifying model of recent lineage tracing data hypothesizes a facultative mechanism of progenitor cell specification. Lineage tracing studies have revealed the existence of multiple castration-resistant populations in the prostate (previously investigated markers include Nkx3.1, Lgr5 and Bmi1). As these populations are not all overlapping (especially in the case of Nkx3.1- and Bmi1-expressing castration-resistant cells), it is reasonable to ask whether specification events for each population also differ. These progenitors, perhaps specified based on localization within a niche, could potentially exist alongside pre-determined and/or static progenitor populations. Future studies examining the molecular differences between these populations may shed light on this hypothesis.

Indeed, the intrinsic properties of progenitor cells may dictate clinical behaviors in prostatic disease. Therefore, an additional line of inquiry presented here addresses a common prostatic disease, benign prostatic hyperplasia (BPH). BPH causes progressive lower urinary tract symptoms (LUTS) and quality of life challenges as males age, the etiology of which remain a mystery (McVary, 2003). Similar to therapeutics used to treat prostate cancer, front-line treatment strategies for BPH block androgen signaling, which is known to disrupt reciprocal signaling interactions between prostate stroma and epithelium to decrease the proliferation of both compartments (Isaacs, 2008). As androgen deprivation is not curative for BPH, other factors may be involved. In particular, estrogens have long been suspected to contribute to the etiology of BPH (Prins and Putz, 2008; Nicholson and Ricke, 2011). As men age, the estradiol/dihydroxytestosterone ratio increases within the prostatic epithelial and stromal compartments, and is significantly increased within BPH tissue (Krieg et al., 1981).

While it has been hypothesized that BPH can result from aberrant stem cell activation and subsequent hyper-proliferation (Isaacs, 1987; 2008), lack of sufficient *in vivo* models has made this hypothesis difficult to test directly (Hudson, 2004; Hieble, 2011; Prajapati et al., 2013). While correlations can be drawn from the study of human tissue samples, the natural history of disease progression cannot be fully understood in these snapshots alone, and methods of tissue preservation can serve as huge constraints to downstream analysis. Therefore, animal models are critical for systematic and mechanistic investigations of human disease. Murine models that accurately recapitulate the human condition enable the study of the natural history of the disease from the time of initiation throughout progression in genetically similar hosts.

To address this challenge, I adapted a recently published estradiol-mediated model of murine bladder outlet obstruction, which was reported to recapitulate several components of

human BPH (Nicholson et al., 2012). Using Magnetic Resonance Imaging (MRI) to longitudinally monitor the pathophysiological progression of prostatic enlargement, I asked whether canonical benchmarks of human BPH were demonstrated in mice treated with low doses of estradiol and testosterone (Chapter 3). Despite bearing some resemblance to the human condition, the mouse model did not reproduce several important histological or pathological aspects of human pathological BPH (McAuley et al., 2017). Mice experienced a significant increase in prostatic volume concomitant with a decrease in urethral lumen volume, but did not demonstrate overt hyperplasia in either the epithelial or stromal compartments. Taken together, these data suggest that underlying mechanisms of estradiol-mediated prostatic enlargement in this model probably do not include conical prostatic hyperplasia, as seen in human BPH. Using this model, we noted a significant decrease in epithelial cell death as a result of estradiol treatment. Importantly, this parameter does match the human condition, and can also be recapitulated in canine models. In BPH patients, the size increase of the prostate is maintained over time (and is not necessarily the result of rapid growth and proliferation of cells). This abnormal size is maintained by a decrease in the rate of cell death, and not by an increase in the rate of cell doubling (Coffey and Walsh, 1990; Partin and Coffey, 1994).

Moreover, my unpublished results demonstrate that there is no significant upregulation of Sox2 in human BPH nodules as compared to the patient-matched adjacent normal transition zone. These data have been corroborated by other reports that utilized qPCR from total RNA isolates as well as immunohistochemistry to show there was no significant difference between human normal and BPH tissues (Le Magnen et al., 2013; Yu et al., 2014). While these data do not directly support or contradict the embryonic re-awakening hypothesis, it is important to keep investigating all possible mechanisms underlying expansion of both the stromal and epithelial

compartments in human BPH. In this context, it is possible that the time points of human tissue examined (after disease onset) were not optimal, if Sox2 upregulation occurs prior or closer to initiation of the disease. Other stem cell circuitry factors (e.g., Nanog, Oct4), perhaps not Sox2, may be involved in the aberrant epithelial proliferation observed in human BPH. Alternatively, if there are multiple sources of stem cells in the prostate, it is possible that the Sox2-positive lineage does not significantly contribute to pathophysiological epithelial expansion in BPH. It would also be valuable to understand how frontline therapeutics for BPH may impact Sox2 expression, as a clientele gene of Sox2 may be easily targetable with adjuvant therapies. Future studies are required to continue refining models and uncovering mechanisms of human BPH initiation and progression.

Notably, both prostatic development and disease is tightly regulated by androgen signaling. Androgen-deprivation therapy (ADT) to disrupt this signaling axis represents a frontline therapeutic intervention for prostate cancer patients (Rosenthal and Sandler, 2010; Zong and Goldstein, 2012). ADT, often used in conjunction with surgical resection, includes use of luteinizing hormone-releasing analogs (LHRH), LHRH antagonists and anti-androgens that prevent androgen synthesis and androgen receptor signaling (Rosenthal and Sandler, 2010; Beltran et al., 2011). The clinical behavior of localized prostate cancer is highly variable—while some men will have aggressive cancer leading to metastasis and death from the disease (Lorente et al., 2015; Cattrini et al., 2017), many others will have indolent cancers that are cured with initial therapy or may be safely monitored (Network et al., 2015). Clinical and pathological parameters used to stratify patients into different risk categories include Gleason score, PSA levels, and clinical and pathological staging. Despite these being the best tools available, they fail to adequately predict outcome for many patients. Therefore, a major therapeutic need

remains to dissect the mechanisms of castration resistance: not only to identify biomarkers that more accurately predict patient outcomes, but to also develop more targeted therapies for these castration-resistant prostate cancer (CRPC) patients (Zong and Goldstein, 2012; Lorente et al., 2015; Narayanan et al., 2015; Beltran et al., 2016).

Questions about SOX2 function in human prostate cancer progression have begun to be explored. Indeed, our group has previously shown that overexpression of SOX2 in a hormone-sensitive cell line is sufficient to drive castration-resistance and tumor formation in a castrate host (Kregel et al., 2013). We and others have shown that silencing of SOX2 results in significant growth suppression of prostate cancer cells (Kregel et al., 2013; Kar et al., 2017). More recently, using a novel mouse model of aggressive prostate cancer, it was hypothesized that tumor cells acquire lineage plasticity via upregulation of Sox2 as a driving mechanism to escape luminal cell-specific drug therapies that target the AR (Ku et al., 2017; Mu et al., 2017). Both models utilize a murine model of prostate cancer that is considered to represent a highly progressive and advanced model of prostate cancer.

Potential functions of SOX2 as a driver for human prostate tumor initiation remain a mystery. SOX2 expression appears to be upregulated in many human cancers as compared to normal tissue, and its increased expression tends to correlate with a worse prognosis. This has been shown in small lung cell, lung, esophageal cancer, as well as non-epithelial cancers such as glioblastoma and sarcoma (Wuebben and Rizzino, 2017). Interestingly, SOX2 appears to fulfill a tumor suppressor function in gastric tumors driven by canonical Wnt signal activation (Sarkar et al., 2016). In murine models of skin squamous cell carcinoma (Boumahdi et al., 2014) and medulloblastoma (Vanner et al., 2014), lineage ablation of Sox2-expressing cells abrogated tumor initiation and lead to tumor regression. In contrast, the Sox2 lineage was found to be

dispensable for initiation, growth, and metastasis of melanoma (Schaefer et al., 2017). Taken together these findings highlight the criticality of context-dependent signaling concerning Sox2 in relation to its function and cellular lineage.

To test more directly whether SOX2 expression contributes significantly to prostate tumor initiation, a future experiment will use immortalized PrECs, which do not express SOX2 and do not possess endogenous malignant potential. To increase malignant potential, PrECs can be transformed via exogenous overexpression of c-Myc and AR (Vander Griend et al., 2014). SOX2-deficient and –sufficient cultures (via lentiviral overexpression) will be examined for differences in proliferation and tumorigenecity *in vivo*. These data will begin to shed light on SOX2 may contribute to prostate tumor initiation. We hypothesize that Sox2-sufficient malignant PrECs will be more resistant to anti-androgen therapies such an enzalutamide, as expression of Sox2 will decrease cellular dependence on androgen signaling. However, PrECs are comprised of mostly basal cells and therefore do not accurately represent luminal cells, thought to be the more sensitive tumor cell-of-origin (Wang et al., 2009; 2014b), and therefore may not reflect common initiation mechanisms of prostate cancer *in vivo*. A potential complementary experimental system to utilize is prostate organoids, a three-dimensional culture of primary tissue isolated from either mice or humans (Gao et al., 2014; Karthaus et al., 2014). Prostate organoids more accurately reflect *in vivo* tissue geometry and importantly, representation of all of prostatic cell lineages.

Major questions that remain in the field center on the origin of castration-resistant prostate cancer, and the underpinning mechanisms of how castration-resistance dictates disease course, and/or is acquired as a result of treatment resistance. Luminal cells appear to be more sensitive to malignant transformation ((Wang et al., 2014b). Our group and others have begun to

establish the potential link between Sox2 expression and prostate cancer biology, specifically how tumor cells may escape frontline, luminal cell-specific therapeutics that target AR (Kregel et al., 2013; Jiang et al., 2017; Kar et al., 2017; Ku et al., 2017; Mu et al., 2017). Further studies, particularly whether castration-resistant Sox2-expressing luminal cells are more prone to oncogenic transformation, are required to understand how Sox2 expression in tumorigenic cells may alter natural history of the disease.

As expression of SOX2 in human prostate cancer might indicate a phenotypic switch of the cancer cells, it is crucial to understand resultant changes in gene expression as a result of an upregulation of SOX2. This is equally true for tumor initiation and progression in prostate cancer. SOX2 itself does not represent a highly druggable target protein: as a transcription factor, it is difficult to design highly specific small-molecule inhibitors to its active site that are also targeted to only cancer cells of interest (Fontaine, 2015). From the perspective of therapeutic design, it is possible that some clientele genes of SOX2 represent highly druggable targets. For instance, one potential avenue forward in prostate cancer may be targeting Bcl-2 in Sox2-overexpressing prostate tumors.

The work presented here has vast implications for both researchers and clinicians. My work seeks to understand the function of Sox2 in normal adult prostate epithelial cells as well as the underlying biology of Sox2+ cells as they may relate to tissue homeostasis. These lines of inquiries are important to fill gaps in knowledge in the scientific community. Additionally, these data may serve to be a point of comparison for the study of Sox2 in the role of prostate tumor initiation or progression. Understanding how Sox2 function is operating in the normal tissue is critical to precisely answer questions about its function in malignant tissue and build a more global and holistic understanding of tumor biology.

REFERENCES

Abrahamsson PA. Neuroendocrine cells in tumour growth of the prostate. Endocrine Related Cancer. 1999 Dec;6(4):503–19.

Adikusuma F, Pederick D, McAninch D, Hughes J, Thomas P. Functional Equivalence of the SOX2 and SOX3 Transcription Factors in the Developing Mouse Brain and Testes. Genetics. 2017 May 17;:genetics.117.202549.

Amador-Arjona A, Cimadamore F, Huang C-T, Wright R, Lewis S, Gage FH, et al. SOX2 primes the epigenetic landscape in neural precursors enabling proper gene activation during hippocampal neurogenesis. Proc. Natl. Acad. Sci. U.S.A. 2015 Apr 14;112(15):E1936–45.

Arnold K, Sarkar A, Yram MA, Polo JM, Bronson R, Sengupta S, et al. Adult Stem and Progenitor Cells Are Important for Tissue Regeneration and Survival of Mice. Stem Cell. Elsevier Inc; 2011 Oct 4;9(4):317–29. PMCID: PMC3538360

Avilion AA, Nicolis SK, Pevny LH, Perez L, Vivian N, Lovell-Badge R. Multipotent cell lineages in early mouse development depend on SOX2 function. Genes & Development. 2003 Jan 1;17(1):126–40. PMCID: PMC195970

Bae KM, Su Z, Frye C, McClellan S, Allan RW, Andrejewski JT, et al. Expression of Pluripotent Stem Cell Reprogramming Factors by Prostate Tumor Initiating Cells. The Journal of Urology. Elsevier Inc; 2010 May 1;183(5):2045–53.

Baltus GA, Kowalski MP, Zhai H, Tutter AV, Quinn D, Wall D, et al. Acetylation of sox2 induces its nuclear export in embryonic stem cells. Stem Cells. 2009 Sep;27(9):2175–84.

Barker N, van Es JH, Kuipers J, Kujala P, van den Born M, Cozijnsen M, et al. Identification of stem cells in small intestine and colon by marker gene Lgr5. Nature. 2007 Oct 14;449(7165):1003–7.

Beltran H, Beer TM, Carducci MA, de Bono J, Gleave M, Hussain M, et al. New therapies for castration-resistant prostate cancer: efficacy and safety. European Urology. 2011 Aug;60(2):279–90.

Beltran H, Prandi D, Mosquera J-M, Benelli M, Puca L, Cyrta J, et al. Divergent clonal evolution of castration-resistant neuroendocrine prostate cancer. Nat Med. 2016 Feb 8;22(3):298–305.

Bernard P, Harley VR. Acquisition of SOX transcription factor specificity through protein–protein interaction, modulation of Wnt signalling and post-translational modification. The International Journal of Biochemistry & Cell Biology. 2010 Mar;42(3):400–10.

Berquin IM, Min Y, Wu R, Wu H, Chen YQ. Expression signature of the mouse prostate. J. Biol. Chem. 2005 Oct 28;280(43):36442–51.

Berry SJ, Coffey DS, Walsh PC, LL E. The Development of Human Benign Prostatic Hyperplasia with Age. 3rd ed. The Journal of urology.

Bhatia-Gaur R, Donjacour AA, Sciavolino PJ, Kim M, Desai N, Young P, et al. Roles for Nkx3.1 in prostate development and cancer. Genes & Development. 1999 Apr 15;13(8):966–77. PMCID: PMC316645

Blanpain C, Horsley V, Fuchs E. Epithelial Stem Cells: Turning over New Leaves. Cell. 2007 Feb;128(3):445–58.

Boer B, Kopp J, Mallanna S, Desler M, Chakravarthy H, Wilder PJ, et al. Elevating the levels of Sox2 in embryonal carcinoma cells and embryonic stem cells inhibits the expression of Sox2:Oct-3/4 target genes. Nucleic Acids Research. 2007;35(6):1773–86. PMCID: PMC1874607

Bolger AM, Lohse M, Usadel B. Trimmomatic: a flexible trimmer for Illumina sequence data. Bioinformatics. 2014 Aug 1;30(15):2114–20. PMCID: PMC4103590

Boumahdi S, Driessens G, Lapouge G, Rorive S, Nassar D, Le Mercier M, et al. SOX2 controls tumour initiation and cancer stem-cell functions in squamous-cell carcinoma. Nature. Nature Publishing Group; 2014 Jul 1;511(7508):246–50.

Boyer LA, Lee TI, Cole MF, Johnstone SE, Levine SS, Zucker JP, et al. Core Transcriptional Regulatory Circuitry in Human Embryonic Stem Cells. Cell. 2005 Sep;122(6):947–56. PMCID: PMC3006442

Brazel CY, Limke TL, Osborne JK, Miura T, Cai J, Pevny L, et al. Sox2 expression defines a heterogeneous population of neurosphere-forming cells in the adult murine brain. Aging Cell. 2005 Aug;4(4):197–207.

Briganti A. Oestrogens and prostate cancer: novel concepts about an old issue. European Urology. 2009 Mar;55(3):543–5.

Brockes JP. Amphibian limb regeneration: rebuilding a complex structure. Science. 1997 Apr 4;276(5309):81–7.

Buch T, Heppner FL, Tertilt C, Heinen TJAJ, Kremer M, Wunderlich FT, et al. A Cre-inducible diphtheria toxin receptor mediates cell lineage ablation after toxin administration. Nat Meth. 2005 Jun;2(6):419–26.

Bylund M, Andersson E, Novitch BG, Muhr J. Vertebrate neurogenesis is counteracted by Sox1–3 activity. Nat Neurosci. 2003 Sep 28;6(11):1162–8.

Carnevale FC, Antunes AA, da Motta Leal Filho JM, de Oliveira Cerri LM, Baroni RH, Marcelino ASZ, et al. Prostatic artery embolization as a primary treatment for benign prostatic hyperplasia: preliminary results in two patients. Cardiovasc Intervent Radiol. 2010 Apr;33(2):355–61. PMCID: PMC2841280

Cattrini C, Zanardi E, Vallome G, Cavo A, Cerbone L, Di Meglio A, et al. Targeting androgen-independent pathways: new chances for patietns with prostate cancer? Critical Reviews in Oncology / Hematology. Elsevier; 2017 Oct 1;118:42–53.

Cavallaro M, Mariani J, Lancini C, Latorre E, Caccia R, Gullo F, et al. Impaired generation of mature neurons by neural stem cells from hypomorphic Sox2 mutants. Development. 2008 Jan 2;135(3):541–57.

Ceder JA, Aalders TW, Schalken JA. Label retention and stem cell marker expression in the developing and adult prostate identifies basal and luminal epithelial stem cell subpopulations. Stem Cell Research & Therapy; 2017 Apr 12;:1–12. PMCID: PMC5406885

Chan SS-K, Kyba M. What is a Master Regulator? J Stem Cell Res Ther. 2013;03(02).

Chen J, Zhang Z, Li L, Chen B-C, Revyakin A, Hajj B, et al. Single-molecule dynamics of enhanceosome assembly in embryonic stem cells. Cell. 2014 Mar 13;156(6):1274–85. PMCID: PMC4040518

Chen JL, Li J, Kiriluk KJ, Rosen AM, Paner GP, Antic T, et al. Deregulation of a Hox Protein Regulatory Network Spanning Prostate Cancer Initiation and Progression. Clinical Cancer Research. 2012 Aug 14;18(16):4291–302.

Choi N, Zhang B, Zhang L, Ittmann M, Xin L. Adult Murine Prostate Basal and Luminal Cells Are Self-Sustained Lineages that Can Both Serve as Targets for Prostate Cancer Initiation. CCELL. Elsevier Inc; 2012 Feb 14;21(2):253–65. PMCID: PMC3285423

Chua CW, Epsi NJ, Leung EY, Xuan S, Lei M, Li BI, et al. Differential requirements of androgen receptor in luminal progenitors during prostate regeneration and tumor initiation. eLife Sciences. 2018 Jan 15;7.

Chua CW, Shibata M, Lei M, Toivanen R, Barlow L, Shen M. Culture of mouse prostate organoids. Nature Publishing Group; 2014a Sep 29.

Chua CW, Shibata M, Lei M, Toivanen R, Barlow LJ, Bergren SK, et al. Single luminal epithelial progenitors can generate prostate organoids in culture. Nature Cell Biology. 2014b Sep 21;16(10):951–61. PMCID: PMC4183706

Cieślar-Pobuda A, Knoflach V, Ringh MV, Stark J, Likus W, Siemianowicz K, et al. Transdifferentiation and reprogramming: Overview of the processes, their similarities and differences. BBA - Molecular Cell Research. Elsevier B.V; 2017 Apr 28;1864(7):1359–69.

Claessens F, Joniau S, Helsen C. Comparing the rules of engagement of androgen and glucocorticoid receptors. Cell. Mol. Life Sci. Springer International Publishing; 2017 May 4;74(12):2217–28.

Coffey DS. Similarities of prostate and breast cancer: Evolution, diet, and estrogens. Urology. 2001 Apr;57(4 Suppl 1):31–8.

Coffey DS, Walsh PC. Clinical and experimental studies of benign prostatic hyperplasia. Urologic Clinics of NA. 1990 Aug;17(3):461–75.

Corsinotti A, Wong FC, Tatar T, Szczerbinska I, Halbritter F, Colby D, et al. Distinct SoxB1

networks are required for naive and primed pluripotency. eLife Sciences. 2017 Dec 19;6.

Cunha GR, Donjacour AA, Cooke PS, Mee S, Bigsby RM, Higgins SJ, et al. The endocrinology and developmental biology of the prostate. Endocr. Rev. 1987 Aug;8(3):338–62.

De Nunzio C, Presicce F, Tubaro A. Inflammatory mediators in the development and progression of benign prostatic hyperplasia. Nature Publishing Group. Nature Publishing Group; 2016 Oct 1;13(10):613–26.

Deering RE, Bigler SA, Brown M, Brawer MK. Microvascularity in benign prostatic hyperplasia. Prostate. 1995 Mar;26(3):111–5.

DeKlerk DP, Coffey DS, Ewing LL, McDermott IR, Reiner WG, Robinson CH, et al. Comparison of spontaneous and experimentally induced canine prostatic hyperplasia. J. Clin. Invest. 1979 Sep;64(3):842–9. PMCID: PMC372190

Desclozeaux M, Poulat F, de Santa Barbara P, Capony JP, Turowski P, Jay P, et al. Phosphorylation of an N-terminal motif enhances DNA-binding activity of the human SRY protein. J. Biol. Chem. 1998 Apr 3;273(14):7988–95.

Donohue JF, Hayne D, Karnik U, Thomas DR, Foster MC. Randomized, placebo-controlled trial showing that finasteride reduces prostatic vascularity rapidly within 2 weeks. BJU Int. 2005 Dec;96(9):1319–22.

Driskell RR, Giangreco A, Jensen KB, Mulder KW, Watt FM. Sox2-positive dermal papilla cells specify hair follicle type in mammalian epidermis. Development. 2009 Jul 24;136(16):2815–23.

Ellis P, Fagan BM, Magness ST, Hutton S, Taranova O, Hayashi S, et al. SOX2, a Persistent Marker for Multipotential Neural Stem Cells Derived from Embryonic Stem Cells, the Embryo or the Adult. Dev Neurosci. 2004;26(2-4):148–65.

Engelen E, Akinci U, Bryne JC, Hou J, Gontan C, Moen M, et al. Sox2 cooperates with Chd7 to regulate genes that are mutated in human syndromes. Nat Genet. Nature Publishing Group; 2011 May 1;43(6):607–11.

English HF, Santen RJ, T IJ. Response of glandular versus basal rat ventral prostatic epithelial cells to androgen withdrawal and replacement. Prostate. 1987;11(3):229–42.

Evans GS, Chandler JA. Cell proliferation studies in the rat prostate: II. The effects of castration and androgen-induced regeneration upon basal and secretory cell proliferation. Prostate. 1987;11(4):339–51.

Fantes J, Ragge NK, Lynch S-A, McGill NI, Collin JRO, Howard-Peebles PN, et al. Mutations in SOX2 cause anophthalmia. Nat Genet. 2003 Mar 3;33(4):461–3.

Fauquier T, Rizzoti K, Dattani M, Lovell-Badge R, Robinson ICAF. SOX2-expressing progenitor cells generate all of the major cell types in the adult mouse pituitary gland. Proc.

Natl. Acad. Sci. U.S.A. 2008 Feb 26;105(8):2907–12. PMCID: PMC2268558

Feng J, Liu T, Qin B, Zhang Y, Liu XS. Identifying ChIP-seq enrichment using MACS. Nat Protoc. 2012 Sep;7(9):1728–40. PMCID: PMC3868217

Ferrari S, Harley VR, Pontiggia A, Goodfellow PN, Lovell-Badge R, Bianchi ME. SRY, like HMG1, recognizes sharp angles in DNA. EMBO J. 1992 Dec;11(12):4497–506. PMCID: PMC557025

Ferri ALM. Sox2 deficiency causes neurodegeneration and impaired neurogenesis in the adult mouse brain. Development. 2004 Jun 23;131(15):3805–19.

Fink J, Andersson-Rolf A, Koo B-K. Adult stem cell lineage tracing and deep tissue imaging. BMB Reports. 2015 Dec 31;48(12):655–67.

Firas J, Polo JM. Towards understanding transcriptional networks in cellular reprogramming. Current Opinion in Genetics & Development. Elsevier Ltd; 2017 Oct 1;46(C):1–8.

Foley SJ, Bailey DM. Microvessel density in prostatic hyperplasia. BJU Int. 2000 Jan;85(1):70–3.

Fontaine F. Pharmacological manipulation of transcription factor protein-protein interactions: opportunities and obstacles. 2015 Mar 17;:1–12.

Frank SB, Berger PL, Ljungman M, Miranti CK. Human prostate luminal cell differentiation requires NOTCH3 induction by p38-MAPK and MYC. Journal of Cell Science. 2017 Jun 1;130(11):1952–64.

Frum T, Ralston A. Cell signaling and transcription factors regulating cell fate during formation of the mouse blastocyst. Trends in Genetics. Elsevier Ltd; 2015 Jul 1;31(7):402–10.

Gao D, Vela I, Sboner A, Iaquinta PJ, Karthaus WR, Gopalan A, et al. Organoid Cultures Derived from Patientswith Advanced Prostate Cancer. Cell. Elsevier Inc; 2014 Sep 25;159(1):176–87.

Gao J, Arnold JT, T IJ. Conversion from a paracrine to an autocrine mechanism of androgen-stimulated growth during malignant transformation of prostatic epithelial cells. Cancer Research. 2001 Jul 1;61(13):5038–44.

Gálvez H, Abelló G, Giraldez F. Signaling and Transcription Factors during Inner Ear Development: The Generation of Hair Cells and Otic Neurons. Front. Cell Dev. Biol. 2017 Mar 24;5:841.

Georgas KM, Armstrong J, Keast JR, Larkins CE, McHugh KM, Southard-Smith EM, et al. An illustrated anatomical ontology of the developing mouse lower urogenital tract. Development. 2015 May 12;142(10):1893–908. PMCID: PMC4440924

Goldstein AS, Lawson DA, Cheng D, Sun W, Garraway IP, Witte ON. Trop2 identifies a

subpopulation of murine and human prostate basal cells with stem cell characteristics. Proc. Natl. Acad. Sci. U.S.A. 2008 Dec 30;105(52):20882–7. PMCID: PMC2603432

Goto K, Salm SN, Coetzee S, Xiong X, Burger PE, Shapiro E, et al. Proximal Prostatic Stem Cells Are Programmed to Regenerate a Proximal-Distal Ductal Axis. Stem Cells. 2006 Aug;24(8):1859–68.

Graham V, Khudyakov J, Ellis P, Pevny L. SOX2 functions to maintain neural progenitor identity. Neuron. 2003 Aug 28;39(5):749–65.

Grant CE, Bailey TL, Noble WS. FIMO: scanning for occurrences of a given motif. Bioinformatics. 2011 Apr 1;27(7):1017–8. PMCID: PMC3065696

Grosschedl R, Giese K, Pagel J. HMG domain proteins: architectural elements in the assembly of nucleoprotein structures. Trends in Genetics. 1994 Mar;10(3):94–100.

Grossfeld GD, Coakley FV. Benign prostatic hyperplasia: clinical overview and value of diagnostic imaging. Radiologic Clinics of North America. 2000 Jan;38(1):31–47.

Gu R, Brown RM, Hsu C-W, Cai T, Crowder A, Piazza VG, et al. Lineage tracing of Sox2-expressing progenitor cells in the mouse inner ear reveals a broad contribution to non-sensory tissues and insights into the origin of the organ of Corti. Developmental Biology. Elsevier; 2016 Apr 14;:1–34. PMCID: PMC4875846

Gubbay J, Collignon J, Koopman P, Capel B, Economou A, Münsterberg A, et al. A gene mapping to the sex-determining region of the mouse Y chromosome is a member of a novel family of embryonically expressed genes. Nature. 1990 Jul 19;346(6281):245–50.

Guneyli S, Ward E, Thomas S, Yousuf AN, Trilisky I, Peng Y, et al. Magnetic resonance imaging of benign prostatic hyperplasia. Diagn Interv Radiol. 2016 May 3;22(3):215–9.

Hall PA, Watt FM. Stem cells: the generation and maintenance of cellular diversity. Development. 1989 Aug;106(4):619–33.

Hansen P, Hecht J, Ibrahim DM, Krannich A, Truss M, Robinson PN. Saturation analysis of ChIP-seq data for reproducible identification of binding peaks. Genome Research. 2015 Sep;25(9):1391–400. PMCID: PMC4561497

Hieble JP. Animal Models for Benign Prostatic Hyperplasia. Handbook of Experimental Pharmacology. Berlin, Heidelberg: Springer Berlin Heidelberg; 2011. p. 69–79.

Hochberg DA, Basillote JB, Armenakas NA, Vasovic L, Shevchuk M, Pareek G, et al. Decreased suburethral prostatic microvessel density in finasteride treated prostates: a possible mechanism for reduced bleeding in benign prostatic hyperplasia. The Journal of Urology. 2002 Apr;167(4):1731–3.

Horvay K, Abud HE. Regulation of intestinal stem cells by Wnt and Notch signalling. Adv. Exp. Med. Biol. 2013;786:175–86.

Hou L, Srivastava Y, Jauch R. ARTICLE IN PRESS. Seminars in Cell & Developmental Biology. Elsevier Ltd; 2016 Aug 13;:1–11.

Höfner T, Eisen C, Klein C, Rigo-Watermeier T, Goeppinger SM, Jauch A, et al. Stem Cell Reports. Stem Cell Reports. The Authors; 2015 Mar 10;4(3):503–18.

Huang L, Pu Y, Hepps D, Danielpour D, Prins GS. Posterior HoxGene Expression and Differential Androgen Regulation in the Developing and Adult Rat Prostate Lobes. Endocrinology. 2007 Mar;148(3):1235–45.

Huang Z, Hurley PJ, Simons BW, Marchionni L, Berman DM, Ross AE, et al. Sox9 is required for prostate development and prostate cancer initiation. Oncotarget. 2012 Jun;3(6):651–63. PMCID: PMC3442290

Hudson DL. Epithelial stem cells in human prostate growth and disease. Prostate Cancer Prostatic Dis. 2004 Aug 3;7(3):188–94.

Hudson DL, Guy AT, Fry P, O'Hare MJ, Watt FM, Masters JR. Epithelial cell differentiation pathways in the human prostate: identification of intermediate phenotypes by keratin expression. J. Histochem. Cytochem. 2001 Feb;49(2):271–8.

Isaacs JT. Control of Cell Proliferation and Cell Death in the Normal and Neoplastic Prostate: A Stem Cell Model. Benign prostatic hyerplasia: a workshop. 1987 Mar 20;:85–94.

Isaacs JT. Prostate stem cells and benign prostatic hyperplasia. Prostate. 2008;68(9):1025–34.

Isikbay M, Otto K, Kregel S, Kach J, Cai Y, Vander Griend DJ, et al. Glucocorticoid receptor activity contributes to resistance to androgen-targeted therapy in prostate cancer. Horm Cancer. 2014 Apr;5(2):72–89. PMCID: PMC4440041

Ittmann M, Huang J, Radaelli E, Martin P, Signoretti S, Sullivan R, et al. Animal Models of Human Prostate Cancer: The Consensus Report of the New York Meeting of the Mouse Models of Human Cancers Consortium Prostate Pathology Committee. Cancer Research. 2013 Apr 30;73(9):2718–36.

Iwafuchi-Doi M, Donahue G, Kakumanu A, Watts JA, Mahony S, Pugh BF, et al. The Pioneer Transcription Factor FoxA Maintains an Accessible Nucleosome Configuration at Enhancers for Tissue-Specific Gene Activation. Molecular Cell. Elsevier Inc; 2016 Apr 7;62(1):79–91. PMCID: PMC4826471

Izumi K, Li L, Chang C. Androgen receptor and immune inflammation in benign prostatic hyperplasia and prostate cancer. Clinical Investigation. 2014 Oct;4(10):935–50.

Jang H, Kim TW, Yoon S, Choi S-Y, Kang T-W, Kim S-Y, et al. O-GlcNAc regulates pluripotency and reprogramming by directly acting on core components of the pluripotency network. Cell Stem Cell. 2012 Jul 6;11(1):62–74.

Javed S, Langley SEM. Importance of HOXgenes in normal prostate gland formation, prostate

cancer development and its early detection. BJU Int. 2013 Aug 13;113(4):535–40.

Jho E-H, Zhang T, Domon C, Joo C-K, Freund J-N, Costantini F. Wnt/beta-catenin/Tcf signaling induces the transcription of Axin2, a negative regulator of the signaling pathway. Molecular and Cellular Biology. 2002 Feb;22(4):1172–83. PMCID: PMC134648

Jia X, Li X, Xu Y, Zhang S, Mou W, Liu Y, et al. SOX2 promotes tumorigenesis and increases the anti-apoptotic property of human prostate cancer cell. J Mol Cell Biol. 2011 Aug;3(4):230–8.

Jiang N, Ke B, Hjort-Jensen K, Iglesias-Gato D, Wang Z, Chang P, et al. YAP1 regulates prostate cancer stem cell-like characteristics to promote castration resistant growth. Oncotarget. 2017 Dec 29;8(70):115054–67. PMCID: PMC5777753

Juuri E, Saito K, Ahtiainen L, Seidel K, Tummers M, Hochedlinger K, et al. Sox2+ Stem Cells Contribute to All Epithelial Lineages of the Tooth via Sfrp5+ Progenitors. Developmental Cell. Elsevier Inc; 2012 Aug 14;23(2):317–28.

Kach J, Long TM, Selman P, Tonsing-Carter EY, Bacalao MA, Lastra RR, et al. Selective Glucocorticoid Receptor Modulators (SGRMs) Delay Castrate-Resistant Prostate Cancer Growth. Molecular Cancer Therapeutics. 2017 Apr 1;16(8):1680–92.

Kamachi Y, Kondoh H. Sox proteins: regulators of cell fate specification and differentiation. Development. 2013 Oct 1;140(20):4129–44.

Kamachi Y, Sockanathan S, Liu Q, Breitman M, Lovell-Badge R, Kondoh H. Involvement of SOX proteins in lens-specific activation of crystallin genes. EMBO J. 1995 Jul 17;14(14):3510–9. PMCID: PMC394419

Kamachi Y, Uchikawa M, Collignon J, Lovell-Badge R, Kondoh H. Involvement of Sox1, 2 and 3 in the early and subsequent molecular events of lens induction. Development. 1998 Jul;125(13):2521–32.

Kamachi Y, Uchikawa M, Kondoh H. Pairing SOX off: with partners in the regulation of embryonic development. Trends in Genetics. 2000 Apr;16(4):182–7.

Kamachi Y, Uchikawa M, Tanouchi A, Sekido R, Kondoh H. Pax6 and SOX2 form a co-DNA-binding partner complex that regulates initiation of lens development. Genes & Development. 2001 May 15;15(10):1272–86. PMCID: PMC313803

Kar S, Sengupta D, Deb M, Pradhan N, Patra SK. Biochimica et Biophysica Acta. BBA - Molecular Basis of Disease. Elsevier B.V; 2017 Jan 1;1863(1):253–65.

Karthaus WR, Iaquinta PJ, Drost J, Gracanin A, van Boxtel R, Wongvipat J, et al. Identification of Multipotent Luminal Progenitor Cells in Human Prostate Organoid Cultures. Cell [Internet]. Elsevier Inc; 2014 Sep 25;159(1):163–75. Retrieved from: http://www.sciencedirect.com/science/article/pii/S0092867414010484

Kasper S. Exploring the Origins of the Normal Prostate and Prostate Cancer Stem Cell. Stem Cell Rev. 2008 Jun 19;4(3):193–201.

Kempfle JS, Turban JL, Edge ASB. Sox2 in the differentiation of cochlear progenitor cells. Sci. Rep. 2016 Mar 18;6:23293. PMCID: PMC4796895

Keramari M, Razavi J, Ingman KA, Patsch C, Edenhofer F, Ward CM, et al. Sox2 is essential for formation of trophectoderm in the preimplantation embryo. PLoS ONE. 2010 Nov 12;5(11):e13952. PMCID: PMC2980489

Kiernan AE, Pelling AL, Leung KKH, Tang ASP, Bell DM, Tease C, et al. Sox2 is required for sensory organ development in the mammalian inner ear. Nature. 2005 Apr 21;434(7036):1031–5.

Klüppel M, Wrana JL. Turning it up a Notch: cross-talk between TGF beta and Notch signaling. Bioessays. 2005 Feb;27(2):115–8.

Knoblich JA. Mechanisms of Asymmetric Stem Cell Division. Cell. 2008 Feb;132(4):583–97.

Kojima M, Naya Y, Inoue W, Ukimura O, Watanabe M, Saitoh M, et al. The American Urological Association symptom index for benign prostatic hyperplasia as a function of age, volume and ultrasonic appearance of the prostate. The Journal of Urology. 1997 Jun;157(6):2160–5.

Kondoh H, Kamachi Y. SOX–partner code for cell specification: Regulatory target selection and underlying molecular mechanisms. The International Journal of Biochemistry & Cell Biology. 2010 Mar;42(3):391–9.

Kopp JL, Grompe M, Sander M. Stem cells versus plasticity in liver and pancreas regeneration. Nature Cell Biology. Nature Publishing Group; 2016 Mar 1;18(3):238–45.

Kopp JL, Ormsbee BD, Desler M, Rizzino A. Small increases in the level of Sox2 trigger the differentiation of mouse embryonic stem cells. Stem Cells. 2008 Apr;26(4):903–11.

Kramer G, Steiner GE, Handisurya A, Stix U, Haitel A, Knerer B, et al. Increased expression of lymphocyte-derived cytokines in benign hyperplastic prostate tissue, identification of the producing cell types, and effect of differentially expressed cytokines on stromal cell proliferation. Prostate. 2002 Jun 1;52(1):43–58.

Kregel S, Kiriluk KJ, Rosen AM, Cai Y, Reyes EE, Otto KB, et al. Sox2 Is an Androgen Receptor-Repressed Gene That Promotes Castration-Resistant Prostate Cancer. Yu J, editor. PLoS ONE. 2013 Jan 11;8(1):e53701.

Krieg M, Klötzl G, Kaufmann J, Voigt KD. Stroma of human benign prostatic hyperplasia: preferential tissue for androgen metabolism and oestrogen binding. Acta Endocrinol. 1981 Mar;96(3):422–32.

Ku S-Y, Rosario S, Wang Y, Mu P, Seshadri M, Goodrich ZW, et al. Rb1 and Trp53 cooperate

to suppress prostate cancer lineage plasticity, metastasis, and antiandrogen resistance. Science. 2017 Jan 6;355(6320):78–83. PMCID: PMC5367887

Kurita T. Role of p63 and basal cells in the prostate. Development. 2004 Oct 15;131(20):4955–64.

Kwak JT, Sankineni S, Xu S, Turkbey B, Choyke PL, Pinto PA, et al. Correlation of magnetic resonance imaging with digital histopathology in prostate. Int J CARS. 2015 Aug 29;11(4):657–66.

Kwon O-J, Valdez JM, Zhang L, Zhang B, Wei X, Su Q, et al. Increased Notch signalling inhibits anoikis andstimulates proliferation of prostate luminalepithelial cells. Nature Communications. Nature Publishing Group; 1AD;5:1–15. PMCID: PMC4167399

Kwon O-J, Zhang L, Ittmann MM, Xin L. Prostatic inflammation enhances basal-to-luminal differentiation and accelerates initiation of prostate cancer with a basal cell origin. Proc. Natl. Acad. Sci. U.S.A. 2014 Feb 4;111(5):E592–E600.

Kwon O-J, Zhang L, Xin L. Stem Cell Antigen-1 Identifies a Distinct Androgen-Independent Murine Prostatic Luminal Cell Lineage with Bipotent Potential. Stem Cells. 2015 Oct 27;34(1):191–202. PMCID: PMC4816225

Kyprianou N, T IJ. Activation of programmed cell death in the rat ventral prostate after castration. Endocrinology. 1988a Feb;122(2):552–62.

Kyprianou N, T IJ. Identification of a cellular receptor for transforming growth factor-beta in rat ventral prostate and its negative regulation by androgens. Endocrinology. 1988b Oct;123(4):2124–31.

Kyprianou N, T IJ. Expression of transforming growth factor-beta in the rat ventral prostate during castration-induced programmed cell death. Mol. Endocrinol. 1989 Oct;3(10):1515–22.

Lawson DA, Xin L, Lukacs RU, Cheng D, Witte ON. Isolation and functional characterization of murine prostate stem cells. Proceedings of the National Academy of Sciences. 2007 Jan 2;104(1):181–6. PMCID: PMC1716155

Le Bin GC, Muñoz-Descalzo S, Kurowski A, Leitch H, Lou X, Mansfield W, et al. Oct4 is required for lineage priming in the developing inner cell mass of the mouse blastocyst. Development. 2014 Mar;141(5):1001–10. PMCID: PMC3929414

Le Magnen C, Bubendorf L, Ruiz C, Zlobec I, Bachmann A, Heberer M, et al. Klf4 transcription factor is expressed in the cytoplasm of prostate cancer cells. European Journal of Cancer. Elsevier; 2013 Mar 1;49(4):955–63.

Lee SH, Shen MM. Cell types of origin for prostate cancer. Current Opinion in Cell Biology. 2015 Dec;37:35–41.

Lefebvre V, Dumitriu B, Penzo-Méndez A, Han Y, Pallavi B. Control of cell fate and

differentiation by Sry-related high-mobility-group box (Sox) transcription factors. The International Journal of Biochemistry & Cell Biology. 2007;39(12):2195–214. PMCID: PMC2080623

Lekas AG, Lazaris AC, Chrisofos M, Papatsoris AG, Lappas D, Patsouris E, et al. Finasteride effects on hypoxia and angiogenetic markers in benign prostatic hyperplasia. Urology. 2006 Aug;68(2):436–41.

Leng N, Dawson JA, Thomson JA, Ruotti V, Rissman AI, Smits BMG, et al. EBSeq: an empirical Bayes hierarchical model for inference in RNA-seq experiments. Bioinformatics. 2013 Apr 15;29(8):1035–43. PMCID: PMC3624807

Lesko MH, Driskell RR, Kretzschmar K, Goldie SJ, Watt FM. Sox2 modulates the function of two distinct cell lineages in mouse skin. Developmental Biology. Elsevier; 2013 Oct 1;382(1):15–26.

Li B, Dewey CN. RSEM: accurate transcript quantification from RNA-Seq data with or without a reference genome. BMC Bioinformatics. 2011 Aug 4;12:323. PMCID: PMC3163565

Li D, Zhao L-N, Zheng X-L, Lin P, Lin F, Li Y, et al. Sox2 is involved in paclitaxel resistance of the prostate cancer cell line PC-3 via the PI3K/Akt pathway. Mol Med Report. 2014 Dec;10(6):3169–76.

Li H, Durbin R. Fast and accurate short read alignment with Burrows-Wheeler transform. Bioinformatics. 2009 Jul 15;25(14):1754–60. PMCID: PMC2705234

Li L, Clevers H. Coexistence of quiescent and active adult stem cells in mammals. Science. 2010 Jan 29;327(5965):542–5. PMCID: PMC4105182

Lin B, Coleman JH, Peterson JN, Zunitch MJ, Jang W, Herrick DB, et al. Injury Induces Endogenous Reprogramming and Dedifferentiation of Neuronal Progenitors to Multipotency. Stem Cell. Elsevier Inc; 2017 Dec 7;21(6):761–5.

Lin F, Lin P, Zhao D, Chen Y, Xiao L, Qin W, et al. Sox2 targets cyclinE, p27 and survivin to regulate androgen-independent human prostate cancer cell proliferation and apoptosis. Cell Prolif. 2012 Jun;45(3):207–16.

Liu J, Pascal LE, Isharwal S, Metzger D, Ramos Garcia R, Pilch J, et al. Regenerated Luminal Epithelial Cells Are Derived from Preexisting Luminal Epithelial Cells in Adult Mouse Prostate. Molecular Endocrinology. 2011 Nov;25(11):1849–57.

Liu Z, Kraus WL. Catalytic-Independent Functions of PARP-1 Determine Sox2 Pioneer Activity at Intractable Genomic Loci. Molecular Cell. 2017 Feb 16;65(4):589–9. PMCID: PMC5319724

Lorente D, Mateo J, Zafeiriou Z, Smith AD, Sandhu S, Ferraldeschi R, et al. Switching and withdrawing hormonal agentsfor castration-resistant prostate cancer. Nat Rev Urol. Nature Publishing Group; 2015 Jan 1;12(1):37–47.

Lukacs RU, Memarzadeh S, Wu H, Witte ON. Bmi-1 Is a Crucial Regulator of Prostate Stem Cell Self-Renewal and Malignant Transformation. Cell Stem Cell. 2010 Dec;7(6):682–93.

Malki S, Boizet-Bonhoure B, Poulat F. Shuttling of SOX proteins. The International Journal of Biochemistry & Cell Biology. 2010 Mar;42(3):411–6.

Marikawa Y, Alarcón VB. Establishment of trophectoderm and inner cell mass lineages in the mouse embryo. Mol. Reprod. Dev. 2009 Nov;76(11):1019–32.

Marker PC, Donjacour AA, Dahiya R, Cunha GR. Hormonal, cellular, and molecular control of prostatic development. Developmental Biology. 2003 Jan;253(2):165–74.

Marshall S, Narayan P. Treatment of prostatic bleeding: suppression of angiogenesis by androgen deprivation. The Journal of Urology. 1993 Jun;149(6):1553–4.

Martin KJ, Rasch LJ, Cooper RL, Metscher BD, Johanson Z, Fraser GJ. Sox2+ progenitors in sharks link taste development with the evolution of regenerative teeth from denticles. Proc. Natl. Acad. Sci. U.S.A. 2016 Dec 20;113(51):14769–74.

Masui S, Nakatake Y, Toyooka Y, Shimosato D, Yagi R, Takahashi K, et al. Pluripotency governed by Sox2 via regulation of Oct3/4 expression in mouse embryonic stem cells. Nature Cell Biology. 2007 May 21;9(6):625–35.

Mathelier A, Fornes O, Arenillas DJ, Chen C-Y, Denay G, Lee J, et al. JASPAR 2016: a major expansion and update of the open-access database of transcription factor binding profiles. Nucleic Acids Research. 2016 Jan 4;44(D1):D110–5. PMCID: PMC4702842

McAuley EM, Mustafi D, Simons BW, Valek R, Zamora M, Markiewicz E, et al. Magnetic Resonance Imaging and MolecularCharacterization of a Hormone-Mediated MurineModel of Prostate Enlargement and Bladder OutletObstruction. The American Journal of Pathology. American Society for Investigative Pathology; 2017 Nov 1;187(11):2378–87.

McNeal JE. Origin and evolution of benign prostatic enlargement. Invest Urol. 1978 Jan;15(4):340–5.

McNeal JE. The zonal anatomy of the prostate. Prostate. 1981;2(1):35–49.

McVary KT. Clinical evaluation of benign prostatic hyperplasia. Rev Urol. 2003;5 Suppl 5:S3–S11. PMCID: PMC1502362

Michiel Sedelaar JP, Dalrymple SS, Isaacs JT. Of mice and men-warning: Intact versus castrated adult male mice as xenograft hosts are equivalent to hypogonadal versus abiraterone treated aging human males, respectively. Prostate. 2013 Jun 15;73(12):1316–25.

Moad M, Hannezo E, Buczacki SJ, Wilson L, El-Sherif A, Sims D, et al. Multipotent Basal Stem Cells, Maintained in Localized Proximal Niches, Support Directed Long- Ranging Epithelial Flows in Human Prostates. CellReports. ElsevierCompany; 2017 Aug 15;20(7):1609–22.

Moore KA, Lemischka IR. Stem cells and their niches. Science. 2006 Mar 31;311(5769):1880–5.

Mosteiro L, Pantoja C, Alcazar N, Marión RM, Chondronasiou D, Rovira M, et al. Tissue damage and senescence provide critical signals for cellular reprogramming in vivo. Science. 2016 Nov 24;354(6315):aaf4445.

Mu P, Zhang Z, Benelli M, Karthaus WR, Hoover E, Chen C-C, et al. SOX2 promotes lineage plasticity and antiandrogen resistance in TP53- and RB1-deficient prostate cancer. Science. 2017 Jan 6;355(6320):84–8. PMCID: PMC5247742

Mustafi D, Zamora M, Fan X, Markiewicz E, Mueller J, Conzen SD, et al. MRI accurately identifies early murine mammary cancers and reliably differentiates between in situand invasive cancer: correlation of MRI with histology. NMR Biomed. 2015 Jul 7;28(9):1078–86.

Narayanan S, Srinivas S, Feldman D. Androgen–glucocorticoid interactions in the era of novel prostate cancer therapy. Nature Publishing Group. Nature Publishing Group; 2015 Dec 8;13(1):47–60.

Nemeth JA, Lee C. Prostatic ductal system in rats: regional variation in stromal organization. Prostate. 1996 Feb;28(2):124–8.

Nemeth JA, Sensibar JA, White RR, Zelner DJ, Kim IY, Lee C. Prostatic ductal system in rats: tissue-specific expression and regional variation in stromal distribution of transforming growth factor-beta 1. Prostate. 1997 Sep 15;33(1):64–71.

Network TCGAR, Abeshouse A, Ahn J, Akbani R, Ally A, Amin S, et al. The Molecular Taxonomy of Primary Prostate Cancer. Cell. Elsevier Inc; 2015 Nov 5;163(4):1011–25.

Nichols J, Zevnik B, Anastassiadis K, Niwa H, Klewe-Nebenius D, Chambers I, et al. Formation of pluripotent stem cells in the mammalian embryo depends on the POU transcription factor Oct4. Cell. 1998 Oct 30;95(3):379–91.

Nicholson TM, Moses MA, Uchtmann KS, Keil KP, Bjorling DE, Vezina CM, et al. Estrogen Receptor-a is a Key Mediator and Therapeutic Target for Bladder Complications of Benign Prostatic Hyperplasia. Journal of Urology. Elsevier Ltd; 2015 Feb 1;193(2):722–9.

Nicholson TM, Ricke EA, Marker PC, Miano JM, Mayer RD, Timms BG, et al. Testosterone and 17β-Estradiol Induce Glandular Prostatic Growth, Bladder Outlet Obstruction, and Voiding Dysfunction in Male Mice. Endocrinology [Internet]. 2012 Nov;153(11):5556–65. Retrieved from: http://press.endocrine.org/doi/suppl/10.1210/en.2012-1522

Nicholson TM, Ricke WA. Androgens and estrogens in benign prostatic hyperplasia: Past, present and future. Differentiation. 2011 Nov;82(4-5):184–99.

Nishan U, Damas-Souza DM, Barbosa GO, Muhammad N, Rahim A, Carvalho HF. Life Sciences. Life Sciences. Elsevier Inc; 2015 Dec 15;143(C):168–73.

Niwa H, Toyooka Y, Shimosato D, Strumpf D, Takahashi K, Yagi R, et al. Interaction between

Oct3/4 and Cdx2 determines trophectoderm differentiation. Cell. 2005 Dec 2;123(5):917–29.

Notara M, Ahmed A. Benign prostate hyperplasia and stem cells: a new therapeutic opportunity. Cell Biol Toxicol. 2012 Oct 12;28(6):435–42.

Ohmoto M, Ren W, Nishiguchi Y, Hirota J, Jiang P, Matsumoto I. Genetic Lineage Tracing in Taste Tissues Using Sox2-CreERT2 Strain. Chemical Senses. 2017 Jun 8.

Okazawa M, Murashima A, Harada M, Nakagata N, Noguchi M, Morimoto M, et al. Developmental Biology. Developmental Biology. Elsevier; 2015 Apr 1;400(1):139–47.

Okubo T, Clark C, Hogan BLM. Cell lineage mapping of taste bud cells and keratinocytes in the mouse tongue and soft palate. Stem Cells. 2009a Feb;27(2):442–50. PMCID: PMC4337989

Okubo T, Clark C, Hogan BLM. Cell Lineage Mapping of Taste Bud Cells and Keratinocytes in the Mouse Tongue and Soft Palate. Stem Cells. 2009b Feb;27(2):442–50.

Oliveira DSM, Dzinic S, Bonfil AI, Saliganan AD, Sheng S, Bonfil RD. The mouse prostate: a basic anatomical and histological guideline. Bosn J of Basic Med Sci. 2015 Aug 20.

Ousset M, Van Keymeulen A, Bouvencourt G, Sharma N, Achouri Y, Simons BD, et al. Multipotent and unipotent progenitors contribute to prostate postnatal development. Nature Cell Biology. 2012 Nov;14(11):1131–8.

oz JMN, Stange DE, Schepers AG, van de Wetering M, Koo B-K, Itzkovitz S, et al. The Lgr5 intestinal stem cell signature: robust expression of proposed quiescent “ þ 4” cell markers. EMBO J. Nature Publishing Group; 2012 Jun 12;31(14):3079–91.

Papaioannou VE. Concepts of Cell Lineage in Mammalian Embryos. 1st ed. Forces and Tension in Development. Elsevier Inc; 2016. p. 185–97.

Pareek G, Shevchuk M, Armenakas NA, Vasjovic L, Hochberg DA, Basillote JB, et al. The effect of finasteride on the expression of vascular endothelial growth factor and microvessel density: a possible mechanism for decreased prostatic bleeding in treated patients. The Journal of Urology. 2003 Jan;169(1):20–3.

Park D, Zhong Y, Lu Y, Rycaj K, Gong S, Chen X, et al. Stem cell and neurogenic gene-expression profiles link prostate basal cells to aggressive prostate cancer. Nature Communications. Nature Publishing Group; 2016 Feb 20;7:1–15. PMCID: PMC4773505

Partin AW, Coffey DS. Benign and malignant prostatic neoplasms: human studies. Recent Prog. Horm. Res. 1994;49:293–331.

Pevny LH, Nicolis SK. Sox2 roles in neural stem cells. The International Journal of Biochemistry & Cell Biology. 2010 Mar;42(3):421–4.

Pignon J-C, Grisanzio C, Carvo I, Werner L, Regan M, Wilson EL, et al. Cell Kinetic Studies Fail to Identify Sequentially Proliferating Progenitors as the Major Source of Epithelial

Renewal in the Adult Murine Prostate. Languino LR, editor. PLoS ONE. 2015 May 29;10(5):e0128489.

Pignon J-C, Grisanzio C, Geng Y, Song J, Shivdasani RA, Signoretti S. p63-expressing cells are the stem cells of developing prostate, bladder, and colorectal epithelia. Proc. Natl. Acad. Sci. U.S.A. 2013 May 14;110(20):8105–10. PMCID: PMC3657776

Potten CS, Loeffler M. Stem cells: attributes, cycles, spirals, pitfalls and uncertainties. Lessons for and from the crypt. Development. 1990 Dec;110(4):1001–20.

Prajapati A, Gupta S, Mistry B, Gupta S. Prostate Stem Cells in the Development of Benign Prostate Hyperplasia and Prostate Cancer: Emerging Role and Concepts. BioMed Research International. 2013;2013(3):1–10.

Prins GS, Putz O. Molecular signaling pathways that regulate prostate gland development. Differentiation. 2008 Jul;76(6):641–59.

Pritchard CC, Nelson PS. Gene expression profiling in the developing prostate. Differentiation. International Society of Differentiation; 2008 Jul 1;76(6):624–40.

Que J, Luo X, Schwartz RJ, Hogan BLM. Multiple roles for Sox2 in the developing and adult mouse trachea. Development. 2009 May 8;136(11):1899–907.

Que J, Okubo T, Goldenring JR, Nam KT, Kurotani R, Morrisey EE, et al. Multiple dose-dependent roles for Sox2 in the patterning and differentiation of anterior foregut endoderm. Development. 2007 May 23;134(13):2521–31.

Ring KL, Tong LM, Balestra ME, Javier R, Andrews-Zwilling Y, Li G, et al. Direct Reprogramming of Mouse and Human Fibroblasts into Multipotent Neural Stem Cells with a Single Factor. Stem Cell. Elsevier Inc; 2012 Jul 6;11(1):100–9.

Rios AC, Fu NY, Lindeman GJ, Visvader JE. In situ identification of bipotent stem cells in the mammary gland. Nature. Nature Publishing Group; 2014 Feb 11;506(7488):322–7.

Roarty K, Rosen JM. Wnt and mammary stem cells: hormones cannot fly wingless. Curr Opin Pharmacol. 2010 Dec;10(6):643–9. PMCID: PMC2981611

Rompolas P, Mesa KR, Greco V. Spatial organization within a niche as a determinant of stem-cell fate. Nature. Nature Publishing Group; 2013 Nov 27;502(7472):513–8.

Roose H, Cox B, Boretto M, Gysemans C, Vennekens A, Vankelecom H. Major depletion of SOX2. Sci. Rep. Springer US; 2017 Nov 27;:1–11.

Rosenthal SA, Sandler HM. Treatment strategies for high-risk locally advanced prostate cancer. Nat Rev Urol. Nature Publishing Group; 2010 Jan 1;7(1):31–8.

Rossant J, Tam PPL. Blastocyst lineage formation, early embryonic asymmetries and axis patterning in the mouse. Development [Internet]. 2009 Feb 6;136(5):701–13. Retrieved from:

http://eutils.ncbi.nlm.nih.gov/entrez/eutils/elink.fcgi?dbfrom=pubmed&id=19201946&retmode=ref&cmd=prlinks

Rossant J, Tam PPL. Perspective. Stem Cell. Elsevier Inc; 2017 Jan 5;20(1):18–28.

Sahu B, Laakso M, Ovaska K, Mirtti T, Lundin J, Rannikko A, et al. Dual role of FoxA1 in androgen receptor binding to chromatin, androgen signalling and prostate cancer. EMBO J. Nature Publishing Group; 2011 Sep 13;30(19):3962–76.

Salm SN, Burger PE, Coetzee S, Goto K, Moscatelli D, Wilson EL. TGF-β maintains dormancy of prostatic stem cells in the proximal region of ducts. The Journal of Cell Biology. 2005 Jul 5;170(1):81–90.

Sampson N, Madersbacher S, Berger P. [Pathophysiology and therapy of benign prostatic hyperplasia]. Wien. Klin. Wochenschr. 2008;120(13-14):390–401.

Sanz-Navarro M, Seidel K, Sun Z, Bertonnier-Brouty L, Amendt BA, Klein OD, et al. Plasticity within the niche ensures the maintenance of a Sox2+ stem cell population in the mouse incisor. Development. 2017 Nov 27;:dev.155929.

Sarkar A, Hochedlinger K. The Sox Family of Transcription Factors: Versatile Regulators of Stemand Progenitor Cell Fate. Stem Cell. Elsevier Inc; 2013 Jan 3;12(1):15–30. PMCID: PMC3608206

Sarkar A, Huebner AJ, Sulahian R, Anselmo A, Xu X, Flattery K, et al. Sox2 Suppresses Gastric Tumorigenesis in Mice. CellReports. The Author(s); 2016 Aug 3;:1–23.

Schaefer SM, Segalada C, Cheng PF, Bonalli M, Parfejevs V, Levesque MP, et al. Sox2 is dispensable for primary melanoma and metastasisformation. Oncogene. Nature Publishing Group; 2017 Apr 3;36(31):4516–24.

Schiebler ML, Tomaszewski JE, Bezzi M, Pollack HM, Kressel HY, Cohen EK, et al. Prostatic carcinoma and benign prostatic hyperplasia: correlation of high-resolution MR and histopathologic findings. Radiology. 1989 Jul;172(1):131–7.

Sciavolino PJ, Abrams EW, Yang L, Austenberg LP, Shen MM, Abate-Shen C. Tissue-specific expression of murine Nkx3.1 in the male urogenital system. Dev. Dyn. 1997 May;209(1):127–38.

Seo E, Basu-Roy U, Zavadil J, Basilico C, Mansukhani A. Distinct Functions of Sox2 Control Self-Renewal and Differentiation in the Osteoblast Lineage. Molecular and Cellular Biology. 2011 Oct 28;31(22):4593–608.

Shafer MER, Nguyen AHT, Tremblay M, Viala S, Béland M, Bertos NR, et al. Lineage Specification from Prostate Progenitor Cells Requires Gata3-Dependent Mitotic Spindle Orientation. Stem Cell Reports. ElsevierCompany; 2017 Mar 6;:1–14.

Shahi P, Seethammagari MR, Valdez JM, Xin L, Spencer DM. Wnt and Notch Pathways Have

Interrelated Opposing Roles on Prostate Progenitor Cell Proliferation and Differentiation. Stem Cells. 2011 Apr 5;29(4):678–88.

Shappell SB, Thomas GV, Roberts RL, Herbert R, Ittmann MM, Rubin MA, et al. Prostate pathology of genetically engineered mice: definitions and classification. The consensus report from the Bar Harbor meeting of the Mouse Models of Human Cancer Consortium Prostate Pathology Committee. Cancer Res. 2004. p. 2270–305.

Shen MM, Abate-Shen C. Molecular genetics of prostate cancer: new prospects for old challenges. Genes & Development. 2010 Sep 15;24(18):1967–2000.

Siegle JM, Basin A, Sastre-Perona A, Yonekubo Y, Brown J, Sennett R, et al. SOX2 is a cancer-specific regulator of tumourinitiating potential in cutaneous squamous cellcarcinoma. Nature Communications. Nature Publishing Group; 2014 Jul 24;5:1–12.

Signoretti S, Waltregny D, Dilks J, Isaac B, Lin D, Garraway L, et al. Short Communication. The American Journal of Pathology. American Society for Investigative Pathology; 2000 Dec 15;157(6):1769–75.

Slack JM. Stem cells in epithelial tissues. Science. 2000 Feb 25;287(5457):1431–3.

Snippert HJ, Clevers H. Tracking adult stem cells. EMBO Rep. 2011 Feb;12(2):113–22. PMCID: PMC3049439

Soufi A, Donahue G, Zaret KS. Facilitators and impediments of the pluripotency reprogramming factors' initial engagement with the genome. Cell. 2012 Nov 21;151(5):994–1004. PMCID: PMC3508134

Soufi A, Garcia MF, Jaroszewicz A, Osman N, Pellegrini M, Zaret KS. Pioneer Transcription Factors Target Partial DNA Motifs on Nucleosomes to Initiate Reprogramming. Cell. Elsevier Inc; 2015 Apr 23;161(3):555–68. PMCID: PMC4409934

Soufi A, Zaret KS. Understanding impediments to cellular conversion to pluripotency by assessing the earliest events in ectopic transcription factor binding to the genome. Cell Cycle. 2013 May 15;12(10):1487–91. PMCID: PMC3680528

Srinivas S, Watanabe T, Lin CS, William CM, Tanabe Y, Jessell TM, et al. Cre reporter strains produced by targeted insertion of EYFP and ECFP into the ROSA26 locus. BMC Dev. Biol. 2001;1:4. PMCID: PMC31338

Staack A, Donjacour AA, Brody J, Cunha GR, Carroll P. Mouse urogenital development: a practical approach. Differentiation. 2003a Sep;71(7):402–13.

Staack A, Donjacour AA, Brody J, Cunha GR, Carroll P. Mouse urogenital development: a practical approach. Differentiation. 2003b Aug 30;(71):402–13.

Steevens AR, Sookiasian DL, Glatzer JC, Kiernan AE. SOX2 is required for inner ear neurogenesis. Sci. Rep. 2017 Jun 22;7(1):1241062.

Sugimura Y, Cunha GR, Donjacour AA. Morphogenesis of ductal networks in the mouse prostate. Biol. Reprod. 1986 Jun;34(5):961–71.

Suh H, Consiglio A, Ray J, Sawai T, D'Amour KA, Gage FH. In Vivo Fate Analysis Reveals the Multipotent and Self-Renewal Capacities of Sox2+ Neural Stem Cells in the Adult Hippocampus. Cell Stem Cell. 2007 Nov;1(5):515–28.

Sun Q-Z, Guan T-Y, Qi J-G, Cao J-Y, Wu G, Yang N, et al. [Histological characteristics of the prostate in men who receive re-TURP for benign prostatic hyperplasia and their clinical significance]. Zhonghua Nan Ke Xue. 2010 Feb;16(2):118–22.

Sutton MT, Yingling M, Vyas A, Atiemo H, Borkowski A, Jacobs SC, et al. Finasteride targets prostate vascularity by inducing apoptosis and inhibiting cell adhesion of benign and malignant prostate cells. Prostate. 2006 Aug 1;66(11):1194–202.

Szczyrba J, Niesen A, Wagner M, Wandernoth PM, Aumüller G, Wennemuth G. Neuroendocrine Cells of the Prostate Derive from the Neural Crest. Journal of Biological Chemistry. 2017 Feb 3;292(5):2021–31.

Takahashi K, Yamanaka S. Induction of Pluripotent Stem Cells from Mouse Embryonic and Adult Fibroblast Cultures by Defined Factors. Cell. 2006 Aug;126(4):663–76.

Taranova OV, Magness ST, Fagan BM, Wu Y, Surzenko N, Hutton SR, et al. SOX2 is a dose-dependent regulator of retinal neural progenitor competence. Genes & Development. 2006 May 1;20(9):1187–202. PMCID: PMC1472477

Tata PR, Mou H, Pardo-Saganta A, Zhao R, Prabhu M, Law BM, et al. Dedifferentiation of committed epithelial cells into stem cells in vivo. Nature. Nature Publishing Group; 2013 Nov 13;503(7475):218–23.

Tetteh PW, Basak O, Farin HF, Wiebrands K, Kretzschmar K, Begthel H, et al. Replacement of Lost Lgr5-Positive Stem Cells through Plasticity of Their Enterocyte-Lineage Daughters. Stem Cell. Elsevier Inc; 2016 Feb 4;18(2):203–13.

Tetteh PW, Farin HF, Clevers H. Plasticity within stem cell hierarchiesin mammalian epithelia. Trends in Cell Biology. Elsevier Ltd; 2015 Feb 1;25(2):100–8.

Teulière J, Faraldo MM, Deugnier M-A, Shtutman M, Ben-Ze'ev A, Thiery JP, et al. Targeted activation of beta-catenin signaling in basal mammary epithelial cells affects mammary development and leads to hyperplasia. Development. 2005 Jan;132(2):267–77.

Thomsen MK, Francis JC, Swain A. The role of Sox9 in prostate development. Differentiation. International Society of Differentiation; 2008 Jul 1;76(6):728–35.

Thomson AA. Mesenchymal mechanisms in prostate organogenesis. Differentiation. International Society of Differentiation; 2008 Jul 1;76(6):587–98.

Timms BG. Prostate development: a historical perspective. Differentiation. International Society

of Differentiation; 2008 Jul 1;76(6):565–77.

Toivanen R, Mohan A, Shen MM. Basal Progenitors Contribuet to Repair. Stem Cell Reports. ElsevierCompany; 2016 May 10;6(5):660–7. PMCID: PMC4939748

Toivanen R, Shen MM. Prostate organogenesis: tissue induction, hormonal regulation and cell type specification. Development. 2017 Apr 11;144(8):1382–98. PMCID: PMC5399670

Tsujimura A. Proximal location of mouse prostate epithelial stem cells: a model of prostatic homeostasis. The Journal of Cell Biology. 2002 Jun 24;157(7):1257–65.

Tsuruzoe S, Ishihara K, Uchimura Y, Watanabe S, Sekita Y, Aoto T, et al. Inhibition of DNA binding of Sox2 by the SUMO conjugation. Biochemical and Biophysical Research Communications. 2006 Dec;351(4):920–6.

Turkbey B, Mani H, Shah V, Rastinehad AR, Bernardo M, Pohida T, et al. Multiparametric 3T Prostate Magnetic Resonance Imaging to Detect Cancer: Histopathological Correlation Using Prostatectomy Specimens Processed in Customized Magnetic Resonance Imaging Based Molds. The Journal of Urology. Elsevier Inc; 2011 Nov 1;186(5):1818–24.

Uzgare AR, Isaacs JT. Enhanced redundancy in Akt and mitogen-activated protein kinase-induced survival of malignant versus normal prostate epithelial cells. Cancer Research. 2004 Sep 1;64(17):6190–9.

Uzgare AR, Xu Y, Isaacs JT. In vitro culturing and characteristics of transit amplifying epithelial cells from human prostate tissue. J. Cell. Biochem. 2003;91(1):196–205.

Valdez JM, Zhang L, Su Q, Dakhova O, Zhang Y, Shahi P, et al. Notch and TGF-beta Form a Reciprocal Positive Regulatory Loop that Suppresses Murine Prostate Basal Stem/Progenitor Cell Activity. Stem Cell. Elsevier Inc; 2012 Nov 2;11(5):676–88.

van Amerongen R, Bowman AN, Nusse R. Developmental stage and time dictate the fate of Wnt/β-catenin-responsive stem cells in the mammary gland. Cell Stem Cell. 2012 Sep 7;11(3):387–400.

Van Hoof D, Munoz J, Braam SR, Pinkse MWH, Linding R, Heck AJR, et al. Phosphorylation dynamics during early differentiation of human embryonic stem cells. Cell Stem Cell. 2009 Aug 7;5(2):214–26.

van Lohuizen M, Verbeek S, Scheijen B, Wientjens E, van der Gulden H, Berns A. Identification of cooperating oncogenes in E mu-myc transgenic mice by provirus tagging. Cell. 1991 May 31;65(5):737–52.

Vander Griend DJ, Karthaus WL, Dalrymple S, Meeker A, DeMarzo AM, T IJ. The Role of CD133 in Normal Human Prostate Stem Cells and Malignant Cancer-Initiating Cells. Cancer Research. 2008 Dec 1;68(23):9703–11.

Vander Griend DJ, Litvinov IV, Isaacs JT. Conversion of Androgen Receptor Signaling From a

Growth Suppressor in Normal Prostate Epithelial Cells to an Oncogene in Prostate Cancer Cells Involves a Gain of Function in c-Myc Regulation. Int. J. Biol. Sci. 2014 Oct 6;10(6):627–42. PMCID: PMC4062956

Vanner RJ, Remke M, Gallo M, Selvadurai HJ, Coutinho F, Lee L, et al. Quiescent Sox2+ Cells Drive Hierarchical Growth and Relapse in Sonic Hedgehog Subgroup Medulloblastoma. Cancer Cell. 2014 Jul 14;26(1):33–47. PMCID: PMC4441014

Varga J, Greten FR. Cell plasticity in epithelial homeostasis and tumorigenesis. Nature Cell Biology. 2017 Sep 25;19(10):1133–41.

Visschere PJL, Vral A, Perletti G, Pattyn E, Praet M, Magri V, et al. Multiparametric magnetic resonance imaging characteristics of normal, benign and malignant conditions in the prostate. European Radiology. European Radiology; 2016 Aug 1;:1–15.

Walsh PC, Wilson JD. The induction of prostatic hypertrophy in the dog with androstanediol. J. Clin. Invest. 1976 Apr;57(4):1093–7. PMCID: PMC436755

Wang B-E, Wang X, Long JE, Eastham-Anderson J, Firestein R, Junttila MR. Castration-resistant Lgr5+ cells are long-lived stem cells required for prostatic regeneration. Stem Cell Reports. The Authors; 2015 May 12;4(5):768–79.

Wang J, Zhu HH, Chu M, Liu Y, Zhang C, Liu G, et al. Symmetrical and asymmetrical division analysisprovides evidence for a hierarchy of prostateepithelial cell lineages. Nature Communications. Nature Publishing Group; 2014a Aug;5:1–13.

Wang X, Julio MK-D, Economides KD, Walker D, Yu H, Halili MV, et al. A luminal epithelial stem cell that is a cell of origin for prostate cancer. Nature. Nature Publishing Group; 2009 Sep 14;461(7263):495–500.

Wang X-D, Leow CC, Zha J, Tang Z, Modrusan Z, Radtke F, et al. Notch signaling is required for normal prostatic epithelial cell proliferation and differentiation. Developmental Biology. 2006 Feb 1;290(1):66–80.

Wang Y, Hayward S, Cao M, Thayer K, Cunha G. Cell differentiation lineage in the prostate. Differentiation. 2001 Oct;68(4-5):270–9.

Wang ZA, Mitrofanova A, Bergren SK, Abate-Shen C, Cardiff RD, Califano A, et al. Lineage analysis of basal epithelial cells reveals their unexpected plasticity and supports a cell-of-origin model for prostate cancer heterogeneity. Nature Cell Biology. Nature Publishing Group; 2013 Feb 24;15(3):274–83. PMCID: PMC3743266

Wang ZA, Toivanen R, Bergren SK, Chambon P, Shen MM. Luminal Cells Are Favoredas the Cell of Origin for Prostate Cancer. CellReports. The Authors; 2014b Sep 11;8(5):1339–46. PMCID: PMC4163115

Wegner M. All purpose Sox: The many roles of Sox proteins in gene expression. The International Journal of Biochemistry & Cell Biology. 2010 Mar;42(3):381–90.

Weina K, Wu H, Knappe N, Orouji E, Novak D, Bernhardt M, et al. TGF-β induces SOX2 expression in a time-dependent manner in human melanoma cells. Pigment Cell Melanoma Res. 2016 Jul;29(4):453–8.

Wicklow E, Blij S, Frum T, Hirate Y, Lang RA, Sasaki H, et al. HIPPO Pathway Members Restrict SOX2 to the Inner Cell Mass Where It Promotes ICM Fates in the Mouse Blastocyst. Downs KM, editor. PLoS Genet. 2014 Oct 23;10(10):e1004618.

Wuebben EL, Rizzino A. The dark side of SOX2: cancer - a comprehensive overview. Oncotarget. 2017 Jul 4;8(27):44917–43. PMCID: PMC5546531

Wuidart A, Ousset M, Rulands S, Simons BD, Van Keymeulen A, Blanpain C. Quantitative lineage tracing strategies to resolve multipotency in tissue-specific stem cells. Genes & Development. 2016 Jun 13;30(11):1261–77.

Xie Q, Liu Y, Cai T, Horton C, Stefanson J, Wang ZA. Dissecting cell-type-specific roles of androgen receptor in prostate homeostasis and regeneration through lineage tracing. Nature Communications. Nature Publishing Group; 2017 Jan 13;8:1–14. PMCID: PMC5264212

Xie Q, Wang ZA. Transcriptional regulation of the Nkx3.1gene in prostate luminal stem cell specification and cancer initiation via its 3′ genomic region. Journal of Biological Chemistry. 2017 Aug 18;292(33):13521–30.

Xin L, Ide H, Kim Y, Dubey P, Witte ON. In vivo regeneration of murine prostate from dissociated cell populations of postnatal epithelia and urogenital sinus mesenchyme. Proceedings of the National Academy of Sciences. 2003 Sep 30;100 Suppl 1:11896–903. PMCID: PMC304104

Xue Y, Smedts F, Debruyne FM, la Rosette de JJ, Schalken JA. Identification of intermediate cell types by keratin expression in the developing human prostate. Prostate. 1998 Mar 1;34(4):292–301.

Yamashita YM, Yuan H, Cheng J, Hunt AJ. Polarity in Stem Cell Division: Asymmetric Stem Cell Division in Tissue Homeostasis. Cold Spring Harbor Perspectives in Biology. 2010 Jan 5;2(1):a001313–3.

Yoo YA, Roh M, Naseem AF, Lysy B, Desouki MM, Unno K, et al. Bmi1 marks distinct castration-resistant luminalprogenitor cells competent for prostateregeneration and tumour initiation. Nature Communications. Nature Publishing Group; 2016 Sep 22;7:1–13.

Yu X, Cates JM, Morrissey C, You C, Grabowska MM, Zhang J, et al. SOX2 expression in the developing, adult, as well as, diseased prostate. Prostate Cancer and Prostatic Disease. Nature Publishing Group; 2014 Aug 5;17(4):301–9.

Yuan H, Corbi N, Basilico C, Dailey L. Developmental-specific activity of the FGF-4 enhancer requires the synergistic action of Sox2 and Oct-3. Genes & Development. 1995 Nov 1;9(21):2635–45.

Zappone MV, Galli R, Catena R, Meani N, De Biasi S, Mattei E, et al. Sox2 regulatory sequences direct expression of a (beta)-geo transgene to telencephalic neural stem cells and precursors of the mouse embryo, revealing regionalization of gene expression in CNS stem cells. Development. 2000 Jun;127(11):2367–82.

Zaret KS, Lerner J, Iwafuchi-Doi M. Chromatin Scanning by Dynamic Binding of Pioneer Factors. Molecular Cell. 2016 Jun 2;62(5):665–7. PMCID: PMC4893772

Zhang D, Jeter C, Gong S, Tracz A, Lu Y, Shen J, et al. Histone 2B-GFP Label-Retaining Prostate Luminal Cells Possess Progenitor Cell Properties and Are Intrinsically Resistant to Castration. Stem Cell Reports. 2018 Jan 9;10(1):228–42. PMCID: PMC5768933

Zhao B, Choi JP, Jaehne M, Gao YRE, Desai R, Tuckermann J, et al. Glucocorticoid receptor in prostate epithelia is not required for corticosteroid-induced epithelial hyperproliferation in the mouse prostate. Prostate. 2014 May 23;74(10):1068–78.

Zhao H-Y, Zhang Y-J, Dai H, Zhang Y, Shen Y-F. CARM1 Mediates Modulation of Sox2. Jin D-Y, editor. PLoS ONE. 2011 Oct 28;6(10):e27026.

Zhao L, Koopman P. SRY protein function in sex determination: thinking outside the box. Chromosome Res. 2012 Jan;20(1):153–62.

Zhao SG, Chang SL, Erho N, Yu M, Lehrer J, Alshalalfa M, et al. Associations of Luminal and Basal Subtyping of Prostate Cancer With Prognosis and Response to Androgen Deprivation Therapy. JAMA Oncol. 2017 Dec 1;3(12):1663.

Zhu Sen, Zhao D, Yan L, Jiang W, Kim J-S, Gu B, et al. BMI1 regulates androgen receptor in prostatecancer independently of the polycomb repressivecomplex 1. Nature Communications. Springer US; 2018 Feb 7;:1–13.

Zipori D. The nature of stem cells: state rather than entity. Nat Rev Genet. 2004 Nov;5(11):873–8.

Zong Y, Goldstein AS. Adaptation or selection—mechanisms of castration-resistant prostate cancer. Nat Rev Urol. Nature Publishing Group; 2012 Dec 18;10(2):90–8.